Constraint on dark matter using neutron stars

WASIF HUSAIN

Doctor of Philosophy

THE UNIVERSITY
of ADELAIDE

Supervisor: Prof. Anthony W. Thomas
Associate Supervisor: Prof. Derek Leinweber

A thesis submitted in fulfilment of
the requirements for the degree of
Doctor of Philosophy

School of Physics, Chemistry and Earth Science
Faculty of Science, Engineering and Technology

The University of Adelaide
Australia

24 July 2023

Abstract

In this study, the nature and properties of dark matter are explored with the help of neutron stars. Dark matter is assumed to have a particle nature, and different dark matter candidates are considered and tested using neutron stars. If neutron stars capture dark matter from the halo, their properties must change, with various candidates affecting them in different ways. Based on these changes, the nature of dark matter is studied, and possible directions for future studies are explored.

In addition to dark matter capture, the recent hypothesis concerning the possible decay of neutrons into dark matter, as suggested by Fornal and Grinstein, and Strumia, is thoroughly studied. Constraints on the properties of dark matter have been established, and observable signals from neutron stars are suggested. Using neutron star cooling, possible decay modes of dark bosons into Standard Model particles are also investigated.

Declaration

I certify that this work contains no material which has been accepted for the award of any other degree or diploma in my name, in any university or other tertiary institution and, to the best of my knowledge and belief, contains no material previously published or written by another person, except where due reference has been made in the text. In addition, I certify that no part of this work will, in the future, be used in a submission in my name, for any other degree or diploma in any university or other tertiary institution without the prior approval of the University of Adelaide and where applicable, any partner institution responsible for the joint award of this degree.

I give permission for the digital version of my thesis to be made available on the web, via the University's digital research repository, the Library Search and also through web search engines, unless permission has been granted by the University to restrict access for a period of time.

Signature

Research publications

Following are the research papers published or accepted in renown peer-reviewed journals during my 3.3 years of PhD candidature.

(1) Wasif Husain, Dipan Sengupta and Anthony Thomas

"Constraining dark boson decay using neutron stars".

Published in a special issue of the journal 'Universe' on the subject of 'Neutron Lifetime', 2023.

https://www.mdpi.com/2359642

Abstract: Inspired by the well known anomaly in the lifetime of the neutron, we investigate its consequences inside neutron stars. We first assess the viability of the neutron decay hypothesis suggested by Fornal and Grinstein within neutron stars, in terms of the equation of state and compatibility with observed properties. This is followed by an investigation of the constraint information on neutron star cooling can place on the decay rate of the dark boson into standard model particles, in the context of various BSM ideas.

(2) Wasif Husain and Anthony Thomas

"Novel neutron decay mode inside neutron stars",

Published in Journal of Physics G: Nuclear and Particle Physics, 2022.

https://doi.org/10.1088/1361-6471/aca1d5

Abstract: We explore the suggestion that the neutron lifetime puzzle might be resolved by neutrons decaying into dark matter through the process, n $\rightarrow \chi\chi\chi$, with χ having a mass one third of that of the neutron. In particular, we examine the consequences of such a decay mode for the properties of neutron stars. Unlike an earlier suggested decay mode, in order to satisfy the constraints on neutron star mass and tidal deformability, there is no need for a strong repulsive force between the dark matter particles. This study suggests the possibility of having hot dark matter at the

core of the neutron star and presents a possible mechanism of dark matter cooling, and examines the possible signal of neutrons decaying in this way inside the neutron star right after its birth.

(3) Wasif Husain, Theo F. Motta and Anthony Thomas,

" Consequences of neutron decay inside neutron stars ",

Published in Journal of Cosmology and Astrophysics (JCAP), 2021.

https://doi.org/10.1088/1475-7516/2022/10/028

Abstract: The hypothesis that neutrons might decay into dark matter is explored using neutron stars as a testing ground. It is found that in order to obtain stars with masses at the upper end of those observed, the dark matter must experience a relatively strong self-interaction. Conservation of baryon number and energy then require that the star must undergo some heating, with a decrease in radius, leading to an increase in speed of rotation over a period of days.

(4) Wasif Husain and Anthony Thomas

“Possible nature of Dark Matter”,

Published in Journal of Cosmology and Astrophysics (JCAP), 2021.

https://doi.org/10.1088/1475-7516/2021/10/086

Abstract: We present a study of neutron star models that contain dark matter (DM) in the core. The DM is assumed to have a particle nature and to be self-interacting. Using constraints on the mass and radius of neutron stars, we investigate the allowed properties of either bosonic or fermionic DM particles. For this purpose three different models of neutron stars are considered, the first involving nucleons only, the second including hyperons, and the last involving strange matter in the core. Different EoS are constructed for the various cases of fermionic and bosonic DM. These EoSs are solved for selected properties of the DM particles and the results are tested against mass, radius and tidal deformability constraints for neutron stars. The distribution of energy density of DM and ordinary matter inside the neutron stars is also presented. It is found that if the DM is fermionic in nature it does not just sit in the core but it is present everywhere in the star, from the centre to outside the surface and may even envelop.

Acknowledgements

This study is supported by the University of Adelaide scholarship; without its support, this study would not have been possible.

I want to express my sincere gratitude to Prof. Anthony W. Thomas, my primary PhD supervisor, for his wise counsel, unwavering encouragement, and tolerance. Throughout all of my academic research and daily life, his vast knowledge and experience have inspired me. I want to thank my associate supervisor, Prof. Derek Leinweber; his guidance, patience, and encouragement throughout my research journey have been invaluable to me. I want to express my gratitude to Sharon and Silvana for their kind assistance and support.

Finally, I'd like to thank my parents, my wife, Saba, my brothers and sisters, and my friends. Without their wonderful support, understanding, and encouragement in the past years, it would have been impossible for me to complete my study.

Contents

List of Figures

List of Tables

CHAPTER 1

Dark matter

Our universe is full of mysteries such as dark energy, black holes, dark matter, and many more. Dark matter is a mysterious matter that is non-luminous, non-interacting (or very weakly interacting) with ordinary matter (except through gravity), and exists in abundance in galaxies and clusters, giving galaxies the shape they have. In fact, on the scale of galaxies, dark matter dominates over ordinary matter. The primary evidence of the presence of dark matter comes from the rotation and shape of galaxies. Some of the galaxies would not have formed if there were not enough dark matter to bind the stars in them. The term 'dark' in dark matter does not mean that the matter is 'dark or black'. In fact, it is called dark matter because it is unseen and does not interact with light.

Most of the studies that have been done to understand the universe involve the study of the electromagnetic spectrum present in the universe. It would not be wrong if one says that to study the universe, we primarily depend on how the light coming out of stars and galaxies interacts with other objects. But the universe is supposed to be unbiased, so there is no particular reason why it should have been specifically selected to reveal its mysteries that way. Naively speaking, on a larger scale, on the scale of galaxies and clusters, the mass required to keep the galaxies and clusters the way they are increases, but the luminosity, or light, does not. This led scientists to hypothesize the existence of an invisible and non-interacting form of matter. That is known as the "missing light problem" or "the dark matter problem". Dark matter has been inferred to exist based on its gravitational effects on visible matter, but its composition and properties remain unknown. Dark matter is a different kind of matter that does not interact with light and therefore remains unseen and unknown.

The nature of dark matter is one of the burning questions in physics. Apart from astrophysics and cosmology research groups, the search for dark matter is also taking place in particle physics experiments such as colliders and direct dark matter detection experiments, and different theoretical dark matter models have been proposed. From the particle physics point of view, dark matter can be a bunch of new and different particles, but they have to be electrically neutral. The Standard Model of particle physics does not have a suitable candidate or mechanism for dark matter, and one must think beyond the Standard Model to discover the nature of dark matter.

Based on the cosmic microwave background (CMB) measured by WMAP (Bennett et al. 2003; Spergel et al. 2003) and SDSS collaboration for power spectrum galaxy density fluctuations (Eisenstein et al. 2005; Tegmark et al. 2004), it has been shown that most of the matter in the universe is in a form that is not observable. In the universe, baryonic matter accounts for only 4% of total energy, while dark matter contributes approximately 26%, and the rest is dark energy.

1.1 Historical background

It was theorised almost a century ago that there must be more matter in the universe than the luminosity would suggest in order to give enough gravitational attraction to galaxies and clusters to hold them together, otherwise, they would have flown apart. To date, there are substantial astrophysical and cosmological evidences that suggests the presence of dark matter. These evidences are based on gravitational effects that are observed, such as the deflection of light, the gravitational potential of galaxies, and the dynamical effects of clusters and galaxies. Since the evidence is related to gravity, it has been suggested that our understanding of gravity might be in error, and one should modify the gravitational equations, but this argument is weak, because it does not produce the effects at the scales of galaxies and clusters and fails to explain the anisotropies in the CMB.

Zwicky 1937, argued that there has to be more non-luminous matter present in clusters and galaxies to keep them in the form they are. This idea built up gradually because the idea

sounds radical, and it was hard to digest having a matter that is non-luminous and does not interact with anything but gravity, whose purpose is to just stay in galaxies and bind them like glue. Later, Kahn and Woltjer 1959 studied the motion of the Andromeda galaxy and argued that the motion of Andromeda towards us suggests that there must be dark matter in our local group of galaxies. The presence of enormous halos around galaxies was suggested by Roberts and Rots 1973 and Rubin et al. 1978. In 1974, two more studies were done by Ostriker et al. 1974 and Einasto et al. 1974 that firmed up the idea of the presence of non-luminous matter in the galaxies and showed that the masses of stars and the light present in galaxies are not enough to explain the dynamics of the galaxies.

1.2 Observational evidences of the presence of dark matter

Here, some of the evidences for the presence of dark matter are given below at different galactic scales that strongly demand the existence of dark matter to explain the physics at different scales.

1.2.1 Rotational curves

The gravitational effects of spiral galaxies are one of the primary sources of evidence for the presence of dark matter. Most of the visible matter is contained as a bulge on a disc. Using Gauss' theorem, the velocity of the star at the distance R from the centre of the galaxy can be given as

$$v = \sqrt{\frac{GM}{R}}, \tag{1.1}$$

where M is the visible mass inside the sphere (Gaussian surface). As R increases or one moves away from the centre of the galaxy, the visible matter fades away, therefore total mass inside the Gaussian surface remains constant. Consequently, the velocity of stars must fall as $v \propto \sqrt{\frac{1}{R}}$. In contrast, the velocity of stars away from the centre of the spiral galaxies shows flat rotational curves, indicating constant velocity. For the constant velocity v_c of the outer

stars of spiral galaxies. The total mass inside the sphere of radius R can be given as

$$M = \frac{Rv_c^2}{G}, \tag{1.2}$$

which indicates a continuous increment in the mass of the galaxy far beyond the region where the visible matter starts to fade away. Consequently, it indicates that there must be more matter inside the spiral galaxies than the visible matter; otherwise, the shape of the galaxies would be different than observed. If one assumes a spherically symmetric distribution of invisible matter, the density needed for producing flat rotation curves can be given by

$$\rho = \frac{v_c^2}{4\pi G R^2}. \tag{1.3}$$

The presence of invisible matter is required to hold the galaxies in the shape they are. This invisible matter is called dark matter. By analyzing the rotation curves of galaxies, astronomers can estimate the amount of dark matter present in a galaxy and its distribution.

1.2.2 Galaxy clusters

Galaxy clusters contain massive quantities of gases in the intergalactic medium, and they are huge in size. The gases in the intergalactic medium can accelerate due to gravity, reach very high velocities, and emit X-rays, which are analysed together with the modeling of the galaxy clusters and used to calculate the mass of the galaxy clusters. The calculated mass of the galaxy cluster is compared with the visible mass, which indicates that the calculated mass is much more than the visible mass, which indicates that there must be a huge amount of invisible matter or dark matter present in the galaxy cluster. However, this method of calculating the mass of the galaxy clusters is not considered very reliable because it requires the approximate modelling of the galaxy clusters.

The method of calculating the mass of galaxy clusters based on gravitational lensing is considered to be more reliable. The method is based on observing the images of distant objects and reconstructing the modified path of the light due to the presence of heavy masses in the path, affecting the geometry of spacetime. The gravitational lensing of the objects behind a galaxy cluster appears in several distorted images spread across a circle. If D_S

denotes the distance to the source and D_L stands for the distance to the galaxy cluster, then the angular radius, θ, of the circle is given by Einstein 1936

$$\theta = \sqrt{\frac{4GM(Ds - D_L)}{c^2 D_s D_L}} \tag{1.4}$$

where M is the mass of the galaxy cluster. Gravitational lensing is used to calculate the mass of galaxy clusters. Studies have shown that the visible mass contributes to 10-20% of the total mass of the galaxy clusters, while the majority of the mass is contributed by dark matter or invisible matter.

1.2.3 Large and cosmological scales

On large scales, dark matter is inferred from its gravitational effects on visible matter, such as stars and galaxies. Astronomers observe the rotational velocities of stars in galaxies and find that they are moving too quickly to be explained by visible matter alone. This implies the presence of additional, unseen matter, which is thought to be dark matter. Similarly, observations of the cosmic microwave background radiation, the leftover radiation from the Big Bang, provide evidence for the existence of dark matter through its gravitational effects on the structure and evolution of the universe. On cosmological scales, dark matter is also inferred from observations of the large-scale structure of the universe. The distribution of galaxies and galaxy clusters on the largest scales is consistent with the presence of a significant amount of dark matter, which provides the gravitational scaffolding for the visible matter to form galaxies and clusters. Cosmological simulations, which model the growth of structure in the universe, also require the presence of dark matter to reproduce the observed distribution of galaxies. Other indirect evidence for dark matter comes from observations of gravitational lensing, the bending of light by the gravitational field of massive objects. The gravitational lensing of distant galaxies by intervening dark matter halos can be used to infer the distribution of dark matter in the universe. Overall, the evidence for the existence of dark matter on both large and cosmological scales is robust and supported by multiple lines of observation and analysis. While the nature of dark matter remains a mystery, its presence is crucial for our understanding of the structure and evolution of the universe.

Today, much progress has been made, and consequently, the distribution and total amount of dark matter present in galaxies are far better understood than in the 1970s. Some of the studies that contribute to the rapid understanding of the presence of dark matter in galaxies and clusters are cosmic microwave background fluctuations, optical surveys of large areas, high red-shifts, and sharp X-ray images.

The progress in understanding the role of dark matter is not limited to observational research only. Over the years, theoretical aspects of dark matter have also been explored. There are some properties that a good candidate for dark matter has to satisfy, and they are given as follows:

1.3 The properties of dark matter

Although dark matter is unknown and we know almost nothing about it. Nevertheless, physicists have been able to infer some of its properties based on its gravitational effects on visible matter. Following are the properties that a good candidate for dark matter must have in order to be consistent with the observations.

1.3.1 Abundance

Dark matter makes up about 85% of the total matter in the universe, with the remaining 15% being ordinary matter. This means that dark matter is much more abundant than ordinary matter, which is why it has such a profound effect on the large-scale structure of the universe. The abundance of dark matter can also be inferred from the way in which galaxies form and evolve. Computer simulations of galaxy formation show that dark matter plays a crucial role in shaping the distribution of visible matter, as well as in the formation of galaxies themselves. By comparing these simulations to observations of real galaxies, physicists can estimate the abundance of dark matter. Moreover, the abundance of dark matter has been inferred through a variety of indirect methods, including the observation of galaxy clusters, the cosmic microwave background radiation, and computer simulations of galaxy formation. While its

exact nature remains a mystery, its abundance is a testament to its importance in shaping the large-scale structure of the universe.

1.3.2 Electric charge

Due to the fact that dark matter does not interact with light and remains unseen, most of the physics community agrees with the argument that dark matter must be electrically neutral. Otherwise, light would be scattered by it. From astrophysical observations and direct dark matter laboratory experiments, the constraints on heavy millicharged particles are deduced in McDermott et al. 2011; Kouvaris 2013; Dolgov et al. 2013. If millicharged dark matter particles coupled strongly with the baryon and photon plasma during the recombination epoch, then they would act like baryons, and the current cosmic microwave background would be affected in several ways (McDermott et al. 2011; Kouvaris 2013). Depending on the mass of the dark matter particle, Kouvaris 2013 suggests a limit on the charge of dark matter that is $q_{DM} \leq 2.24\times\ 10^{-4}\ m_{DM}$/TeV)$^{1/2}$ for $m_{DM} >> m_p$, while direct detection as suggested by Nobile et al. 2016 gives an upper bound on the charge of dark matter particles as $q_{DM} \leq 7.6\times\ 10^{-4}\ m_{DM}$/TeV)$^{1/2}$.

1.3.3 Cold

Cold dark matter particles are believed to be non-relativistic, i.e., moving at speeds much slower than the speed of light, and to have low kinetic energy, which means they are "cold" in the sense that they have a low temperature. This property of dark matter is inferred from its effects on the large-scale structure of the universe as well as from observations of the cosmic microwave background radiation. Numerical simulations of the formation of structures in the early universe suggest that dark matter particles were non-relativistic at the time when large-scale structures began to form. This means that the particles were moving much slower than the speed of light and were governed primarily by gravity rather than other fundamental forces. This non-relativistic behaviour is consistent with the hypothesis that dark matter consists of particles that interact weakly with other matter and form large-scale structures

through gravitational attraction. The non-relativistic nature of dark matter particles has important implications for their detection and characterization, as well as for the formation and evolution of galaxies and other astrophysical systems.

Hot dark matter would cause inconsistencies with the observations because hot or relativistic dark matter particles can travel a large distance before falling into a potential well, which is also known as the streaming length. However, at the scale of a typical galaxy, the cold dark matter simulation suggests the presence of several sub-structural dark matter halos. Apparently, that can lead to too many subhalos. But this problem can be eased if dark matter is warm and has a mass of approximately 2–3 keV.

1.3.4 Lifetime

Probably one of the most naive observations about dark matter particles is that they are very long-lived, stable particles. The presence of dark matter is necessary for the gravitational effects in galaxies and clusters. If their lifetime were shorter than the age of the universe, then the gravitational effects of dark matter would have been different from the observational findings. The observations of the large-scale structure of the universe and the cosmic microwave background radiation suggest that dark matter has been present since the early universe and has remained unchanged for billions of years. However, some theories propose that dark matter may have a very long but finite lifetime (Audren et al. 2014), which could lead to detectable signals such as the emission of gamma rays or cosmic rays. They must have a decay rate that is longer than the age of the universe to be acceptable.

1.3.5 Self-interaction

The self-interacting property of dark matter refers to the possibility that dark matter particles can interact with each other through a force other than gravity. This is in contrast to the current understanding that dark matter interacts only through gravity, as it does not interact with light or the electromagnetic force.

There is some observational evidence that suggests that dark matter may be self-interacting. One such piece of evidence comes from the observation of colliding galaxy clusters. When two galaxy clusters collide, the dark matter in each cluster is expected to pass through each other due to their lack of electromagnetic interactions. However, simulations of these collisions have shown that the dark matter in each cluster appears to interact with itself, causing it to slow down and become more concentrated in the central region of the collision.

The ellipticity of galaxies and the observational findings put a limit on the dark matter self-interaction, as suggested by Buote et al. 2002; McDaniel et al. 2021 and Randall et al. 2008, respectively. The dark matter-dark matter self-interaction is constrained by σ_{DM-DM}/m_{DM} < 0.47 cm^2/g by Harvey et al. 2015. It is also shown in Tulin and Yu 2018a; Spergel and Steinhardt 2000 that the velocity dependence in σ_{DM-DM} might help solve some small-scale structural problems of the universe. However, the dark matter self-interaction cross-section within the limit σ_{DM-DM}/m_{DM} < 1 cm^2/g is helpful to solve the problem associated with the number of sub-structures in DM halo numerical simulations.

These observations have led to the development of models of dark matter that include self-interactions. Such models could help to explain the observed distribution of dark matter in galaxies and clusters and could have implications for the formation and evolution of these structures. However, the nature and strength of these self-interacting forces of dark matter are still unknown, but they could be due to the exchange of a new particle, such as a dark photon. Ongoing and future observational studies of galaxy clusters, galactic dynamics, and gravitational lensing will provide further insights into the properties of dark matter and its interactions with itself and with ordinary matter.

1.3.6 Non-baryonic

One of the most widely accepted explanations for dark matter is that it is non-baryonic in nature, meaning that it is composed of particles such as neutrons and protons. Baryonic matter accounts for only a small fraction of the total matter in the universe. One of the main pieces of evidence for the non-baryonic nature of dark matter comes from studies of the cosmic

microwave background (CMB), the radiation left over from the Big Bang. Measurements of the CMB show that the amount of baryonic matter in the universe is not sufficient to account for the observed gravitational effects on the large-scale structure of the universe. The non-baryonic nature of dark matter particles is widely accepted among physicists as the most likely explanation for their abundance in the universe. Ongoing experiments and observations will continue to provide clues to the properties of dark matter particles and help shed light on this enigmatic substance that makes up the majority of the matter in the universe.

1.4 Dark matter candidates

There are numerous dark matter models that have been proposed over the years since the presence of dark matter has been suggested in the universe. The list of dark matter candidates is quite long. Here are some of the most established dark matter candidates covered. Although some of the dark matter candidates are considered more promising and preferred over the others, there is no dark matter candidate that qualifies to be the perfect candidate and solves all the problems associated with dark matter. Some of the promising dark matter candidates are given as follows:

1.4.1 Weakly Interacting Massive Particles (WIMPs)

As the name suggests, the main features of this dark matter candidate are that it is massive and interacts very weakly with visible matter. This class of dark matter particles was first proposed by Steigman and Turner 1985. WIMPs are suggested to have a mass of the order of 100 GeV and have a weak scale coupling of about 10^{-2}. Having been born out of the decay of inflation in the early universe, if the WIMPs are in a thermal bath with the other particles, the Boltzmann equation can be solved at a density that is proportional to the inverse of the annihilation cross-section of the WIMPs to find the moment when the WIMPs stop being destroyed or created. This is also known as the "Free Out" epoch of the WIMPs. This density should remain constant in the future. When the dimensional analysis cross-section is inserted into the Boltzmann equation of the early universe, the resulting calculation predicts a

number density of Weakly Interacting Massive Particles (WIMPs) that matches the density inferred from astrophysical observations. This agreement supports the hypothesis that WIMPs constitute a significant fraction of dark matter and provides a valuable tool for exploring their properties and interactions.

1.4.2 Axions

Axions are one of the most promising dark matter candidates. The candidate came from the solution of the strong CP violation problem, and therefore it not only solves the dark matter problem but also the strong CP violation problem. In the quantum chromodynamics (QCD) Lagrangian, there exists a term $F\tilde{F}$, which has a coefficient θ, which could have any value but experiments suggest that the value of θ has to be smaller than 10^{-9}, which is a very strict restriction on the value, also known as fine tuning (Baker et al. 2006). In principle, there is nothing to stop a coefficient from being extremely small, but when a parameter that can take any value is exceptionally close to zero, it raises the question, why? Peccei and Quinn 1977; Weinberg 1978; Wilczek 1978 promoted the coefficient to a dynamic field and suggested that there is a protective global symmetry. When this symmetry breaks, the term has to vanish, and therefore the coefficient must be nearly zero. But breaking the suggested symmetry requires the production of a new particle, and this particle is called 'axion', which is a pseudo-Nambu-Goldstone boson. Sikivie 1982; Preskill et al. 1983; Abbott and Sikivie 1983; Dine and Fischler 1983 give the astrophysics aspects of axions in detail, and the possible production mechanism of axions can be found in (Turner 1990; Raffelt 1990). The axions are naturally non-interacting or very weakly interacting, and are produced as a result of symmetry breaking. A cold bunch of axions can cling together gravitationally and guide the evolution of galaxies, and physicists suspect that axions may have been produced in bulk in the early universe. Thus, axions could be a good candidate for dark matter. The mass of axions has to be extremely small. Indeed, studies suggest that the axions could have mass in the order of a few μeV. It has been suggested by Sikivie 1983; Asztalos et al. 2002 that the axions can be detected in a magnetic field by axion-photon resonance, but axions have not been observed yet.

1.4.3 Neutrinos

Neutrinos, a class of particles that interact very weakly with visible matter, have a very light mass, and they are also considered one of the candidates for dark matter. Fukuda et al. 1998 and Ahmad et al. 2002 did the oscillation experiment of neutrinos, which indicated that at least two of the neutrinos present in the Standard Model are massive. The tritium beta decay experiment suggests that $m_{\nu_e} \leq 2.5$ MeV with 95% confidence. Bonn et al. 2000 and Lobashev et al. 1999 indicate that the astrophysics density of light neutrinos ($m_\nu \leq$ MeV) is supposed to be $\Omega_\nu h^2 = \Sigma m_\nu/(94.0)$ eV, while the WMAP shows that $\Omega_\nu h^2 < 0.0076 \rightarrow \Sigma m_\nu \leq 0.7$ eV. The oscillation experiments force the mass of neutrinos $m_\nu \geq 50$ MeV; therefore, 0.0005 < $\Omega_\nu h^2$ < 0.0076, a known constituent of dark matter, would be non-relativistic today. However, being fermions of this mass window, they cannot be a significant constituent of galaxies due to Pauli blocking. Although Lee and Weinberg 1977 considers massive neutrinos as dark matter candidates, the neutrinos have to be hot, and they cannot be abundant in galaxies. This makes them unsuitable for an ideal dark matter candidate to explain the properties of galaxies.

1.4.4 Sterile neutrino

They are hypothetical particles that are assumed to be interactive only via gravity. They do not interact via any force described in the Standard Model. The term, 'sterile' in the name suggests that they are different 'inert' neutrinos compared to the neutrinos present in the Standard Model. They do not take part in electroweak interactions. Sterile neutrinos have been proposed in different contexts to address different problems (Feng et al. 2003). As a dark matter candidate, it has been claimed that they may have been created in the early universe in a variety of ways, and depending on the mechanism of their creation, they can be constrained by using their effect on the small-scale structure in the universe (Abazajian 2006). It has been claimed in Abazajian et al. 2001 that the sterile neutrinos may mix with active neutrinos and that the probability of their decay into photons and active neutrinos is very low. In particular,

the sterile neutrino inverse-lifetime

$$\tau^{-1} \sim G^2 m_\nu^5 \theta^2, \tag{1.5}$$

where θ is the mixing parameter. Forcing the mixing not to exceed the limit $\theta < 3.3 \times 10^{-4}(\frac{10keV}{m_\nu})^5$, making the lifetime of sterile neutrinos bigger than the age of the universe. The observations have excluded the Dodelson-Widrow model of sterile neutrinos (Abazajian 2006; Abazajian et al. 2001).

1.4.5 Dark photons

The light boson with mass $m_V < 2m_e$ is a viable candidate for dark matter. Dark photons can be stable and may be produced in the early universe via annihilation or scattering processes such as $e^+e^- \rightarrow V\gamma$ or $\gamma e^\pm \rightarrow Ve^\pm$ where V indicates a dark photon. It may also be produced by photon-dark photon resonance. An et al. 2015 showed the production of dark photons via condensate seeded by inflationary perturbations. Dark photons are force carriers in the dark sector, similar to ordinary photons in the visible sector. The light-dark photons (scalar or vector) can be constrained with experiments that depend on their wavelike behaviour or their possible portal with the visible sector.

1.4.6 Neutrons decay into dark matter

Perhaps the newest theory of dark matter is that the neutron might decay into dark matter, as proposed by Fornal and Grinstein 2018a; Fornal and Grinstein 2020. The neutrons show a different lifetime when observed by different methods, such as the beam and bottle methods. Neutrons in a beam have a longer lifetime compared to neutrons in a bottle. In fact, the difference between the two lifetime measurement methods is always approximately 8 seconds. To explain this, Fornal and Grinstein 2018a; Fornal and Grinstein 2020 suggest that neutrons might decay into dark matter in the beam method, making dark matter go undetected (the method uses the number of protons present after a while), while in the bottle method its effect is counted (the method uses the number of neutrons remaining after a while). If we consider

this approach, the neutron decay puzzle seems to get fixed. In this study, this hypothesis has been tested using neutron stars.

1.4.7 Supersymmetry (SUSY) particles

Supersymmetry is the theory that physicists propose in order to fill the gaps in the Standard Model. One can call supersymmetry an extension of the Standard Model. It links the bosons and fermions such that every particle in the Standard Model will have a supersymmetric partner. The supersymmetric partners will interact through forces similar to Standard Model particles. Like many theories, Pagels and Primack 1982 proposed that the light supersymmetric partners of the Standard Model particles are stable, interact weakly, and are neutral in charge. They could therefore stay in the galaxies without being discovered. Some of the promising supersymmtric dark matter candidates are neutralinos, gravitinos, and axinos. They are the supersymmetric partners of neutrinos, gravitons (Feng et al. 2003) and axions (Bonometto et al. 1989). But none of the SUSY particles have been observed yet.

1.5 Cosmological challenges for dark matter

Despite the overwhelming presence of dark matter in the universe, there are still many open questions and challenges to understanding dark matter from a cosmological perspective. Although at the larger scale, at distances bigger than 1 Mpc, the asymmetric cold dark matter model is good for explaining the observed structural properties of the universe, on the smaller scale, there are issues that need to be addressed. Some of the literature regarding this can be found in Zavala and Frenk 2019; Bullock and Boylan-Kolchin 2017. Following are the major challenges for a dark matter model:

1.5.1 Too big to fail problem

There is a discrepancy between observations of dwarf galaxies and theoretical predictions based on the standard model of dark matter. According to the theory, dark matter halos in

which dwarf galaxies form should have a large number of subhalos, or smaller clumps of dark matter, that host satellite dwarf galaxies. However, observations of dwarf galaxies in the local group, which includes the Milky Way and Andromeda galaxies, show a deficit of such satellites compared to the number predicted by the theory. This discrepancy arises because the predicted subhalos are expected to be massive enough to host galaxies, but most of them have not been observed to do so. This has led some to suggest that the standard model of dark matter may not be accurate on small scales and that alternative theories, such as warm dark matter or self-interacting dark matter, may be needed to explain the observed properties of dwarf galaxies. One proposed solution to the too big to fail problem is that the baryonic dark matter in the subhalos may be able to affect the dark matter distribution and disrupt the formation of satellite galaxies. This could occur through processes such as supernova explosions or the heating of gas by radiation from stars, which can drive gas out of the subhalos and alter their density profiles. This would make it more difficult for satellite galaxies to form in the subhalos, and could potentially resolve the discrepancy between observations and theory. Overall, the too big to fail problem highlights the need for a better understanding of the nature of dark matter and the processes that govern the formation and evolution of galaxies on small scales. It remains an active area of research in astrophysics, and cosmology. The n-body simulation of the asymmetric cold dark matter at the galactic scale predicts a higher number of subhalos than are actually found in the galaxy. The masses of such subhalos are so massive that they may create stars but fail to form them, while the lower-mass subhalos are able to form the stars. This problem is known as the too big to fail problem. The solution to this problem is suggested by considering warm dark matter or self-interacting dark matter (Bullock and Boylan-Kolchin n.d.). There are some weak constraints on the dark matter mass and self-interaction suggested by different cosmological simulations. For warm dark matter, the mass of the dark matter particles must be greater than a few KeV, while the self-interaction cross section of the dark matter particles must be in the range 0.5–10 cm^2/g (Tulin and Yu 2018b).

1.5.2 Core vs. Cusp problem

The "core vs. cusp" problem in galaxy formation refers to a discrepancy between observations of the density profiles of dark matter halos and the predictions of the standard model of dark matter. According to the theory, dark matter halos should have a density profile that rises steeply towards the center, forming a cusp-like shape. However, observations of some galaxies suggest that their dark matter halos have a flatter density profile towards the center, forming a core-like shape. The core vs. cusp problem has important implications for our understanding of galaxy formation and the nature of dark matter. If the cusp-like density profile is correct, it would suggest that dark matter interacts very weakly with itself and other matter, and would support the standard model of dark matter. On the other hand, if the core-like density profile is correct, it would suggest that dark matter interacts more strongly with itself or with visible matter and would require modifications to the standard model of dark matter. One proposed solution to the core vs. cusp problem is the idea that the feedback from baryonic matter, such as gas and stars, could modify the density profile of dark matter halos. This could occur through processes such as supernova explosions, which can drive gas out of the central regions of galaxies and reduce the density of dark matter. Alternatively, interactions between dark matter particles, such as self-interacting dark matter, could lead to the formation of a core-like density profile. The core vs. cusp problem remains an active area of research in astrophysics and cosmology, and there is an ongoing debate over the interpretation of observational data and the theoretical predictions of different models of dark matter. Further observations of galaxies and improved simulations of galaxy formation will be necessary to fully understand this problem and its implications for our understanding of the universe. The density profiles predicted by n-body simulations indicate a steep rise in the density of dark matter at smaller radii, while the rotational curves suggest that the density profile remains flat. Indeed, the asymmetric dark matter simulation indicates density $\rho(r) \propto 1/r^{\gamma}$, where γ must be in the range 0.8-1.4, as suggested by Navarro et al. 2010, while the rotational curves indicate that γ must be 0–0.5 for smaller radii. Several solutions to the problem have been proposed, including the effects of baryonic feedback, which can flatten the core to the density suggested by the rotational curves.

1.5.3 Missing satellite problem

The "missing satellite" problem in galaxy formation refers to a discrepancy between the number of observed satellite galaxies in the local group (the group of galaxies that includes the Milky Way and Andromeda) and the number predicted by the standard model of dark matter. According to the theory, dark matter halos should be filled with smaller subhalos, which in turn should host satellite galaxies. However, observations of the local group suggest that there are far fewer satellite galaxies than predicted by the standard model of dark matter. This discrepancy has led to the "missing satellite" problem, which has important implications for our understanding of galaxy formation and the nature of dark matter. The n-body simulation of dark matter halos predicts that at the size of the Milky Way galaxy, there must be thousands of subhalos of dark matter that are massive enough to create galaxies, but observations found that there are only approximately 100 galaxies orbiting the Milky Way. This lack of galaxies indicates that there is something wrong with our approach to dark matter properties on a smaller scale. The missing satellite problem highlights the need for a better understanding of the nature of dark matter and the processes that govern the formation and evolution of galaxies on small scales. It remains an active area of research in astrophysics and cosmology, and further observations and theoretical studies will be necessary to fully understand this problem and its implications for our understanding of the universe.

1.6 Dark matter probes

Since the presence of dark matter came to our knowledge, there have been numerous attempts to understand its nature, both experimentally and theoretically.

1.6.1 Experimental efforts to discover dark matter

There are some laboratories, such as accelerators and colliders, built on Earth to detect any sign of dark matter. The CMS (Compact Muon Solenoid) and ATLAS (A Toroidal LHC ApparatuS) collaborations at the Large Hadron Collider (LHC) are searching for any sign of

dark matter during proton-proton collisions. The basic idea behind their work is that the dark matter particles must have escaped the system, leading to a significant reduction in the total energy and momentum of the system. The collider experiment targets the dark matter models, which suggest that dark matter particles may interact with ordinary particles by the exchange of Z or Higgs bosons, supersymmetric particles, heavy mediators in effective field theories, etc. The experimental detection includes the detection of any invisible particle produced through the mediation of a Standard Model boson and the old searches for invisible particles produced via new particle mediators. Although no signal of dark matter has been detected yet by the LHC, it has been useful in setting limits on cross-sections, couplings, and masses. There are several approaches to searching for dark matter, including indirect detection, direct detection, and collider experiments.

1.6.1.1 Direct dark matter detection

The dark matter density in our solar system is of order 0.4 GeV/cm^3 (Catena and Ullio 2010; Nesti and Salucci 2013; Sivertsson et al. 2018) and the dark matter halo is considered to be relatively non-rotating compared to the rotational disc of the galaxy. Thus, the dark matter particle will have a relative velocity of approximately 200 km/sec. The rotation of our Earth around the Sun will lead to several trillion dark matter particles interacting and passing through Earth each year. The interaction between dark matter particles and the nucleons on Earth will take place through scattering processes. The basic idea is, if dark matter interacts with the nucleons, then measuring the recoil energy of the nucleon can help detect the dark matter particles. There are several detection centers running to search for dark matter particles, but such searches are still limited by our poor understanding of velocity and the density of dark matter in our solar system. Aprile et al. 2017 shows the effects of velocity and density in dark matter detection. Although the sensitivity of detecting dark matter has increased with every passing generation, but such detection techniques are not suitable for the axions like particle because they are extremely light and their recoil energy is extremely tiny, but specific detection experiments can be designed (Graham et al. 2015) for axion like particles interaction with electromagnetic fields.

1.6.1.2 Indirect dark matter detection

This method of dark matter detection is based on the idea of detecting the decay products of dark matter or the possible production of particles by the interaction between dark matter and nucleons. The main decay products, or annihilation products, are photons, protons, electrons, and neutrinos. Photons are relatively easy to detect, while neutrinos are very hard to detect. The indirect detection of dark matter in experiments depends on the type of dark matter one is expected to detect. This type of dark matter detection method is more suitable in regions where the dark matter density is higher. Some of the density profiles of dark matter are presented in Navarro et al. 1996; Merritt et al. 2006; Burkert 1995. If there is a small coupling between dark matter and Standard Model particles, the interaction or annihilation of dark matter particles can result in the production of Standard Model particles. The probability of interaction between dark matter particles depends on their relative velocity and on their annihilation cross section into Standard Model particles. The study by Aguilar et al. 2016 puts very strong constraints on the dark matter annihilation cross sections.

1.6.1.3 Dark matter search in colliders

The high energy particle colliders are designed to study new physics scenarios by colliding particles. The Large Hadron Collider (LHC) may be the most prominent collider designed to study new physics. The basic idea behind the colliders is that the particles at very high energy collide with each other and generate heavy particles, which decay into new particles. Colliders, such as the LHC, have been used to search for dark matter particles indirectly by producing them and observing their interactions with other particles. One approach is to look for missing energy signatures in the detector. If dark matter particles are produced in a collision, they would escape undetected and result in an imbalance in the measured energy and momentum of the collision products. This missing energy could be a potential signature of dark matter. Another approach is to search for the production of new particles that could be the constituents of dark matter. For example, some models of dark matter predict the existence of a particle called a WIMP (weakly interacting massive particle). Colliders can be used to produce and study the properties of these particles. However, detecting dark matter particles

in colliders is challenging because they interact weakly with other particles. This means that the probability of producing dark matter particles is low, and they may escape undetected even if they are produced. Despite these challenges, colliders continue to be an important tool in the search for dark matter. New experiments and detectors are being developed to increase the sensitivity of collider searches for dark matter, and researchers are exploring new theoretical models that could lead to the production of dark matter particles in colliders.

1.6.2 Theoretical efforts to understand dark matter

There are several theoretical efforts to understand dark matter, such as axions, WIMPs, supersymmetry particles, extra dimensions, modified gravity, etc., yet its exact nature and properties remain a mystery. Most of these models have been explained above.

In this study, theoretical models to understand the nature of dark matter have been developed. Although, because of the non-interacting nature of dark matter with ordinary matter, it is very hard to explore it. But as we are aware that dark matter interacts with gravity, it may be that we can study dark matter with the help of objects that are very compact and have the highest order of gravity. The most compact objects in the universe are black holes, their gravity is so huge that even light cannot escape them. Since nothing can escape the black holes, they themselves are a mystery, and physicists do not have a clue about what they are made of. The next most compact objects after black holes are neutron stars. They are super compact and have an escape velocity of about 60% of the velocity of light, and they are often called the astrophysical laboratories of the universe. Luckily, there are some observational constraints on the properties of neutron stars that can be used for the study of dark matter. Therefore, neutron stars could be handy in the study of dark matter.

Neutron stars can capture dark matter particles, which may then settle down in the core. Of course, the capturing of dark matter particles inside the neutron star is a matter of speculation, but there are some mechanisms suggested by authors such as Busoni 2021; Bell et al. 2019; Press and Spergel 1985. In this study, we are not concerned with how dark matter is captured, but we are focusing on whether dark matter is captured inside the neutron stars, how it will

affect their properties, and how much dark matter should be inside the neutron stars to see changes in their properties.

Apart from the dark matter capture theory, neutron stars could also prove extremely useful to test the relatively new hypothesis of neutron decay into dark matter, suggested in Fornal and Grinstein 2018b; Fornal and Grinstein 2020; Strumia 2022. Before moving any further, it will be worthwhile to know and understand some of the most promising properties and constraints on neutron star properties that can be used to study dark matter.

CHAPTER 2

Neutron stars

Neutron stars are very compact objects present in the universe. The extreme conditions inside the neutron star, such as energy density, pressure, and temperature, make them ideal to test the physics under extreme conditions that cannot be created in a laboratory. Therefore, neutron stars are often called astrophysical laboratories.

Neutron stars are special stars that come into existence when an ordinary star of mass in the range of 8-25 solar masses dies (Beck, D.H. 2019). When an ordinary star within the mass range given above runs out of fuel, it cannot sustain itself against gravity, and it collapses. As the core collapses and sends a strong ripple of energy, the outer layers are blown into space in a supernova remnant. In the collapse of the core, electrons and protons present in the core interact together and create neutrons, which is why the collapse of the core becomes a very compact neutron star. The death of an old star leads to the birth of a neutron star. The name of the star is kept because of the fact that it is mostly made of neutrons. It is suggested that a typical neutron star is made of up to 90% of neutrons.

Soon after the discovery of the neutron, the presence of neutron stars was proposed by Baade and Zwicky (Baade and Zwicky 1934). They suggested that a supernova remnant can create an extremely dense, super-tiny object that is mostly made of neutrons. The size of such objects should be very small. In fact, the size should be in the range of just a few kilometers. Being so tiny in size, it is extremely hard to detect such an object. Because of their relatively small size, the possibility of finding them was ignored for almost three decades until 1967, when Bell and Hewish (Hewish et al. 1968) discovered the first pulsar named PSR B1919+21. At that time, pulsars were not recognised as neutron stars, but later, Goldman (Gold 1968) showed that pulsars are nothing but neutron stars rotating extremely fast.

Pulsars have a very strong magnetic field, and their magnetic poles are not aligned with their rotational axis. Therefore, when a pulsar rotates, the radiation coming out of it also rotates with it and sweeps. The rotation of the pulsars is only detected when an observer is in the line of sight of the radiation. To the far observer, the signal is detected as the turning on and off of light as a pulse, which is why they are named pulsars. Sometimes they are also referred to as the light houses of the universe. Based on their pulsating behaviour, pulsars are placed into different categories, such as ordinary pulsars, millisecond pulsars, binary pulsars, and gamma-ray pulsars. Ordinary pulsars have periods ranging from a few milliseconds to several seconds and are typically found in the galactic plane or in supernova remnants. Millisecond pulsars have much shorter periods, typically around 1–10 milliseconds, and are thought to be spun up by the accretion of matter from a binary companion. Binary pulsars are pulsars in orbit around another star, which can be used to test the theory of general relativity and measure the masses of neutron stars. Gamma-ray pulsars are pulsars detected at high energies by space-based gamma-ray observatories, such as Fermi and Integral. In addition to these categories, there are also so-called "anonymous" pulsars that have not been associated with any known astrophysical object or phenomenon. Despite their diverse observational properties, all pulsars are believed to be rotating neutron stars. The detailed studies about pulsars may be found in Graham-Smith 1977; de Groot 1977; Lyne and Graham-Smith 1990.

The extreme conditions of the neutron stars make them very special. Let's go through the most important properties of the neutron stars that might help us find the characteristics of dark matter.

2.1 Gravity

As mentioned earlier, neutron stars are extremely compact. Indeed, their gravity is so huge that they are second only to black holes when it comes to escape velocity. In other words, black holes are the only objects in the universe that are more compact than neutron stars. The neutron stars can have an escape velocity as high as $0.6c$ (c is the velocity of light). So it is very hard for particles other than light to escape them. Due to their gravitational power,

neutron stars might capture some of the dark matter particles so that they stay trapped inside their core and alter the properties of the neutron star. The consequences of having dark matter inside the neutron star core are explored later.

2.2 Mass

Most of the neutron stars have a mass of approximately 1.4 $M_\odot$ but Refs. Ter 5I and Ter 5J Ransom et al. 2005, PSR J1903+0327, and PSR J0437-4715 Champion et al. 2008; Verbiest et al. 2008 all have masses of about 1.7 $M_\odot$ with 95%, confidence limit. The NICER collaboration recently measured the mass of two pulsars, PSR J0030+0451 and PSR J0740+6620. In 2019, the NICER collaboration first measured the mass of PSR J0030+0451 and suggested that it is 1.34 ± 0.15 $M_\odot$ (Riley et al. 2019). In 2021, an updated analysis of the data was released, including additional observations and improved analysis techniques, resulting in a new measurement of the mass of PSR J0030+0451 to be 1.44 ± 0.15 $M_\odot$ (Riley et al. 2021). Similarly, the mass of PSR J0740+6620 was measured by the NICER collaboration in 2019 (Miller et al. 2019), suggesting a mass of 2.14 ± 0.10 $M_\odot$. An updated analysis of the data in 2021 by Miller et al. 2021, including additional observations and improved analysis techniques, confirmed the previous measurement, resulting in a mass of 2.14 ± 0.10 $M_\odot$ for PSR J0740+6620.

It is worth noting that the PSR J0348+0432 pulsar also has a mass just over 2 $M_\odot$ (Antoniadis et al. 2013a), which suggests that the upper limit on the mass of neutron stars is still unknown. Nevertheless, any viable physics model that accounts for high energy densities should predict the maximum mass of a neutron star to be at least 2 $M_\odot$. The determination of the mass of the neutron star has great importance because it brings together nuclear physics and gravity under extreme conditions and gives physicists an opportunity to understand and test their knowledge at higher densities. The mass of a neutron star is determined by the mass function, which is based on the Keplerian parameters. (Tamagaki 1993; Shapiro and Teukolsky 1983; Bahcall 1978)

$$f(M_p, M_c, i) = \frac{(M_c \sin(i))^3}{(M_p + M_c)^2} = \frac{P_b v_1^3}{2\pi G}, \tag{2.1}$$

where P_b is the eccentricity projection of the neutron star's orbital semi-major axis on the line of sight, $x = a_1 \sin(i)$, where i represents the inclination of the orbit and longitude of the periaster (ω_0) and time (T_0). These parameters are related to the mass of a neutron star (M_p) and its partner star (M_c) by Kepler's third law.

2.3 Radius

Compared to other cosmological objects, neutron stars are extremely small. Hence, it is very hard to directly determine their radius. It took 30 years to discover the first neutron star after their prediction. The typical size of a neutron star is 10-14 km (Steiner et al. 2013; Lattimer and Steiner 2014). The radius of a neutron star is measured using the X-ray flux emitted from the neutron star

$$r = \sqrt{\frac{FD^2}{\sigma T^2}}, \tag{2.2}$$

$$R = r\sqrt{1 - 2\frac{GM}{c^2 r}}, \tag{2.3}$$

where R is the radius of the neutron star and 'r' is the effective radius. T represents the surface temperature, and M gives the mass of the neutron star. σ is the Stefan-Boltzmann constant, and F is the X-ray flux radiation of the neutron star. The precision of the measurement of radius by this method greatly depends on the accuracy of the measurement of the surface temperature. If the surface temperature is not accurately known, it may mislead the value of the radius of a neutron star by a huge margin. The authors Steiner et al. 2013 and Lattimer and Steiner 2014 suggested that the neutron stars can have radii in the range 10.4 km to 12.9 km.

The other method to measure the radii of neutron stars uses gravitational lensing around the neutron stars. The method of using gravitational lensing is said to be more accurate with better equipment in the future. It is worth noting that in the surface temperature method, if the surface temperature of a neutron star is not uniform, it may lead to an error of up to 50%.

2.4 Spin

Neutron stars are one of the fastest rotating objects in the universe. Neutron stars typically rotate with angular frequencies of 600–700 rotations per second. This incredible rotational spin of neutron stars is achieved by the conservation of angular momentum. The progenitor stars are massive in size and have a low angular frequency, while the neutron star born after the core collapse of such a massive star, due to conservation of angular momentum, rotates with much higher angular frequencies. The fastest rotating neutron star found is PSR J1748-2446ad (Hessels et al. 2006) which rotates at a frequency of 716 Hz. Typically, neutron stars have a very high magnetic field, of the order of 10^{12}-10^{15}G. Due to the loss of energy (mass) in the form of electromagnetic radiation, it is expected for neutron stars to spin down over a period of time. But this is not observed; rather, neutron stars appear to rotate with constant frequency, and they are often referred to as universal clocks. The general acceptance among physicists is that neutron stars accrete the mass of their companion stars of lower energy density, which increases their spin.

Kaaret et al. 2007 claimed that a neutron star of rotating frequency 1122 Hz has been found, but the observation has not been repeated to confirm the claim and could have errors due to the burst mechanism of burning material. Anyway, the spin of neutron stars puts a weak constraint on the equation of state of neutron stars, and both the frequencies 716 Hz and 1122 Hz are well under the Kepler frequency, which is the maximum frequency a neutron star can have before mass shedding takes place.

2.5 Moment of inertia

The moment of inertia of neutron stars is highly dependent on the stiffness of their equation of state. The moment of inertia of neutron stars is of the order of 10^{36} - 10^{38} kg.m^2 Ruderman 1972. The moment of inertia of the Crab nebula, calculated based on its luminosity, is found in the range 4×10^{37} - 8×10^{37} kg.m^2 by most authors Baym and Pethick 1975; Trimble and Rees 1970; Borner and Cohen 1973. If the moment of inertia and mass of the neutron star were

known with more accuracy, then together they could put a strong constraint on the radius of the neutron star. Recently, in a neutron star binary system, the mass and radius were calculated for EXO 1745-248, mass = 1.4 $M_\odot$ and radius = 11 km; mass = 1.7 $M_\odot$ and radius = 9 km and for 4U 1608-52 mass = 1.8 $M_\odot$ and radius = 10 km (details can be found in Lattimer and Schutz 2005a). Both estimated radii have errors of 1 km. The above measurements are model dependent rather than the actual measurement of the moment of inertia of PSR J0737-6069A. The actual, precise measurement of the moment of inertia remains to be made.

2.6 Neutron star binary system and gravitational waves

Gravitational waves are one of the many predictions of Albert Einstein. He suggested that the presence of compact objects in a binary system may create ripples in the fabric of space-time, which are known as gravitational waves. The gravitational waves carry important information about how the internal structure of the compact objects and the gravitational waves may be affected by the effects of rotations and tides. On August 17, 2017, the LIGO (Laser Interferometer Gravitational-Wave Observatory) and VIRGO (VIRGO Interferometer Gravitational-Wave Observatory) collaborations (Abbott et al. 2017a) detected the first gravitational wave signal from the merger of a neutron star binary system. This observation puts a strong constraint on the equation of state of the neutron stars. The observation indicated that a neutron star of mass 1.4 $M_\odot$ must have tidal deformability in the range 75–580, and the radius of neutron stars must be between 10-14 km.

In a binary system, when the neutron stars are far away from each other, they behave like a point mass, and they orbit each other very slowly. When they come close to each other. Gravitational waves typically transmit important information about the inside matter of neutron stars when the distance between them is comparable to the radii of the stars. At this time, the internal structure of the neutron stars is quite relevant. Each neutron star's tidal field induces a mass-quadrupole moment on the neighbouring object.

Tidal deformability, which is determined by the tidal Love number and depends on the equation of state of the neutron star, is proportional to the induced quadrupole moment in

relation to the external tidal field. The tidal deformability is given by,

$$\Lambda = -Q_{ij}/\epsilon_{ij}, \tag{2.4}$$

and in terms of the tidal Love number

$$\Lambda = \frac{2}{3}k_2\Big(\frac{c^2R}{GM}\Big)^5, \tag{2.5}$$

where Λ represents the tidal deformability of the neutron star, k_2 gives the second order tidal Love number, where M stands for the mass and R represents the radius of the neutron star.

2.7 Temperature

The surface temperature is useful to understand the characteristic properties of the neutron star, and it may also give insights into the constituents of neutron star matter. The surface temperature of neutron stars is determined by analysing the photons radiating from their surface. Although neutron stars are not perfectly black bodies yet, their spectra are treated as black body spectra. The observational data collected is compared with the luminosity of the neutron star rather than the surface temperature. Because luminosity is directly proportional to the fourth power of the temperature, even a small uncertainty can make a huge difference in the luminosity. In terms of surface temperature T, the luminosity L is given by

$$L = 4\pi R^2\sigma T^4, \tag{2.6}$$

where σ is the Boltzmann constant and R is the observational distance.

2.8 Neutron star cooling

Neutron stars are very hot at the time of their birth. They may have a temperature of the order of $10^{11}K$. But they cool down rapidly, and their cooling primarily depends on the number of nucleons participating in the cooling mechanism. The fastest and simplest mechanism

responsible for neutron star cooling is called the Urca process, which is given as

$$n \rightarrow p + l + \overline{\nu}_l, \quad p + l \rightarrow n + \nu_l. \tag{2.7}$$

The direct Urca process is primarily responsible for neutron star cooling when the neutron stars have a proton content higher than 10% of the total number of particles inside the neutron star. But there are other mechanisms that are active at any given fraction of protons and at any energy density, but the cooling through these mechanisms is very slow. The modified Urca (Lattimer et al. 1991) process is one such mechanism, given as

$$N + n \rightarrow N + p + l + \overline{\nu}_l, \quad N + p + l \rightarrow N + n + \nu_l. \tag{2.8}$$

There are other slow neutron star cooling processes. Bremsstrahlung and Cooper pair formation are possible, depending on the number of baryons taking part in the process. The Bremsstrahlung process is given by

$$N + N \rightarrow N + N + \nu + \overline{\nu}. \tag{2.9}$$

When the temperature of neutron stars falls below a critical temperature, nucleons form a Cooper pair, given as

$$n + n \rightarrow [nn] + \nu + \overline{\nu}, \quad p + p \rightarrow +\nu + \overline{\nu}. \tag{2.10}$$

The presence of different kinds of matter inside the neutron stars may alter their cooling process. The presence of hyperons or strange matter inside the core may produce different spectra and provide insight into the matter present in the core. A more detailed study has been provided in Balberg and Barnea 1998; Takatsuka and Tamagaki 1999; Takatsuka et al. 2006; Nishizaki et al. 2002.

2.9 Core of the neutron star

Neutron stars cover a huge range of energy densities, from the core to the atmosphere. Based on the energy density, the inside regions of the neutron stars can be classified into different regions, such as the atmosphere, crust, and core. For the sake of brevity, only specific

information about the interior of neutron stars is given in this study. The atmosphere is the outermost part of the neutron star, which is only a few millimetres thick, but in a hot neutron star, the thickness of the atmosphere could be tens of centimetres. The electromagnetic radiation spectrum that is created in the atmosphere contains vital data about the surface temperature, magnetic fields, mass, radius, and chemical composition of the matter. At the core of the neutron stars, the energy density could reach up to 10 times the normal nuclear matter density. It is not known with confidence how particles behave at such high energy densities. The core of the neutron star contributes most of its mass, while the radius of the neutron star depends on the crust, or low energy density region. Various authors suggest different matters present at the core of the neutron stars, such as strange quark matter, hyperons, etc. In this study, we have taken into account the three possible cases to model the core of the neutron stars, i.e., hyperons, strange matter, and nucleons only. The details of the models are given in later chapters.

2.9.1 Meson condensation

Bahcall and Wolf 1965 suggested that the core of neutron stars might contain mesons (pions). Generally, the Bose-Einstein condensation of mesons (pions) in nuclear matter is restricted by the repulsion among the nucleons. However, excitation of pion like quasi-particles in a superdense medium, may occur (Sawyer 1972; Scalapino 1972; Migdal 1977) and condense, with loss of transition invariance. Studies have shown correlations among nucleons and a possible condensation of pions.

The creation of kaons may take place in the core as

$$e + N \rightarrow K^{-} + N + \nu_e, \tag{2.11}$$

and

$$n + N \rightarrow p + K^{-} + N, \tag{2.12}$$

where N stands for a nucleon, and the presence of nucleons ensures that the process satisfies conservation of energy and momentum in a highly dense medium. In 1980 (Kaplan and

Nelson 1988) it was suggested that the Bose condensation of kaons may take place when densities exceed three times the density of nuclear matter. The process is also explained by Ramos et al. 2000.

The condensation of mesons is also suggested by Kolomeitsev and Voskresensky 2003 using strong interactions. The K-meson condensation relies on the presence of hyperons and affects the properties of the nuclear matter. The first and second order phases of transition depend on the strength of attractive forces between kaons and nucleons, and the occurrence of any kind of suggested condensation softens the equating of state at the core at higher energy densities.

2.9.2 Deconfined quarks

Quarks make hadrons, and the degrees of freedom of quarks may have significant effects on the properties of nuclear matter at higher energy densities. At lower energy, a single quark is never observed in a free state. Quarks are always bound to other quarks, which is also called quark confinement. The force among the quarks grows at low energy (Dremin and Kaidalov 2006). But as the energy density increases, the baryons may decompose into quarks. The authors Ivanenko and Kurdgelaidze 1965 displayed that at the core of neutron stars, deconfined quark matter may exist. The properties of non-interacting quark matter were calculated using quantum chromodynamics (QCD) with perturbation theory, but the calculations (Collins and Perry 1975; Kurkela et al. 2010) were limited to higher energy densities $>>$ 1 GeV/fm^3, and it is not likely for the chemical potential of particles at the core of neutron stars to reach this value. Later, some other theories were presented to explore the properties of compact stars. The authors Blaschke et al. 2009 displayed some phase transitions at different energy density regions inside the neutron stars.

All known models of neutron stars have some drawbacks, and none of them is perfect. Quark and baryon phase transition models lack self-consistency, which is very important. The calculations are done with the use of perturbation theory at relatively low energy densities, and the calculations indicate phase transitions at energy densities that seem unrealistic.

2.9.3 Possibility of mixed phases

As the name indicates, in this phase, two more different phases can coexist in the form of droplets. Iosilevskiy 2010 and Glendenning 1992 have discussed the possible existence of such phases inside compact objects like neutron stars. Since the structure of matter is calculated by balancing surface tension (at the edge between droplets), energy density, kinetic energy of ingredient particles, and electrostatic energy, the existence of such a phase is theoretically possible under the assumption that the electric charge of one transition phase is counterbalanced by the other coexisting transition phase.

It was assumed that the short range strong nucleon-nucleon repulsive force may form a solid core inside the neutron stars (Canuto et al. 1975). Later, it was realised that nucleon-nucleon interaction takes place through the exchange of vector mesons. The more accurate calculations suggested that the repulsive short-distance potential does not crystallize the core.

CHAPTER 3

Recipe to model the dark matter inside the neutron stars

In this study, different candidates for dark matter are being explored with the help of neutron stars. For our purpose, neutron stars can be useful in two ways to study dark matter. First, neutron stars, being super compact, can capture the dark matter that will remain trapped inside them. The presence of dark matter must change its properties, which can be tested against observational constraints. Of course, different properties of the dark matter will affect the neutron stars differently. The second is that, to solve the puzzle of the lifetime of the neutrons, it has been proposed that the neutrons might decay into dark matter. If this is the case, then there must be plenty of neutrons that have decayed inside the neutron star, and neutron stars must have enough dark matter trapped inside to alter the properties of the neutron star, which can be tested like the dark matter capture cases. The details of the different dark matter candidate models have been given in the following chapters. Here, one point is worth noting. That is, the dark matter capture mechanism is not proposed in this study. It has been assumed that the dark matter is captured and settles inside the neutron stars, then how it will behave and what the observable signals of various dark matter candidates could be. The various dark matter capture mechanisms are proposed in Refs. Bell et al. 2020; Busoni 2021; Busoni 2022; Press and Spergel 1985; Bell et al. 2019; Bertone and Fairbairn 2008; Li et al. 2012a

To model neutron stars, it is required to have a dark matter equation of state, a model for the nuclear matter of the neutron stars, and the structural equations for the very compact objects. Since multiple dark matter candidates are explored in this study, it is therefore required to have a separate equation of state for each of the dark matter candidates.

The cases of bosonic or fermionic dark matter as well as neutrons decaying into dark matter have been explored in this study, and the different observable signals have been proposed. An

equation of state is derived for the bosonic dark matter, which is based on the model proposed in Li et al. 2012b; Li et al. 2012a. For fermionic dark matter, the approach suggested in Kouvaris and Nielsen 2015 and Mukhopadhyay et al. 2017 are considered. It is assumed that both of these dark matter candidates have been captured from the dark matter halo and settled at the core of neutron stars.

Next, an equation of state for neutron decay into dark matter is derived, which is based on the hypothesis suggested by Fornal and Grinstein 2018a; Fornal and Grinstein 2020, to solve the neutron decay time anomaly. They suggested that approximately 1% of the time, neutrons decay into dark matter χ and an extreme light ϕ boson.

An equation of state is also formulated based on the hypothesis suggested by Strumia in reference Strumia 2021 to solve the neutron's lifetime puzzle, but unlike the suggestion of Fornal and Grinstein that neutrons decay into χ and ϕ, Strumia suggested the decay of the neutron into three dark matter particles, χ. He claimed that this decay mode successfully satisfies the observable constraints on the maximum mass of the neutron stars and that dark matter does not have to be self-repulsive, unlike the Fornal and Grinstein hypothesis. Strumia assumed that dark matter has a fractional baryon number (i.e., 1/3). The details of these dark matter equations of state are provided in the following chapters.

After having the dark matter equation of state, it is required to model the nuclear matter inside the neutron stars. As mentioned above, neutron stars have extreme energy densities and pressure at the core, which is why modelling neutron stars is a difficult task. In fact, it is a puzzle among physicists to predict physics when the nuclear matter density is several times the normal nuclear matter density. Different physicists have proposed different theories at extreme densities. In this study, the equation of state (EoS) based on the quark meson coupling model has been constructed for modelling the nuclear matter inside the neutron star because it has shown promising results. To include the effects of nucleon structure, Guichon proposed the quark-meson coupling model (QMC) (Guichon 1988a) and suggested a new saturation mechanism for nuclear matter at the quark level. The authors in reference Rikovska Stone et al. 2007a suggested a methodology based on the QMC model to calculate the EoS of cold stellar matter in β equilibrium for a non-rotating neutron star. Since it is not known with

certainty in which form matter exists at the core of a neutron star, equations of state based on nucleons only, hyperons included, and strange matter Rikovska Stone et al. 2007a are taken into consideration.

Apart from the equation of state of nuclear matter and dark matter, it is required to have structural equations. To find the structural equations, TOV (Tolman Oppenheimer Volkoff) equations are very effective and are considered in this study. Since, in this study, it is assumed that the dark matter and the nuclear matter do not interact with each other, the TOV equations have been modified for two non-interacting fluids.

The process of modelling neutron stars containing dark matter inside the core, can be summarized in the following steps:

(1) Supply the equation of state of nuclear matter and dark matter to the pressure differential equation of the TOV equation and integrate them from the center of the star towards the surface.
(2) Integrate the mass differential equation of the TOV equation simultaneously with step (1).
(3) Integrate the tidal deformability equations suggested by Hinderer (Hinderer 2008; Hinderer et al. 2010) from the center to the surface.
(4) Repeat steps (1), (2), and (3) until reaching the surface. The surface is the region of the neutron stars, where the pressure and the energy density become zero.

3.1 Observable constraints on the properties of the neutron stars

Based on observational studies, strict constraints have been imposed on the properties of neutron stars. A good model of neutron stars must satisfy the observed properties of neutron stars in order to be considered realistic. Constraints on the properties of the neutron stars are summarized as follows:

(1) Almost all the neutron stars that have been discovered to date have radii within the range of 10–14 km (typically). Moreover, the discovery of gravitational waves by the collaboration of LIGO and VIRGO (Abbott et al. 2018) indicates that a neutron star of mass 1.4 $M_\odot$ should have a radius of 10–14 km. So, a realistic neutron star model must predict the radius in this range.

(2) Most of the neutron stars discovered to date have masses of approximately 1.4 $M_\odot$, but the discoveries of PSR J1614-2230 of Demorest et al. 2010 and PSR J0348+0432 Antoniadis et al. 2013b with masses of 1.928 $M_\odot$ and 2.01 $M_\odot$ set a lower limit on the maximum mass of neutron stars. A good model of neutron stars must predict the maximum mass of a neutron star to be at least 2 $M_\odot$.

(3) Compared to the radius, the moment of inertia is more sensitive to the equation of state. Lattimer and Schultz in Lattimer and Schutz 2005b showed the moment of inertia values up to an accuracy of 10%. This results in an accurate measurement of pressure and radius. The values that are computed must adhere to Lattimer and Schultz's research.

(4) The tidal deformability and the Love number should be consistent with the empirical analysis Abbott et al. 2017b; Abbott et al. 2019 made on data collected from gravitational wave detection by the LIGO and VIRGO observatories.

Apart from these, there are other observable properties such as the Kepler period, spin, angular momentum, and compactness, but these properties do not impose a strict constraint on the equation of state.

As with other authors, this study avoids working with fast spinning neutron stars that are close to their mass-shedding frequency. The methodology described above only works for non-spinning or slowly spinning compact stars. The method works only for stars spinning at frequencies such that $R\Omega << c$, where R is the radius of the neutron star, Ω is the frequency, and c is the speed of light.

CHAPTER 4

Neutron star matter equation of state

In this chapter, the equation of state (EoS) of nuclear matter inside neutron stars is derived for densities several times the density of normal nuclear matter. The EoS of nuclear matter inside neutron stars is an important theoretical quantity that describes the relationship between the pressure and energy density of the dense matter inside the neutron star. The EoS is particularly important for understanding the structure and properties of neutron stars, as it governs the behaviour of the matter under extreme conditions of density and pressure.

At densities several times the density of normal nuclear matter, the behaviour of the nuclear matter is expected to deviate significantly from the behaviour of normal nuclei. Therefore, to derive the EoS of nuclear matter under these extreme conditions, the quark meson coupling model is selected. The details of the model are given in the following sections:

4.1 Equation of state of nuclear matter

For the equation of state of nuclear matter inside the neutron stars, the quark meson coupling (QMC) model has been adopted. Since it is not known in which form matter exists inside the neutron star core, where the nuclear matter number densities may increase up to 10 times the number density of normal matter, for modelling the nuclear matter inside the neutron stars at such higher densities, three different EoSs have been derived for different types of matter at the neutron star core. The EoSs considered matter at the core of the neutron are, namely, nucleons only, hyperons included, and strange matter. As the names indicate, nucleons only EoS considers only nucleons at higher energy densities, the existence of hyperons or strange matter is not taken into consideration. For the hyperons included in EoS, it is assumed that

at higher energy densities, the nucleons may transform into hyperons, and hyperons may populate the core. For the case of strange matter, it has been assumed that at higher energy densities, the nucleons decompose into quarks, and at the core, deconfined quark matter exists. The strange matter EoS is taken from Ref. Alcock et al. 1986, which is also considered in Urbanec et al. 2013.

4.1.1 Quark Meson Coupling model equation of state

The QMC model was proposed by Guichon, who suggested that the structure of the nucleons might play a significant role in describing the properties of nuclear matter. For determining the structure of the nucleons, it is important to understand the relevant degrees of freedom of hadrons. At first glance, the quark meson coupling (QMC) model and quantum hadrodynamics (QHD) seem to be connected, but in the QHD model, baryons are treated as a point like particles, and the structure of baryons is ignored. But in contrast, the QMC model treats baryons as collections of three quarks confined in a very small region based on the MIT bag model, and these bags of quarks interact with each other through the exchange of mesons. Inside the bag, quarks are confined as color singlet hadrons, and as the energy density increases, nucleons begin to overlap. Therefore, the structure of the hadrons is expected to play a significant role in determining the properties at the higher energy densities. However, a strict restriction on QMC is that quark bags do not overlap.

By considering baryons as bags of massless quarks that are directly related to exchange mesons and modify the motion of the quarks, Guichon proposed a new mechanism for nuclear saturation. The physics of finite nuclei is successfully defined by this model.

The Ref. Guichon et al. 1996 showed that it is possible to find a nuclear Hamiltonian that is consistent with relativity and might be applied at high energy densities, as demonstrated by the Ref. Guichon et al. 2006. A general formalisation of nuclear matter with a mixture of N, Λ, Σ, and Ξ baryons is produced in Ref. Guichon et al. 2006. The QCD simulations indicated that quarks in the baryons are confined by a Y-shaped string and the color attached to the quarks. Outside of this region, a typical non-perturbative medium exists where quarks

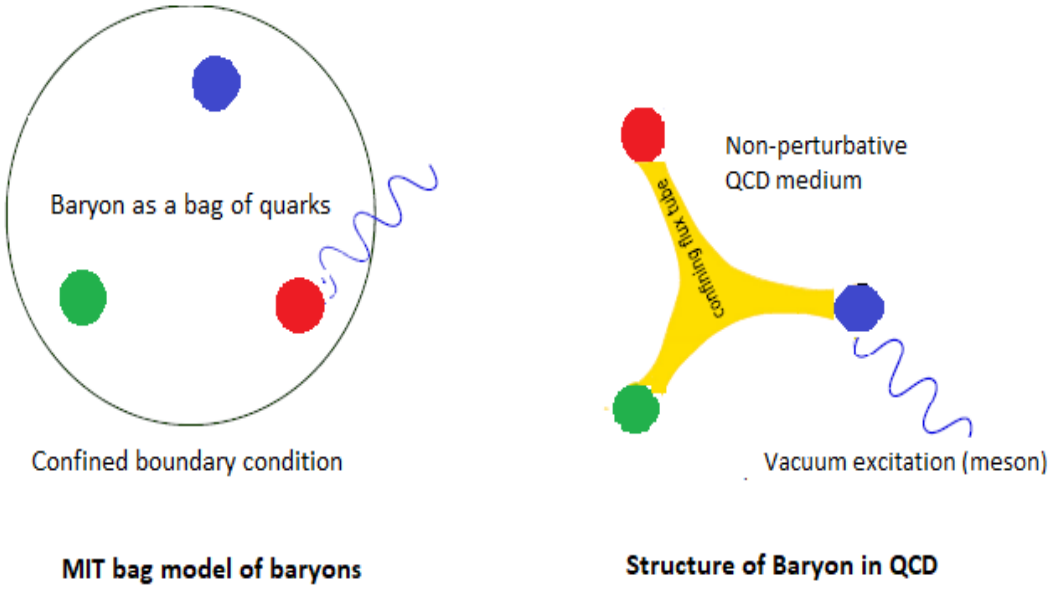

FIGURE 4.1: Structure of baryon in different theories (Rikovska Stone et al. 2007b).

from other hadrons can freely flow, changing the structure of the medium. So, the strict condition of non-overlapping quark bags that restrict quarks from travelling through their boundaries must be considered an average portrayal of a complex situation. The bag's size and boundaries shouldn't be strictly interpreted in terms of their physical meaning. At higher energy densities, we may expect the bags to overlap considerably, and the QMC model may breakdown. Although coupling inside the bag seems unnatural, it is proposed that the more realistic underlying representation of quarks is just attached to the gluon, and in the rest of the non-perturbative volume, nothing prevents quarks from feeling the vacuum fluctuations. To keep the model simple, only σ, ω and ρ mesons are considered.

4.1.1.1 Effective mass and energy

Using the Born-Oppenheimer approximation, Guichon et al. 1996 calculated, for a given position and velocity of the quark bag, the energy of the bag coupled with σ, ω and ρ, in the nuclear mean field associated with them. The quantum numbers of the octet baryons are given in Table 4.1. From the Hamiltonian, classical and canonical quantization give the energy. This work is an extension of the previous QMC model. In the earlier version of the model, it

	p	n	Λ	Σ^-	Σ^0	Σ^+	Ξ^-	Ξ^0
t	1/2	1/2	0	1	1	1	1/2	1/2
m	1/2	-1/2	0	-1	0	1	-1/2	1/2
S	0	0	-1	-1	-1	-1	-2	-2

TABLE 4.1: t is isospin, m is isospin projection, and S is strangeness of octet members.

was limited to nuclear matter and finite nuclei, and the presence of hyperons was excluded, whereas in this study, the hyperons are included and the model has been kept limited to consider the spin $\frac{1}{2}$ SU(3) octet (N, Λ, Σ, Ξ) and baryons are specified by $|f \geq |tms >$ (Table 4.1).

The hypothesis is that strange quarks do not couple with the meson field as a consequence of the fact that the σ, ω and ρ mesons represent the correlated pion exchanges. This is also a major part of the explanation of the observed small spin-orbit splitting in Λ hypernuclei, as the strange quark carries all the spin of the Λ hyperon. It is assumed that the Up (u) and the Down (d) quarks are massless, and the couplings do not violate isospin symmetry. The baryon of flavour f at position $\vec{R}$ (from the centre of the bag) has the energy in the rest frame of the σ field, which can be given by

$$E = \sqrt{P^2 + M_f(\sigma)^2} + g^f_\omega \omega + g_\rho \vec{b}.\vec{I^t}, \tag{4.1}$$

where $M_f(\sigma)$ is its effective mass that is the rest frame energy of the quark bag, $\vec{P}$ stands for the momentum of the baryon, and $\vec{I^t}$ is the isospin operator for the isospin t, defined by

$$< tms|\Sigma_q \vec{\tau_q}/2|t'm's' >= \delta_{(tt')}\delta_{(ss')}\vec{I}^{tt'}_{mm'}. \tag{4.2}$$

Here, the Pauli matrix, $\vec{\tau_q}$ is acting on the u (Up) and d (Down) quarks, b represents the third component of the ρ meson mean field. The flavoured quarks have omega coupling,

$$g^f_\omega = \omega^\omega_f g_\omega = (1 + s/3)g_\omega, \tag{4.3}$$

where g_ω denotes the $\omega - N$ coupling constant. The vector mean field, ω, is linear with the baryon density according to Guichon's research, which is given in Guichon 1988b. The scalar mean field, i.e., the σ field, depends on the source term. The quark wave function

self-consistently adjusts in response to the applied scalar field such that the ω field increases faster than σ field does, when the energy density increases. The structure of the nucleon introduces an effect that opposes the scalar field; therefore, the attractive σ does not increase as fast as the repulsive ω field does. One gets the parameterized mass of the baryon when solving the quark bag equations using the QMC model. The effective mass of a baryon is as follows (see Appendix A)

$$M_f(\sigma) = M_f - \omega_f^\sigma g_\sigma \sigma + \frac{d\tilde{\omega}_f^\sigma (g_\sigma \sigma)^2}{2}, \tag{4.4}$$

where d stands for the scalar polarisability and g_σ represents the σ-N coupling constant in the free space. At the hadronic level, an effective Lagrangian can be constructed, and one may solve the relativistic mean field equations in the usual way Serot and Walecka 1986. The couplings are controlled by the $\tilde{\omega}_f^\sigma$ and ω_f^σ and a first approximation is set to $\tilde{\omega}_f^\sigma = \omega_f^\sigma$ = 1 + s/3. The hyperfine color interaction breaks this relation, and the exact values are given in Rikovska Stone et al. 2007a.

4.1.1.2 Hamiltonian of the nuclear system

By combining the energies of the baryons and the energy held in the meson fields, the total energy of the nuclear system is obtained. If the masses of the mesons σ, ω, and ρ are m_σ, m_ω, and m_ρ, respectively, then the total energy of the system can be given by

$$E_{total} = \Sigma_{j=1}^{n} E_{baryon} + E_{meson} \tag{4.5}$$

$$\begin{aligned} E_{total} = \sqrt{P_f^2 + M_f(\sigma)^2} + g_\omega^f \omega + g_\rho \vec{b}.\vec{I^t} + \frac{1}{2}\int \vec{dr}[(\nabla\sigma)^2 + m_\sigma^2\sigma^2] \\ -\frac{1}{2}\int \vec{dr}[(\nabla\omega)^2 + m_\omega^2\omega^2] - \frac{1}{2}\int \vec{dr}[(\nabla\vec{b})^2 + m_\rho^2\vec{b^2}]. \end{aligned} \tag{4.6}$$

In the hypothesis, meson fields are considered time independent. If $\sigma_{solution}$, $\omega_{solution}$ and $\rho_{solution}$ are the solutions for the σ, ω and ρ meson equations of motion. Therefore, the Hamiltonian of the nuclear system is as follows

$$H(R_x, P_x) = E_t(R_x, P_x, \sigma \to \sigma_{solution}, \omega \to \omega_{solution}, \rho \to \rho_{solution}) \tag{4.7}$$

$$\frac{\delta E}{\delta \sigma} = \frac{\delta E}{\delta \omega} = \frac{\delta E}{\delta b_\alpha} = 0. \tag{4.8}$$

The effective mass depends on scalar σ, ω and ρ meson fields. The σ is non-linear, and it needs to be solved, as Ref. Guichon et al. 2006

$$\sigma = \bar{\sigma} + \delta\sigma \tag{4.9}$$

where $\delta\sigma$ is the small deviation in the σ field and the $\bar{\sigma}$ is the nuclear ground state expectation value in the nuclear system $\bar{\sigma} =< \sigma >$, whereas ω and ρ are linear and can be solved the usual way. As shown in references Rikovska Stone et al. 2007b and Guichon et al. 2006 the Hamiltonian term depending on the σ meson field in terms of the one body kinetic operator ($K(\bar{\sigma})$) is given by

$$H_\sigma = \int d\vec{r}\Big[K(\bar{\sigma}) - \frac{\bar{\sigma}}{2} < \frac{\partial K}{\partial \bar{\sigma}} > + \frac{\delta\sigma}{2}\Big(\frac{\partial K}{\partial \bar{\sigma}} - < \frac{\partial K}{\partial \bar{\sigma}} >\Big)\Big], \tag{4.10}$$

where ($K(\bar{\sigma})$) is the kinetic operator, which depends on the creation ($a_k^\dagger$) and annihilation operators (a_k). If k indicates the momentum of a baryon of flavour f, we have

$$K(\bar{\sigma}) = \frac{1}{2V}\Sigma_{k,k',f} e^{i(\vec{k}-\vec{k'}).\vec{r}}(\sqrt{k^2 + M_f[\bar{\sigma}(\vec{r})]^2} + \sqrt{k'^2 + M_f[\bar{\sigma}(\vec{r})]^2})(a^\dagger_{\vec{k}f} a_{\vec{k'}f}), \tag{4.11}$$

in the mean field approximation, where the meson field variation has to be zero, $\delta\sigma(r) = 0$. The self-consistent solution in a uniform system for a constant $\bar{\sigma}(r)$ field is shown in Guichon et al. 2006,

$$\bar{\sigma}(r) = -\frac{1}{m_\sigma^2} < \frac{\partial K}{\partial \bar{\sigma}} >, \tag{4.12}$$

The scalar meson field $\delta\sigma$ fluctuation is

$$\delta\sigma(\vec{r}) = \int d\vec{r}\frac{d\vec{q}}{(2\pi)^3}\frac{ie^{\vec{q}.(\vec{r}-\vec{r'})}}{q^2 + \tilde{m}_\sigma^2}(-\frac{\partial K(\vec{r})}{\partial \bar{\sigma}} + < \frac{\partial K(\vec{r})}{\partial \bar{\sigma}} >), \tag{4.13}$$

where $\tilde{m}_\sigma$ is the effective mass of the σ meson, which is

$$\tilde{m}_\sigma^2 = m_\sigma^2 + < \frac{\partial^2 K}{\partial \bar{\sigma}^2} > \tag{4.14}$$

The Hartree-Fock approximation is used to calculate the energy density of nuclear matter. The one body kinetic operator and Hamiltonian density are

$$< K(\bar{\sigma}) >= \frac{2}{(2\pi)^3}\Sigma_f \int_0^{k_f} d\vec{k}\sqrt{k^2 + M_f^2(\bar{\sigma})}, \tag{4.15}$$

$$\begin{aligned}\frac{< H_\sigma >}{V} =& < K(\bar{\sigma}) > + \frac{1}{2m_\sigma^2}(< \frac{\partial K}{\partial \bar{\sigma}} >)^2 \frac{1}{(2\pi)^6}\Sigma_f \int_0^{k_f} d\vec{k_1} d\vec{k_2} \frac{1}{(\vec{k_1} - \vec{k_2})^2 + \tilde{m}_\sigma^2} \\ & \times \frac{\partial}{\partial \bar{\sigma}}\sqrt{k_1^2 + M_\sigma^2}\frac{\partial}{\partial \bar{\sigma}}\sqrt{k_2^2 + M_\sigma^2}.\end{aligned} \tag{4.16}$$

Now the potentials for ω and ρ meson exchange Fock contributions need to be constructed, which are

$$\frac{< V_\omega >}{V} = \frac{G_\omega}{2}(\Sigma_f \omega_f^\omega n_f)^2 - G_\omega \Sigma_f (\omega_f^\omega)^2 \frac{1}{(2\pi)^6}\int_0^{k_f(f)} d\vec{k_1} d\vec{k_2} \frac{m_\omega^2}{(\vec{k_1} - \vec{k_2})^2 + m_\omega^2} \tag{4.17}$$

$$\begin{aligned}\frac{< V_\rho >}{V} = & \frac{G_\rho}{2}(\Sigma_{tms} m n_{tms})^2 - G_\rho \Sigma_{tmm's} \vec{I^t_{mm'}} \vec{I^t_{m'm}} \frac{1}{(2\pi)^6}\int_0^{k_F(tms)} d\vec{k_1} \\ & \int_0^{k_F(tm's)} d\vec{k_2} \frac{m_\rho^2}{(\vec{k_1} - \vec{k_2})^2 + m_\omega^2},\end{aligned} \tag{4.18}$$

where G_σ, G_ω, and G_ρ are

$$G_\sigma = \frac{g_\sigma^2}{m_\sigma^2}, \tag{4.19}$$

$$G_\omega = \frac{g_\omega^2}{m_\omega^2}, \tag{4.20}$$

$$G_\rho = \frac{g_\rho^2}{m_\rho^2}. \tag{4.21}$$

In the Hartree-Fock approximation, the total energy includes the contribution of the long range pion exchange in the Fock term only. The authors Serot and Walecka 1986 provides the expression for the impact of long range pion exchange.

$$\begin{aligned}\frac{< V_\pi >}{V} = & \frac{1}{n_B}(\frac{g_A}{2f_\pi})^2 (J_{pp} + 4J_{pn} + J_{nn} - \frac{24}{25}(J_{\Lambda\Sigma^-} + J_{\Lambda\Sigma^0} + J_{\Lambda,\Sigma^+}) \\ & + \frac{16}{25}(J_{\Sigma^-\Sigma^0} + 2J_{\Sigma^-\Sigma^0} + 2J_{\Sigma^+\Sigma^0} + J_{\Sigma^+\Sigma^+}) \\ & + \frac{1}{25}(J_{\Xi^-\Xi^-} + 4J_{\Xi^-\Xi^0} + J_{\Xi^0\Xi^0})).\end{aligned} \tag{4.22}$$

Here $J_{ff'}$ is given by

$$J_{ff'} = \frac{1}{(2\pi)^6} \int_0^{k_F} \int_0^{k'_F} d\vec{p} d\vec{p'} [1 - \frac{m_\pi^2}{(\vec{p} - \vec{p'})^2 + m_\pi^2}]. \tag{4.23}$$

In the above equations, the nucleon's axial coupling constant is $g_A = 1.26$ and the mass of the pion is represented by m_π and the pion decay constant is taken as f_π = 93 MeV. The contact term, J_{ff}, is hard to separate from the short range contributions of heavy mesons, therefore, they are excluded, and only long ranged pion exchange of the Yukawa type is taken into consideration. That is the first term in the brackets on the right hand side of Eq.(4.23). This enforces small changes in the values of parameters G_σ, G_ω and G_ρ which are addressed in the following section.

4.1.1.3 Adjusting the parameters

The masses of the mesons and coupling constants (G_ω, G_ρ and G_σ) need to be fixed. The radius of the free nucleon does not affect the results much. The radius of the nucleon is set to be R_n = 0.8 fm, which gives the optimum results as suggested by Thomas 1984. The masses of mesons such as π, ω and ρ are set to their physical values except for the mass of σ meson. Due to the large $\pi\pi$ resonance width in the physical region, the mass of σ meson is not well known. However, m_σ = 700 MeV is set because it produces the best results, as indicated by the authors in Guichon et al. 2006. Anyway, in the case of modelling the neutron stars, the mass of σ meson is not very important because it mainly affects the nuclear surface. G_ω, G_ρ and G_σ are adjusted to reproduce the asymmetry and the binding energy at the saturation point for the symmetric nuclear matter. First, the contributions of pions are taken as 0. The coupling constants are adjusted in such a way that they produce the asymmetry energy, a_s = 30 MeV, and binding energy, E = - 15.865 MeV, of nuclear matter at saturation point, which is taken to be 0.16 fm^{-3}. The values of these coupling constants are stated in Table 4.2.

Model	$m_\sigma(MeV)$	π_n	$E(MeV)$	$G_\sigma(fm^2)$	$G_\omega(fm^2)$	$G_\rho(fm^2)$	$K_\infty(MeV)$
QMC700	700	0	-15.865	11.33	7.27	4.56	340

TABLE 4.2: Final coupling constants after the fixation.

In the above Table 4.2, the column π_n is the number by which the pion contribution is multiplied. E denotes the binding energy of symmetric nuclear matter, and K_∞ represents incompressibility. The values acceptable for K_∞ for the QMC700 model range from 200 MeV to 300 MeV, while the value shown in Table 4.2 for K_∞ is clearly above the acceptable values. For the purpose of fixing that effect of the Fock term is included. This depends weakly on the density at saturation point, roughly as $\rho^{1/6}$, and when the contribution of the pions is included in the Fock term, the incompressibility reduces to 322 MeV.

4.1.2 Neutron star matter

The cold nuclear matter inside the neutron star is expected to be in β equilibrium. In this study, it is considered that the nuclear matter inside the neutron star is made from octet baryons, electrons, and negative muons. Any kind of octet baryon, including hyperons, may develop inside the core through weak interactions among the nuclear matter particles.

The expression for the total energy density is simply the addition of the energy density of baryons ϵ_B, energy density of electrons ϵ_{elec}, and the energy density of the muon ϵ_μ.

$$\epsilon = \epsilon_B + \epsilon_{elec} + \epsilon_\mu, \tag{4.24}$$

at the state of equilibrium, the energy has to be minimal, the baryon number must be conserved, and the total electric charge must be zero as the nuclear matter at the interior of the neutron stars is neutral. Therefore, the contribution of the baryonic matter energy density term can be given by

$$\epsilon_B = \frac{< H_\sigma + V_\omega + V_\rho + V_\pi >}{V}. \tag{4.25}$$

Here, the terms on the right hand side of the equation (4.25) have been defined above from the equation (4.16) to (4.22). The pressure due to baryons (P_B) is

$$P_B = n_B^2 \frac{\partial}{\partial n_B}\Big(\frac{\epsilon_B}{n_B}\Big), \tag{4.26}$$

and the expression for the incompressibility modulus (K_∞) is

$$K_\infty = 9\frac{\partial P_B}{\partial n_B}, \tag{4.27}$$

where n_B = $\Sigma_f n_f$ and the derivative with respect to n_B is taken at a constant fraction,

$$\frac{n_f}{n_B}, f = 1, 2, ...8. \tag{4.28}$$

The energy density of the gas of leptons can be calculated by the Fermi expression

$$\epsilon_l = \frac{2}{(2\pi)^3}\int_0^{k_{f(l)}} d\vec{k}\sqrt{k^2 + m_l^2}, \tag{4.29}$$

where m_l represents the mass of the lepton and the number density of the leptons (n_l) is

$$n_l = \frac{k_f^3(l)}{3\pi^2}. \tag{4.30}$$

Nuclear matter in the neutron star is expected to be neutral. Therefore, at equilibrium, by using the Lagrangian multiplier method

$$\delta[\epsilon_B(n_p, ..) + \epsilon_e(n_e) + \epsilon_\mu(n_\mu) + \lambda(\Sigma_f n_f - n_B) + \nu(\Sigma_f n_f q_f - (n_e + n_\nu))] = 0, \tag{4.31}$$

where (λ, ν) are Lagrangian multipliers and q_f stands for the charge of flavour f. Equation (4.31) is the deviation of energy using the Lagrangian multipliers, λ and ν.
The chemical potentials of the particles are defined as

$$\mu_f = \frac{\partial \epsilon_B}{\partial n_f}, \mu_l = \frac{\partial \epsilon_l}{\partial n_l} = \sqrt{k_f^2(l) + m_l^2}. \tag{4.32}$$

Plugging the chemical potentials of the particles into Equation (4.31) at the equilibrium condition, one gets

$$\mu_f + \lambda + \nu q_f = 0, \tag{4.33}$$

$$\mu_e - \nu = 0, \tag{4.34}$$

$$\mu_\mu - \nu = 0, \tag{4.35}$$

$$\Sigma_f n_f - n_B = 0, \tag{4.36}$$

$$\Sigma_f n_f q_f - (n_e + n_\mu) = 0, \tag{4.37}$$

The Lagrangian multipliers μ and ν have to be eliminated in order to solve equations (4.33-4.37). From the above equations, clearly $\mu_\mu = \mu_e$, which is

$$k_f(\mu) = R\sqrt{k_f^2(e) + m_e^2 - m_\mu^2}, \tag{4.38}$$

where R shows the real part. Since $m_\mu > m_e$ the electron enters first in the system, and as the electron density vanishes, the muon density also vanishes rapidly. The method to solve the system of equations (4.31) - (4.37) is provided by Rikovska Stone et al. 2007a. The relative densities of the particles are

$$X = [x_i] = [\frac{n_p}{n_B}, \frac{n_n}{n_B}, \frac{n_\lambda}{n_B}, ..., \frac{n_e}{n_B}, \frac{n_\mu}{n_B}]. \tag{4.39}$$

Every element is found by varying ϵ with $\rho_i = x_i n_B$. When the solution of X_0 is found at some value of n_B, the value of density is increased by an infinitesimally small value, Δn, to know if the cut off density of some particle has been reached. If the cut off density has crossed, that means the new particle has been populated in the system, and it should be taken into account. To verify if a particle has been populated, the energy density of the particle must change the sign below and across the cut off value, if it does change the sign, that means the new particle has been populated. The same procedure is followed for all the particles, and if the condition is met, that means all such particles have appeared and must be included in the system of equations. The system of equations is solved numerically by considering the first approximation of X_0 at the density and increasing it by a small value ($n_B = n_0 + \delta n$). If a certain concentration drops below some value, that is selected to measure the accuracy of the solution, θ, that means the concerned equation is removed from the system. The authors Rikovska Stone et al. 2007a selected the accuracy, $\theta = 10^{-4}$ and verified that $\theta = 10^{-3}$ provides the same results. The system of equations is solved by selecting the initial value $n_B = 0$ for pure neutron matter. The total energy density at equilibrium is calculated after finding the solution at equilibrium ($X(n_B)$) for a selected range of baryon densities. The total pressure ($P(n_B)$) of the system is the sum of the pressures due to leptons and baryons. At equilibrium, total pressure is

$$P(n_B) = n_B^2 \frac{d}{dn_B} \frac{\epsilon(n_B)}{n_B}. \tag{4.40}$$

At the center of the star, where the energy density is several times the nuclear matter energy density, while in the atmosphere, the energy density is comparable to the energy density of terrestrial iron. As one moves further towards the center of the neutron star, the region is supposed to be made of unbound protons, electrons, neutrons, and muons because the atoms will decompose into their constituent elementary particles. As the energy density increases further towards the core of the neutron stars as the threshold for the heavier baryons is reached, they may populate the neutron stars. It has been suggested in various studies Arnett and Bowers 1977; Pandharipande 1971; Balberg et al. 1999; Wiringa 1993 that if energy density is high enough, heavier mesons and strange baryons might populate the system. At the crust, where the baryon number density is expected to be lower than the core when the baryon number density is 0.75 times the density of nuclear matter, nucleons are arranged on a lattice along with neutrons and electron gas. Effective interaction (non-relativistic Skyrme, relativistic mean field) was presented as a method for creating a nucleon-based equation of state in Akmal et al. 1998 Chabanat et al. 1998 to energy densities corresponding to the maximum mass of a neutron star.

4.1.2.1 Parameterized equation of State (EoS) of nuclear matter

For convenience, two parameterized EoSs are given below, one for the nucleons only and the other including hyperons. The parameters of both EoSs are given in Table 4.3. The N-QMC700 is the equation of state for nucleons only matter, while the F-QMC700 equation of state includes hyperons at higher energy densities.

$$P = \frac{N_1 \epsilon^{p1}}{1 + e^{(\epsilon - r)/a}} + \frac{N_2 \epsilon^{p2}}{1 + e^{-(\epsilon - r)/a}}. \tag{4.41}$$

The parameters work well in the energy density range of 0 to 1300 MeV/fm^3.

	N_1	p_1	N_2	p_2	r	a
N-QMC700	0	0	0.008623	1.548	342.4	184.4
F-QMC-700	0.0000002.62	3.197	0.0251	1.286	522.1	113

TABLE 4.3: Table for parameters

For the strange matter neutron stars the EoS state suggested by Alcock et al. 1986 is taken into consideration. This strange matter EoS is given by

$$P = \frac{1}{3}(\epsilon - 4B). \tag{4.42}$$

The EoS is based on the MIT bag model (Chodos et al. 1974) of nucleons, and B is the bag constant, where the value of B is 10^{14}gm/cm^3 as suggested by the author. The EoS suggests the deconfinement of the quark at the core of the neutron stars, where the energy density is several times the energy density of the nuclear matter. However, this EoS only considers colour singlet baryons and does not take strange quarks into consideration (Akmal et al. 1998). This EoS works very poorly in the lower energy density region, which is very important for calculating the radius of the neutron star. Therefore, in the lower energy density regions, nucleon only EoS is used in the region below 300 MeV/fm^3. As displayed by the authors Husain and Thomas 2020, the lower energy density regions are very sensitive to the EoS to determine the properties of the neutron stars. Furthermore, for the sake of better results and accuracy, the Baym-Bethe-Pethick (BBP) EoS Baym et al. 1971 has been used in the region, where the energy density is below 100 MeV/fm^3.

CHAPTER 5

Bosonic and fermionic dark matter EoS

Since the nature of dark matter is not known and we know that all the particles that exist in the universe have either an integer spin (bosons) or (a multiple of) spin 1/2 (fermions), based on our knowledge of particle physics, it may be assumed that the dark matter particles must also have a 1/2 or integer spin. Therefore, in this chapter, dark matter has been classified as fermionic or bosonic. The EoS for bosonic and fermionic dark matter are constructed separately.

5.1 Bosonic dark matter EoS

On general grounds, we know that all bosons must condense below some critical temperature, and must occupy a single quantum ground state. Below the critical temperature, the wavelengths of the dark matter particles overlap, and they are related to each other. In this state, the mean inter-particle distance of the dark matter particles is smaller than the thermal wavelength of the dark matter particles. If the dark matter particles have mass m_χ, scattering length l_χ, and energy density ϵ_χ then the critical temperature for Bose-Einstein condensation to occur must be $T_{cr} = \frac{2\pi l_x}{m_\chi^{5/3} k_B} \epsilon_\chi^{2/3}$, where k_B is Boltzmann's constant. For constructing the bosonic dark matter equation of state, the approach suggested by Li et al. 2012a is adopted. Assuming dark matter consists of a dilute gas of bosonic dark matter particles at an absolute temperature of 0 $^\circ K$, then the dark matter particles must condense. Since the dark matter particles are cold and dilute, only binary collisions of the particles will be relevant, and they can be categorized by using only a single parameter, which is the scattering length of the dark matter-dark matter particles. The interaction potential of the particles will be $V_I = \theta\delta(\vec{r'} - \vec{r})$

(effective potential). Here θ is the coupling constant, which can be given in terms of scattering length, l_χ as $\theta = 4\pi l_\chi/m_\chi$ (Dalfovo et al. 1999). The Gross-Pitaevskii equation (GP) is used to describe the ground state properties of dark matter particles. The energy function of the dark matter particle can be written as (GP equation)

$$E = E_{kinetic} + E_{gravitational} + E_{interaction}, \tag{5.1}$$

$$E = \int (\frac{1}{2m_\chi}|\nabla\psi|^2)\vec{dr} - \frac{1}{2}m_\chi^2 \int\int \frac{|\psi|^2|\psi'|^2}{|\vec{r}-\vec{r'}|}\vec{dr}\vec{dr'} + \int \frac{U_0}{2}|\psi|^4\vec{r}, \tag{5.2}$$

where $\hbar = G = 1$, ψ and ψ' are the condensate wave functions, which are functions of $\vec{r}$ and $\vec{r'}$. The value of U_0 should be $4\pi l_\chi/m_\chi$, as shown by the author Dalfovo et al. 1999. The condensate dark matter mass density in terms of the condensate wave function will be

$$\rho_\chi(\vec{r}) = m_\chi|\psi(\vec{r})|^2 = m_\chi\rho(\vec{r},t). \tag{5.3}$$

A small change in the energy of the system can be given as

$$\delta E = \mu\delta N, \tag{5.4}$$

where N is the total number of dark matter particles, μ stands for the chemical potential of the particle, and the normalization condition $N = \int |\psi|^2\vec{dr}$ is considered in this work. The equation (5.2) takes the form

$$-\frac{\nabla^2\psi(\vec{r})}{2m_\chi} + m_\chi V(\vec{r})\psi(\vec{r}) + U_0|\psi(\vec{r})|^2|\psi(\vec{r})| = \mu\psi(\vec{r}). \tag{5.5}$$

Time dependent gravitationally trapped Bose-Einstein condensate dark matter satisfies the GP equation

$$i\frac{\partial}{\partial t}\psi(\vec{r},t) = -\Big[\frac{\nabla^2}{2m_\chi} + m_\chi V(\vec{r}) + U_0|\psi(\vec{r,t})|^2\Big]\psi(\vec{r},t). \tag{5.6}$$

Using the wave function in terms of action, S, as suggested by the authors in Dalfovo et al. 1999; Duine and Stoof 2004; Pethick and Smith 2008 as

$$\psi(\vec{r},t) = \sqrt{\rho(\vec{r},t)}e^{iS(\vec{r},t)}, \tag{5.7}$$

the decoupled form of equation (5.6) we get

$$\frac{\partial \rho}{\partial t} + \nabla.(\rho_\chi \vec{v}) = 0, \tag{5.8}$$

$$\rho_\chi[\frac{\partial \vec{v}}{\partial t} + (\vec{v}).\nabla]\vec{v} = -\nabla P_\chi - \rho_\chi \nabla(\frac{V}{m_\chi}) - \nabla V_Q. \tag{5.9}$$

Finally, the pressure of the dark matter condensate in terms of the scattering length will be

$$P_\chi = \frac{2\pi\hbar l_\chi}{m_\chi^3}\epsilon_\chi^2, \tag{5.10}$$

where the potential, V_Q, is taken to be $-(\hbar^2/2m_\chi)\nabla^2\sqrt{\rho}_\chi/\sqrt{\rho}_\chi$ and $\vec{v}$ is $\nabla S/m_\chi$. More details can be found in Li et al. 2012a. The pressure of dark matter is directly proportional to the self-interaction scattering length of the dark matter. The weakly self-interacting dark matter may cause the neutron star to collapse quicker.

5.2 Asymmetric fermionic dark matter (AFDM) EoS

If the dark matter is fermionic, then unlike bosonic dark matter, all fermionic dark matter particles can't be in the ground state due to Pauli's exclusion principle. The fermionic dark matter particles must exert a degeneracy pressure. For the self-interacting dark matter particle, one must include an extra term in the equation of state for the self-interaction. For the EoS of self-interacting asymmetric dark matter, the approach suggested in Kouvaris and Nielsen 2015; Mukhopadhyay et al. 2017 is considered. The EoS of the AFDM can be given in simple terms, as

$$\epsilon_\chi = \epsilon_{kin} + \epsilon_{int}, \tag{5.11}$$

$$P = P_{kin} + P_{int}, \tag{5.12}$$

where the first term (sub kin) indicates the energy density and pressure of the non-interacting dark matter, while the second term (sub int) comes from the self-interaction of the dark matter. The value of ϵ_{kin} originates from the kinetic energy of all the fermions occupying different energy states in the Fermi sea up to the Fermi level. Hence, the energy density of dark matter

can be given by ($\hbar = 1, c = 1$)

$$\epsilon_{kin} = \int_0^{p_f} E n_p d^3p = \int_0^{p_f} \sqrt{p^2 + m_\chi^2} n_p d^3p, \tag{5.13}$$

where $n_p d^3p$ represents the number of dark matter particles with momentum in the range $\vec{p}$ and $\vec{p}$+$\vec{dp}$. The pressure, which is the force per unit area, can be given as

$$P_{kin} = \frac{1}{3}\int_0^{p_f} \frac{p^2}{\sqrt{(p^2 + m_\chi^2)}} n_p d^3p. \tag{5.14}$$

The factor 1/3 at the front comes because, on average, approximately 1/3 of the particles are moving in a particular direction. The number density, n_χ is

$$n_\chi = \int_0^{p_f} n_p d^3p = \frac{8\pi p_f^3}{3}, \tag{5.15}$$

where degeneracy = 2 has been taken because dark matter particles are fermions. For simplicity, let us set $x = \frac{(3\pi^2 n_\chi)^{1/3}}{m_\chi}$, the dark matter number density becomes

$$n_\chi = \frac{x^3 m_\chi^3}{3\pi^2}, \tag{5.16}$$

with the help of the above equation of number density, on integration, the pressure given in equation (5.14) and the energy density given in equation (5.13) become

$$P_{kin} = m_\chi^4 \phi(x), \tag{5.17}$$

and

$$\epsilon_{kin} = m_\chi^4 \alpha(x), \tag{5.18}$$

where the functions $\phi(x)$ and $\alpha(x)$ are

$$\phi(x) = \frac{1}{8\pi^2}(x\sqrt{1+x^2}(2x^2/3 - 1) + \log(x + \sqrt{1+x^2})), \tag{5.19}$$

$$\alpha(x) = \frac{1}{8\pi^2}(x\sqrt{1+x^2}(1 + 2x^2) - \log(x + \sqrt{1+x^2})). \tag{5.20}$$

For introducing the interaction among the dark matter particles, an approach similar to vector meson exchange in the hadronic matter is adopted. Let the mass of the dark matter mediator be m_I, this is the particle being exchanged by the dark matter particles and responsible for

the dark matter self-interaction. The Lagrangian for the system can be written as

$$L = -\frac{1}{4}F^{\mu\nu}_{\mu\nu} + \frac{1}{2}m_I^2 A_\mu A^\mu - j_\mu A^\mu. \tag{5.21}$$

The equation of motion

$$(\partial_\nu \partial^\nu + m_I^2)A^\mu = j^\mu, \tag{5.22}$$

which has the solution given by Yukawa potential, V_Y as

$$V_Y = g^2 \frac{e^{-m_I r}}{4\pi r}, \tag{5.23}$$

where g is the coupling constant. To calculate the total energy of the self-interacting system of particles, the sum of all the pairs of particles is performed, and for simplicity, any correlation among particle positions is neglected. The potential energy between two particles can be written as

$$V_{potential(i,j)} = g^2 \frac{e^{-m_I r}}{4\pi r}. \tag{5.24}$$

The total potential energy of all the pairs of particles is

$$E_{total} = \frac{1}{2} n_\chi^2 g^2 \int\int \frac{e^{-m_I r_{i,j}}}{4\pi r_{i,j}} d\Omega_i d\Omega_j, \tag{5.25}$$

integrating over the system (upper limit infinity) considering one particle at the origin. One gets

$$E_\Omega = \frac{1}{2m_I^2} n^2 g^2 \Omega. \tag{5.26}$$

Now, we have the total interaction energy. The energy density of the dark matter self-interaction can be found by

$$\epsilon_{int} = \frac{E_\Omega}{\Omega} = \frac{1}{2m_I^2} n^2 g^2, \tag{5.27}$$

using the value of number density given in the equation (5.16). The ϵ_{int} can be given as

$$\epsilon_{int} = \frac{1}{9\pi^4} \frac{x^6 m\chi^6}{m_I^2}. \tag{5.28}$$

Now, the energy density due to the self-interaction of dark matter is known. The pressure due to dark matter self-interaction can be calculated using the relation

$$P_{int} = n_\chi^2 \frac{d}{dn_\chi}\left(\frac{\epsilon_{int}}{n_\chi}\right), \tag{5.29}$$

which is

$$P_{int} = \frac{1}{9\pi^2}\frac{x^6 m_\chi^6}{m_I^2}. \tag{5.30}$$

Therefore, the final equation of state of self-interacting AFDM is found by plugging the values from equations (5.18), (5.17), (5.28) and (5.30) into the equations (5.11) and (5.12). One gets

$$\epsilon_\chi = m_\chi^4 \alpha(x) + \frac{1}{(3\pi^2)^2}\frac{x^6 m_\chi^6}{m_I^2}, \tag{5.31}$$

$$P_\chi = m_\chi^4 \phi(x) + \frac{1}{(3\pi^2)^2}\frac{x^6 m_\chi^6}{m_I^2}. \tag{5.32}$$

One needs to use the equations (5.31) and (5.32) together to describe the energy density and the pressure of the fermionic dark matter EoS. If one wants to construct the EoS of non-interacting dark matter, then one just needs to remove the second term from both equations (5.31) and (5.32). Non-interacting fermionic dark matter is just a gas of fermionic dark matter particles, which obeys the Pauli exclusion principle. Ref. Kouvaris 2012 showed that fermionic dark matter with an attractive Yukawa self-interaction may form black holes at the core of old neutron stars, and this puts a constraint on the fermionic dark matter EoS.

CHAPTER 6

Neutrons decay into dark matter EoS

Neutrons are one of the fundamental constituents of matter. Neutrons were discovered almost a century ago, but the decay of neutrons is still a puzzle, and the precise lifetime of neutrons is not known. Indeed, different methods of measuring the lifetime of neutrons (the beam and bottle methods) give different results. In recent years, some theoretical physicists have proposed the hypothesis of neutron dark decay, in which neutrons can decay into invisible dark matter particles, in addition to the usual decay products of protons, electrons, and antineutrinos. This hypothesis is motivated by the possibility that dark matter may interact weakly with normal matter, and that neutron decay may provide a way to probe these interactions. Before introducing the hypothesis of neutron's dark decay, let us first understand how neutrons decay in the Standard Model (SM) particles.

6.1 Neutrons decay into Standard Model particles

Neutrons decay through two channels that involve the Standard Model particles. The first neutron decays into a proton, an electron, and an anti-electron neutrino. This type of decay is commonly known as β decay, and the neutron predominately decays through β decay. The photon at the final state of the β decay is suggested in Bales et al. 2016 with a branching ration of order 10^{-2}. The second, neutron decays into a hydrogen atom and an electron anti-neutrino, which have a branching ratio of order 4×10^{-6}, approximately as suggested in Faber et al. 2009. In all of these decay channels, one of the end products is a proton.

Theoretically, the lifetime (τ_n) of the neutron can be calculated by using V_{ud}, the first element of the CKM matrix (Cabibbo-Kobayashi-Maskawa matrix),

$$\tau_n = \frac{4908.6(1.9)s}{(1+3\lambda^2)|V_{ud}|^2}, \tag{6.1}$$

where λ is the ratio of the axial-vector and the vector current coefficient in the matrix element of the neutron decay.

Experimentally, there are two prime methods widely adopted by the physics community to determine the lifetime of neutrons, the beam method and the bottle method. In the beam method, a beam of cold neutrons is fired (the number of neutrons fired in the beam is known), and after a while (after the expected lifetime of neutrons), the number of protons is counted. Based on the number of protons found after the decay and the lifetime of the neutrons is determined by

$$\tau_n^{beam} = -\frac{N_n}{dN_p/dt}. \tag{6.2}$$

By the beam method, the lifetime of the neutrons is found to be 888.0 $\pm$ 2.0 sec, as shown in Byrne et al. 1996; Nico et al. 2005; Yue et al. 2013. The other method of measuring the lifetime of neutrons is the bottle method. In the bottle method, the ultra-cold neutrons are trapped in a tube, and the total number of neutrons in the tube is known. After a while (after the expected lifetime of neutrons), the number of neutrons left in the tube is counted again. Based on these counts, the lifetime of neutrons is determined by

$$\tau_n^{bottle} = -\frac{N_n}{dN_n/dt}. \tag{6.3}$$

The lifetime of the neutrons in the bottle method is found to be 879.4 $\pm$ 0.6 sec, as shown in Serebrov et al. 2005; Pichlmaier et al. 2010; Steyerl et al. 2012; Arzumanov et al. 2015; Serebrov et al. 2018a. Regardless of the method of measurement, the lifetime of the neutrons must be equal, and it is expected that the decay rate must be equal, but the lifetime of the neutrons measured by the different methods has a discrepancy of approximately 4 σ. It is highly unlikely that the discrepancy is the result of some systematic error. The experiment has been repeatedly performed by various groups of scientists with the highest accuracy, but the difference in the lifetime of neutrons in the beam and bottle methods is always approximately

4σ. This controversy inspired a remarkably precise measurement of the lifetime of neutrons trapped in a bottle by the UCNτ Collaboration Gonzalez et al. 2021, with the result of $877.75 \pm 0.28_{\rm stat} + 0.22 - 0.16_{\rm syst}$ s. This agrees well with other recent measurements, such as Ref. Pattie et al. 2018, which reported a neutron lifetime 877.7 ± 0.7 s and Ref. Serebrov et al. 2018a, which reported a value of 881.5 ± 0.7 s. That raises a serious suspicion that there may be some underlying physics that we are unaware of. The results produced by these different methods can be reconciled if one assumes that neutrons have decay channels other than protons, which go uncounted in the beam method. The effect of this unknown channel is counted in the bottle method because, in the bottle experiment, the lifetime of neutrons is determined by the number of neutrons left after the decay, while in the beam method it is determined by the number of protons produced. The lifetimes determined by the beam and bottle methods are connected as

$$\tau_n^{beam} = \frac{\tau_n^{bottle}}{Br(n \to p + something)}. \tag{6.4}$$

The lifetime of a neutron is $\tau_n^{beam} > \tau_n^{bottle}$. If the 99% neutrons β decay into proton, i.e., branching ratio $\approx$ 0.99, and the remaining 1%, branching ratio $\approx$ 0.01, decay into some other particles that go undetected. If one includes the effect of the unknown decay channel, the discrepancy in the lifetime of the neutrons may be solved.

6.2 Neutrons dark decay channel

For neutrons to decay through dark decay channels, there are some constraints that can be put on the total mass of the final particles. The stability of nuclei puts a strong constraint on the mass of the end product of the decay. The total mass of the final particles must respect the following constraints:

(1) $M_f < m_n$ = 939.57 MeV for the decay of the neutron to be kinematically open.

(2) From the stability of stable nuclei, $M_f > m_n - S_{Be}$ = 937.906 MeV, where S_{Be} = 1.664 MeV is the binding energy of Be^8. Be is selected because it gives the strongest bound.

(3) The stability of the protons suggests that $M_f > m_p - m_e$ = 937.77 MeV.

(4) For the stability of the final product and β decay to be forbidden, $M_f < m_p + m_e$ = 938.79 MeV.

In light of the constraint given above, the total mass of the particle after the decay must be in the narrow range 937.906 MeV < M_f < 938.79 MeV. Any model suggesting the neutron has a decay channel excluding the proton, as the final product must be in the narrow range of mass.

6.2.1 Fornal and Grinstein hypothesis

A very interesting hypothesis to solve the discrepancy in the lifetime of the neutron, was suggested by Fornal and Grinstein in Grinstein et al. 2019. The central idea of the hypothesis is that in addition to the neutron β decay mode, $n \rightarrow p + e^- + \bar{\nu_e}$, neutrons could possibly decay into dark sector particles (dark matter) with a small branching ratio of approximately 0.01. They suggested that in the beam experiments, the dark matter particles, being very weakly interactive with the Standard Model particles, would remain undetected, while the dark sector particles would affect the total decay rate of neutrons in the bottle experiments. In fact, in the total decay rate, the contribution of the dark sector particles is included. This hypothesis suggested a substitute model to the idea that the neutrons might be oscillating into their mirror counterparts, although Serebrov et al. 2008 ruled out this idea of neutrons oscillating in their mirror counterparts. Some of the other decay modes have been discussed in Ref. Ivanov et al. 2018.

Fornal and Grinstein suggested the dark fermion, χ is almost degenerate to the neutron. Precisely, the decay can be represented as

$$n \longrightarrow \chi + \phi\,, \tag{6.5}$$

where χ is the dark fermion and ϕ is the dark boson. In fact, the mass of χ must be in the narrow mass band of 937.9 MeV < m_χ < 938.7 MeV (Grinstein et al. 2019 considering ϕ massless) because of the constraints discussed above. The study by Tang et al. 2018a ruled out the possibility of ϕ boson being a photon. In addition, ϕ boson must be extremely light,

almost massless. The author Serebrov et al. 2018b argued that the proposal might be helpful in solving the experimental inconsistency of the reactor anti-neutrino anomaly.

If such a neutron decay channel exists, then the properties of neutron stars could be very helpful in testing the hypothesis. The decay mode shown in Equation (6.5) would start populating a fraction of dark matter particles inside the neutron star as soon as the neutron star comes into existence. The populated dark matter particles must be in chemical equilibrium with the nuclear matter inside the neutron star and would remain gravitationally trapped inside the neutron star. If the dark fermions are non-interacting, the conversion of neutrons, with their high chemical potential, into dark matter particles is highly energetically favoured. Indeed, as shown by Motta et al. 2018a; Baym et al. 2018; McKeen et al. 2018, if one considers the dark fermions to be non-self-interacting, the presence of this decay mode produces neutron stars of maximum mass close to around $0.7\,M_{\odot}$, while the neutron stars of masses above 2 $M_{\odot}$ have been observed Özel and Freire 2016; Demorest et al. 2010; Antoniadis et al. 2013b.

If the hypothesis proposed by Fornal-Grinstein is to survive, the dark matter fermions, χ, must be self-repulsive. Using the observational constraints on the properties of the neutron stars, the constraints on the properties of the dark matter particles can be determined (Husain et al. 2022b; Motta et al. 2018b; Grinstein et al. 2019; Baym et al. 2018; Cline and Cornell 2018; Berryman et al. 2022; Strumia 2021; Rajendran and Ramani 2021; Tang et al. 2018b; Berezhiani et al. 2021). This study will also focus on finding an observational signal for such a neutron decay channel, apart from just testing the proposed dark decay model. For this reason, in this study, the baryon number is ensured to be conserved even when some of the baryons decay into dark fermions, and the consequences of such a decay are drawn.

In Equation (6.5), ϕ, dark boson, which is considered a massless boson, will escape the neutron star immediately and take away a very small amount of energy. The baryonic dark matter particle, χ, must have a mass approximately equal to the mass of the neutron. For the sake of ease of calculation, it is considered degenerate with the neutron. Apart from nuclear matter, the neutron star also has dark fermions inside it. Therefore, the presence of dark fermions has changed the chemical composition of neutron star matter. Indeed, the dark fermions must be in chemical equilibrium with the neutrons. The complete set of equations

for chemical equilibrium, including β equilibrium equations, are given as (Motta et al. 2018b; Motta et al. 2018a; Husain et al. 2022b)

$$\mu_n = \mu_p + \mu_e, \tag{6.6}$$

$$n_p = n_e + n_\mu, \tag{6.7}$$

$$\mu_\mu = \mu_e, \tag{6.8}$$

$$\mu_n = \mu_\chi, \tag{6.9}$$

where μ stands for the chemical potential of each of the particle species. The Hartree term in the energy density of the system, which must include the energy density of the χ dark fermion, is given by

$$\begin{aligned}\epsilon_H = &\frac{1}{2}m_\sigma^2\sigma^2 + \frac{1}{2}m_\omega^2\omega^2 + \frac{1}{2}m_\rho^2\rho^2 + \frac{1}{\pi^2}\int_0^{k_F^n} k^2\sqrt{k^2 + M_N^*(\sigma)^2}dk \\ &+\frac{1}{\pi^2}\int_0^{k_F^p} k^2\sqrt{k^2 + M_N^*(\sigma)^2}dk + \frac{1}{\pi^2}\int_0^{k_F^e} k^2\sqrt{k^2 + m_e^2}dk \\ &+\frac{1}{\pi^2}\int_0^{k_F^\mu} k^2\sqrt{k^2 + m_\mu^2}dk + \frac{1}{\pi^2}\int_0^{k_F^\chi} k^2\sqrt{k^2 + m_\chi^2}dk\,.\end{aligned} \tag{6.10}$$

The full Fock term (Motta et al. 2019) is given as

$$\begin{aligned}\epsilon_{Fock} = &-G_\omega\frac{1}{(2\pi)^6}\Big[\int_o^{k_F^p} d^3k_1\int_o^{k_F^p} d^3k_2\frac{m_\omega^2}{(\vec{k_1}-\vec{k_2})^2 + m_\omega^2} + \int_o^{k_F^n} d^3k_1\int_o^{k_F^n} d^3k_2 \\ &\frac{m_\omega^2}{(\vec{k_1}-\vec{k_2})^2 + m_\omega^2}\Big] - \frac{G_\rho}{4}\frac{1}{(2\pi)^6}\Big[(1)\times\int_o^{k_F^n} d^3k_1\int_o^{k_F^n} d^3k_2\frac{m_\rho^2}{(\vec{k_1}-\vec{k_2})^2 + m_\rho^2} + \\ &(1)\times\int_o^{k_F^p} d^3k_1\int_o^{k_F^p} d^3k_2\frac{m_\rho^2}{(\vec{k_1}-\vec{k_2})^2 + m_\rho^2} + (2)\times\int_o^{k_F^n} d^3k_1\int_o^{k_F^p} d^3k_2\frac{m_\rho^2}{(\vec{k_1}-\vec{k_2})^2 + m_\rho^2} + \\ &(2)\times\int_o^{k_F^p} d^3k_1\int_o^{k_F^n} d^3k_2\frac{m_\rho^2}{(\vec{k_1}-\vec{k_2})^2 + m_\rho^2}\Big] + \frac{1}{(2\pi)^6}\int_o^{k_F^p} d^3k_1\int_o^{k_F^p} d^3k_2\frac{1}{(\vec{k_1}-\vec{k_2})^2 + \tilde{m}_\sigma^2} \\ &\times\frac{M_n^*(\sigma)(-g_\sigma C(\sigma))}{\sqrt{M_n^*(\sigma)+k_1^2}}\times\frac{M_n^*(\sigma)(-g_\sigma C(\sigma))}{\sqrt{M_n^*(\sigma)+k_2^2}} + \frac{1}{(2\pi)^6}\int_o^{k_F^n} d^3k_1\int_o^{k_F^n} d^3k_2\frac{1}{(\vec{k_1}-\vec{k_2})^2 + \tilde{m}_\sigma^2} \\ &\times\frac{M_N^*(\sigma)(-g_\sigma C(\sigma))}{\sqrt{M_N^*(\sigma)+k_1^2}}\times\frac{M_N^*(\sigma)(-g_\sigma C(\sigma))}{\sqrt{M_N^*(\sigma)+k_2^2}}\end{aligned} \tag{6.11}$$

where $M_N^*(\sigma)$ represents the effective mass of the nucleon, which can be calculated using Equation (4.4). k_F stands for the Fermi momentum of each fermion in the system. The $\tilde{m_\sigma}^2$ is given as

$$\tilde{m_\sigma}^2 = m_\sigma^2 + \frac{1}{\pi^2}\Sigma_{p,n}\int_0^{k_F^n} k^2 dk \frac{\partial^2}{\partial\sigma^2}\sqrt{M_N^*(\sigma)+k^2}. \tag{6.12}$$

The meson fields are given as

$$\sigma(n,p) = -\frac{1}{m_\sigma^2\pi^2}\frac{\partial M_N^*}{\partial\overline{\sigma}}\Big[\Sigma_{p,n}\int_0^{k_F} k^2 dk \frac{M_N^*(\sigma)}{\sqrt{M_N^*(\sigma)+k^2}}\Big], \tag{6.13}$$

$$\omega(n,p) = \frac{g_\omega}{m_\omega^2}(n+p), \tag{6.14}$$

$$b(n,p) = \frac{g_\rho}{m_\rho^2}(p-n)/2. \tag{6.15}$$

The pressure (P) is calculated as

$$P = \int \mu_f n_f - \epsilon. \tag{6.16}$$

The number of baryons is given by

$$B_i = 4\pi\int_0^R \frac{r^2 n_i(r)}{[1-\frac{2M(r)}{r}]^{1/2}} dr, \tag{6.17}$$

where n_i is the number of the baryons and i = n, p, χ . The equation of state used here has a binding energy per nucleon of -15.8 MeV, the normal nuclear matter density is 0.148 fm^{-3}, incompressibility of 295 MeV, and a symmetry energy of 30 MeV, the symmetry energy slope is 52.4 MeV.

6.2.2 Strumia hypothesis - $n \to \chi\chi\chi$

Recently, Strumia (Strumia 2022) proposed an alternative model to solve the discrepancy in the lifetime of the neutron. Interestingly, it was suggested that the neutron might decay into dark matter, but the decay is different than suggested by Fornal and Grinstein. Strumia suggested that the dark decay of neutrons might decay into three dark matter particles that are identical, with each of them having a baryon number of 1/3.

In this decay, the final decay particles are only dark matter particles, and no dark bosons exist, and each of the dark matter particles is much lighter than the Fornal and Grinstein suggested dark matter particle. It has also been shown that this decay model eliminates the requirement for dark matter to be self-interactive (repulsive) in order to satisfy constraints on the maximum mass of the neutron star (Husain and Thomas 2022), which is contrary to the model of Fornal and Grinstein. Therefore, this model becomes very interesting to test using neutron stars. Here, a detailed examination of the consequences of this model of neutron decay on the properties of the neutron star is carried out. Following Strumia 2022, the neutron decay can be given as

$$n \rightarrow \chi + \chi + \chi. \tag{6.18}$$

Here, χ is a dark matter particle whose mass must be very close to $m_n/3$ to ensure the stability of the stable atomic nuclei and baryon number of 1/3. Like the constraints imposed on the mass of the dark fermions in the Fornal and Grinstein model, Strumia's dark matter fermions must also follow similar constraints given as

(1) For the Strumia model to be kinematically open, the mass of the dark matter particle must be $m_\chi < m_n/3 \approx$ 313.19 MeV.
(2) For the stability of stable nuclei, the mass of the dark matter particle must be $m_\chi > (m_n - E_{Be})/3 \approx$ 312.63 MeV, because the strongest bound comes from Be^8.
(3) For the proton to be stable, it requires that $m_\chi > (m_p - m_e)/3$ = 312.59 MeV.
(4) For $m_\chi < (m_p + m_e)/3 \approx$ 312.93 MeV, the decay of a Hydrogen atom, H $\rightarrow \chi\chi\chi\nu_e$, would be open.

Like the Fornal and Grinstein model, the Strumia neutron decay also has a narrow range for the mass of dark matter.

The course of developing the EoS for the Strumia model follows a similar process as for the Fornal and Grinstein model. Like in the previous case, the presence of dark matter must change the chemical composition of the neutron star. But unlike the previous case, in modelling the most massive neutron stars, we must include the hyperons at the highest energy

densities because it is quite likely for hyperons to develop at the higher energy densities.

$$\mu_\mu = \mu_e, \tag{6.19}$$

$$\mu_n = \mu_p + \mu_e, \tag{6.20}$$

$$n_p = n_e + n_\mu, \tag{6.21}$$

$$\mu_\chi = \mu_n/3. \tag{6.22}$$

For the sake of simplicity, m_χ = $m_n/3$ has been selected in the calculation for modelling the Strumia's neutron decay model. In the approach to neutron decay, let us include the equation of state that allows hyperons at the core of neutron stars. Assuming that the neutron star may have hyperons at higher energy densities. For the hyperons included in the equation of state, the hyperons appear as the chemical potential increases as one moves towards the core of the neutron star. With the equation of state including hyperons, one must have

$$\mu_\chi = \mu_n/3, \tag{6.23}$$

$$\mu_n = \mu_p + \mu_e, \tag{6.24}$$

$$n_p = n_e + n_\mu + n_{\Xi^-}, \tag{6.25}$$

$$\mu_\mu = \mu_e, \tag{6.26}$$

$$\mu_n = \mu_\Lambda = \mu_{\Xi^0}, \tag{6.27}$$

$$\mu_{\Xi^-} = \mu_n + \mu_e. \tag{6.28}$$

It is worth noting that the Σ baryons in the QMC model (Guichon et al. 2008) experience repulsion, so they do not populate at any energy density of interest. Therefore, they have not been displayed explicitly. The hyperons start to populate when the energy density is greater than three times that of the normal nuclear matter energy density. The Λ hyperon appears first, followed by Ξ^-, and at the highest central energy densities, Ξ^0 appears. The energy density (Motta et al. 2019; Husain et al. 2022a) is calculated using the Hartree-Fock method shown above from equations (6.10 - 6.17). The things that need to be taken care of are: m_χ = m_n/3 and the baryon number of χ is 1/3.

CHAPTER 7

Structural equations of neutron stars

Due to the super-dense matter inside the neutron stars, the spacetime from the center to around the neutron star is not flat, but significantly curved. Therefore, in this chapter, the structural equations based on the general theory of relativity framework are developed, which are essential together with the EoS to compute the properties of the neutron star.

7.1 Static and spherically symmetric neutron stars

The neutron stars are among the most compact objects in the universe, and the spacetime from the center to around them is curved. Therefore, if one wants to calculate the properties of a neutron star, one must consider the physics of curved spacetime using the general theory of relativity. Moreover, if the neutron star is rotating, then one must include the Lense-Thirring or frame-dragging effect. Although in this section the structural equations for a static, spherically symmetric neutron star are presented, this involves solving the Tolman, Oppenheimer, and Volkoff (TOV) equations (Tolman 1934; Oppenheimer and Volkoff 1939), which are based on Einstein's general theory of relativity framework. In simple words, the TOV equation is the relation between the two forces, the gravitational force, which tries to collapse the compact star, and the internal pressure of the compact star, which works in an outward direction against the gravitational force and tries to sustain the star. The pressure varies a lot from the center to the surface of the neutron star, and at the surface, the pressure vanishes, but at the center, neutron stars have one of the highest orders of pressure in the universe.

It is worth noticing that the original TOV equations are derived for compact objects containing only one type of fluid. But in this study, neutron stars contain two different fluids that are

non-interacting, namely, nuclear matter and dark matter. Hence, the TOV equations need to be modified accordingly so that they can work for compact objects made of two non-interacting fluids.

For a static, spherically symmetric, non-rotating neutron star, which is considered to be made of perfect fluids under Einstein's general theory of relativity framework.

The stress-energy tensor for such a system can be given as

$$T^{\alpha\beta} = \begin{pmatrix} -\epsilon_{nucl} - \epsilon_{DM} & 0 & 0 & 0 \\ 0 & P_{nucl} + P_{DM} & 0 & 0 \\ 0 & 0 & P_{nucl} + P_{DM} & 0 \\ 0 & 0 & 0 & P_{nucl} + P_{DM} \end{pmatrix}$$

where $T^{\alpha\beta}$ is the total energy density tensor of the compact star given by $T^{\alpha\beta} = T^{\alpha\beta}_{nucl} + T^{\alpha\beta}_{DM}$. Here, $T^{\alpha\beta}_{nucl}$ is the stress energy tensor for nuclear matter, and $T^{\alpha\beta}_{DM}$ is the stress energy tensor for the dark matter contained inside the compact star. For ease of calculation, the natural units, $G = c = 1$, have been set.

The line element for a non-rotating spherically symmetric neutron star can be given by

$$ds^2 = -e^{2\Phi(r)}dt^2 + e^{2\Lambda(r)}dr^2 + r^2 d\theta^2 + r^2 \sin^2\theta d\phi^2, \tag{7.1}$$

where $\Phi(r)$ and $\Lambda(r)$ are the metric functions that depend on the radial distances, and the covariant form of the metric functions are

$$g_{tt} = -e^{2\Phi(r)}, g_{rr} = e^{2\Lambda(r)}, g_{\theta\theta} = r^2, g_{\phi\phi} = r^2 \sin^2\theta. \tag{7.2}$$

The line element given by equation (7.1) can be written as

$$ds^2 = g_{\mu\nu} dx^\mu dx^\nu. \tag{7.3}$$

Here, the method to determine the relationship between the energy density and the pressure is given briefly. Einstein's mixed tensor is given as

$$G^\mu_\nu = R^\mu_\nu - \frac{1}{2}\delta^\mu_\nu R = 8\pi(T^\mu_{\nu\, DM} + T^\mu_{\nu\, nucl}). \tag{7.4}$$

In the physical sense, the equation given above is the relation between the distribution of energy and matter (both dark matter and nuclear matter), contained in the energy momentum tensor, and the curvature of spacetime. The stress energy tensor, T^{μ}_{ν}, is given by

$$T^{\mu}_{\nu\,nucl} = (\epsilon_{nucl} + P_{nucl})\frac{dx^{\mu}}{d\tau}\frac{dx_{\nu}}{d\tau}\Big|_{nucl} + \delta^{\mu}_{\nu}P_{nucl}, \tag{7.5}$$

$$T^{t}_{t\,nucl} = -\epsilon_{nucl}, T^{i}_{i\,nucl} = P_{nucl}. \tag{7.6}$$

Similarly, the stress energy tensor for dark matter

$$T^{\mu}_{\nu\,DM} = (\epsilon_{DM} + P_{DM})\frac{dx^{\mu}}{d\tau}\frac{dx_{\nu}}{d\tau}\Big|_{DM} + \delta^{\mu}_{\nu}P_{DM}, \tag{7.7}$$

$$T^{t}_{t\,DM} = -\epsilon_{DM}, T^{i}_{i\,DM} = P_{DM}, \tag{7.8}$$

where x^{μ} is the four velocity of the fluid. The tensor divergence of the left hand sides in the above given equations vanishes identically. The four derivative of the stress-energy tensor is established by applying the rule of covariant differentiation, as

$$T^{\mu}_{\nu;\mu}\big|_{nucl} = \frac{\partial T^{\mu}_{\nu}}{\partial x^{\mu}} + \Gamma^{\mu}_{\kappa\mu}T^{\kappa}_{\nu} - \Gamma^{\kappa}_{\nu\mu}T^{\mu}_{\kappa}\big|_{nucl} = 0, \tag{7.9}$$

$$T^{\mu}_{\nu;\mu}\big|_{DM} = \frac{\partial T^{\mu}_{\nu}}{\partial x^{\mu}} + \Gamma^{\mu}_{\kappa\mu}T^{\kappa}_{\nu} - \Gamma^{\kappa}_{\nu\mu}T^{\mu}_{\kappa}\big|_{DM} = 0. \tag{7.10}$$

The non-vanishing Christoffel symbols for the line element, i.e. equation (7.1), are

$$\begin{gathered}\Gamma^{r}_{tt} = e^{2\Phi-2\Lambda}\Phi', \qquad \Gamma^{t}_{tr} = \Phi', \qquad \Gamma^{r}_{rr} = \Lambda', \\ \Gamma^{\theta}_{r\theta} = 1/r, \qquad \Gamma^{\phi}_{r\phi} = 1/r, \qquad \Gamma^{r}_{\theta\theta} = -re^{-2\Lambda}, \\ \Gamma^{\phi}_{\theta\phi} = \cot\theta, \qquad \Gamma^{r}_{\phi\phi} = \frac{-r\sin^{2}\theta}{e^{2\Lambda}}, \qquad \Gamma^{\theta}_{\phi\phi} = -\sin\theta.\cos\theta,\end{gathered} \tag{7.11}$$

where $'$ are derivatives of the quantity with respect to r. Namely, Λ' and Φ' are the derivatives of Λ and Φ that are $\frac{d\Phi}{dr}$ and $\frac{d\Lambda}{dr}$. In flat spacetime or in a local inertial reference frame, the covariant derivatives of the stress energy vanish

$$T^{\mu}_{\nu;\mu}\big|_{nucl} = \frac{\partial}{\partial x^{\mu}}T^{\mu}_{\nu}\big|_{nucl} = 0, \tag{7.12}$$

$$T^{\mu}_{\nu;\mu}\big|_{DM} = \frac{\partial}{\partial x^{\mu}}T^{\mu}_{\nu}\big|_{DM} = 0. \tag{7.13}$$

For the line element stated above, the covariant derivative of the stress energy tensor given in equations (7.9) and (7.10) reduce to

$$T^{\mu}_{\nu;\mu}\big|_{nucl} = (\epsilon_{nucl} + P_{nucl})\Phi' + P'_{nucl}, \tag{7.14}$$

$$T^{\mu}_{\nu;\mu}\big|_{DM} = (\epsilon_{DM} + P_{DM})\Phi' + P'_{DM}, \tag{7.15}$$

which implies that the mixed energy momentum tensor, the middle term of equation (7.4), for the given spacetime metric can be calculated using the expressions below (see Appendix B)

$$\begin{aligned} R^t_t &= [-\frac{1}{4}\Phi'^2 + \frac{1}{4}\Phi'\Lambda' - \frac{1}{2}\Phi'' - \frac{1}{r}\Phi']e^{-\Lambda}, \\ R^r_r &= [-\frac{1}{4}\Phi'^2 + \frac{1}{4}\Phi'\Lambda' - \frac{1}{2}\Phi'' - \frac{1}{r}\Lambda']e^{-\Lambda}, \\ R^{\phi}_{\phi} &= R^{\theta}_{\theta} = -\frac{1}{r^2}e^{-\Lambda}[1 - \frac{1}{2}r\Lambda' + \frac{1}{2}r\Phi'] + \frac{1}{r^2}. \end{aligned} \tag{7.16}$$

The Ricci scalar is given by

$$R = \frac{1}{r^2 e^{2\Lambda}}[2\Phi'\Lambda' r^2 - 2\Phi'' r^2 - 2(\Phi')^2 r^2 - 4r\Phi' + 4r\Lambda' + 2e^{2\Lambda} - 2]. \tag{7.17}$$

Therefore, Einstein's curvature tensor is calculated as

$$G^t_t = R^t_t - \frac{1}{2}R = e^{-2\Lambda}(\frac{1}{r^2} - 2\frac{\Lambda'}{r}) - \frac{1}{r^2}, \tag{7.18}$$

$$G^r_r = R^r_r - \frac{1}{2}R = e^{-2\Lambda}(\frac{2\Phi'}{r} + \frac{1}{r^2}) - \frac{1}{r^2}, \tag{7.19}$$

$$G^{\theta}_{\theta} = R^{\theta}_{\theta} - \frac{1}{2}R = e^{-2\Lambda}(\Phi'' - \Phi'\Lambda' + \Phi'^2 + \frac{\Phi' - \Lambda'}{r}), \tag{7.20}$$

$$G^{\phi}_{\phi} = G^{\theta}_{\theta}. \tag{7.21}$$

Since the neutron star is static, the following relations are used.

$$\frac{dr}{d\tau} = \frac{d\theta}{d\tau} = \frac{d\phi}{d\tau} = 0, \tag{7.22}$$

and

$$\frac{dt}{d\tau} = e^{-\Phi}. \tag{7.23}$$

Using equations (7.18-7.21), with equation (7.6), and equation (7.8), one finds the general relativistic equation at μ = ν = t

$$e^{-2\Lambda}(\frac{1}{r^2} - 2\frac{\Lambda'}{r}) - \frac{1}{r^2} = -8\pi(\epsilon_{nucl} + \epsilon_{DM}), \tag{7.24}$$

at μ = ν = r

$$e^{-2\Lambda}(\frac{2\Phi'}{r} + \frac{1}{r^2}) - \frac{1}{r^2} = 8\pi(P_{nucl} + P_{DM}), \tag{7.25}$$

at μ = ν = θ

$$e^{-2\Lambda}(\Phi'' - \Phi'\Lambda' + \Phi'^2 + \frac{\Phi' - \Lambda'}{r}) = 8\pi(P_{nucl} + P_{DM}). \tag{7.26}$$

Simplifying equation (7.24) for the purpose of solving for $e^{2\Lambda}$,

$$e^{-2\Lambda}2\Lambda' r - e^{-2\Lambda} + 1 = 8\pi(\epsilon_{nucl} + \epsilon_{DM})r^2. \tag{7.27}$$

Rearranging the left hand side and noticing that it is the derivative form of the function

$$-\frac{d}{dr}(e^{-2\Lambda}r - r) = 2(4\pi(\epsilon_{nucl} + \epsilon_{DM})r^2), \tag{7.28}$$

and the total mass of the neutron star enclosed within the sphere of radius 'r' can be determined by

$$m(r) = 4\pi \int_0^r dr.r^2(\epsilon_{nucl} + \epsilon_{DM}), \tag{7.29}$$

which is the sum of the mass of the dark matter and the mass of the nuclear matter inside the radius, r

$$m(r) = m_{nucl}(r) + m_{DM}(r). \tag{7.30}$$

The contribution of the mass of dark matter and the mass of nuclear matter can be given as

$$m_{DM}(r) = 4\pi \int_0^r dr.r^2\epsilon_{DM}(r), \tag{7.31}$$

$$m_{nucl}(r) = 4\pi \int_0^r dr.r^2\epsilon_{nucl}(r). \tag{7.32}$$

Integration of equation (7.28) yields,

$$e^{-2\Lambda} = 1 - \frac{2m(r)}{r}. \tag{7.33}$$

Here, $m(r)$ is the total mass, including the mass of the nuclear matter and the dark matter inside the radius r. Eliminating $e^{-2\Lambda}$ from equation (7.25) by plugging its value from equation (7.33),

$$8\pi(P_{nucl} + P_{DM}) = \frac{-2m}{r^3} + 2(1 - \frac{2m}{r})\frac{\Phi'}{r}, \tag{7.34}$$

which leads to the differential function in Φ' as

$$\Phi' = \frac{4\pi r^3(P_{nucl} + P_{DM}) + m}{r^2(1 - \frac{2m}{r})}. \tag{7.35}$$

At the surface of the neutron star

$$\Phi = \frac{1}{2}\log(1 - \frac{2M}{R}), \tag{7.36}$$

where M and R represent the total mass and radius of the neutron star, respectively. Finally, from the expressions given in Appendix B, the differential equation involving the pressure gradient, radius, and density of the neutron star is found as given below

$$\frac{dP}{dr}\Big|_{nucl} = -\frac{(\epsilon_{nucl} + P_{nucl})(m + 4\pi r^3(P_{nucl} + P_{DM}))}{r^2(1 - \frac{2m}{r})}, \tag{7.37}$$

$$\frac{dP}{dr}\Big|_{DM} = -\frac{(\epsilon_{DM} + P_{DM})(m + 4\pi r^3(P_{nucl} + P_{DM}))}{r^2(1 - \frac{2m}{r})}. \tag{7.38}$$

The above equations are important relations among radius, pressure, and energy density because when the equation of state is plugged with these equations, they give insight into how pressure varies from the core to the surface with changes in energy density. The established relation is one of the essential equations needed to calculate the properties of the neutron star. The structural equations of the single fluid compact star are known as TOV equations. Since, in this study, two non-interacting fluids are considered inside the neutron stars, the TOV equations are called 'modified TOV equations' or 'the two fluid TOV equations'. These equations must be integrated under the boundary conditions, which are that the energy density and pressure vanish at the surface of the neutron star. Therefore, at the surface of the neutron star, one must get $P = 0, \epsilon = 0$, when $R = Radius$.

In a general sense, both in classical mechanics and the general theory of relativity framework, the outward working pressure of the mass shell counters the gravitational force that acts

inwards towards the center of the compact star and tries to collapse the star. But it is worth noticing that in the classical mechanics framework, there is no limit on how massive neutron stars can be. Based on classical mechanics theory, neutron stars can be as massive as one wants them to be, having $P << \epsilon$, $P << m << r$, results in $dP/dr = \epsilon m/r^2$. Whereas, in the general relativistic framework, neutron stars can't be arbitrarily massive, as the neutron stars become more massive at a certain point, the gravitational force overcomes the internal pressure of the compact stars, and they collapse under their own gravity and form black holes.

To determine the properties of neutron stars, we need a nuclear equation of state and a dark matter equation of state, which have been calculated in the earlier sections, that are the input to the structural equations (modified TOV equations). These equations are numerically integrated from the center to the surface. The steps to integrate take place as

(1) First, choose the central energy densities of the neutron star for the nuclear matter and the dark matter (ϵ_{nucl} and ϵ_{DM}) and calculate the pressure at the center from the corresponding equations of state for both fluids, respectively. These values serve as input to the modified TOV equations.
(2) Determine the mass ($m = m_{nucl} + m_{DM}$) of the shell by the equation (7.30).
(3) Plugging the values found above in the pressure gradient and (dP/dr) is determined at an infinitesimal small distance (dr) by the modified TOV equations.
(4) Find the pressure (P) for the next step by using the Euler integration method (one can choose any integration method).
(5) Determine the pressures (P_{nucl} and P_{DM}). Using these values of the pressures, calculate the energy densities of the nuclear matter and the dark matter by inverting the respective equations of state. After finding the energy densities of both fluids, calculate the mass for the shell of thickness dr.
(6) Repeat these steps until we reach $P = 0, \epsilon = 0$, which are the boundary conditions. At that point, mass (M) is the total mass, and radius (R) is the total radius of the neutron star.

The results of two fluid TOV equations are comparable to one fluid TOV equation as given in Motta et al. 2018b; Motta et al. 2018a, and there is no major difference between the two approaches (it may be because the dark matter contribution to the neutron star mass is small compared to nuclear matter). Therefore, for the rest of the calculations, one fluid TOV equation is adopted for the sake of ease of calculation.

7.2 Moment of inertia

The moment of inertia of the neutron star is calculated by using the equation

$$I = \frac{J}{\Omega}, \tag{7.39}$$

where J is the angular moment of the neutron star and Ω is the rotational velocity. It is worth noticing that rotating neutron stars can be slightly heavier than non-rotating ones because they have an additional centrifugal force that counterbalances the gravitational attraction. The shape of a neutron star also deforms due to rotation, specifically, at the equator, they have a bulge and their radii stretch, whereas at the poles, they tend to flatten a little. Therefore, rotating neutron stars are not perfectly spherical in shape, instead, they have an oval shape. This deformation of shape makes calculations a bit harder for the rotating neutron stars because it changes the spacetime structure from the center to the surface of the neutron star. This suggests that the line element of a spinning neutron star is dependent on the star's rotational speed. Consequently, the metric tensor must include an additional non-diagonal term ($g^{t\phi}$) to account for the general relativistic effect of the local inertial frame dragging. While the local inertial frame is dragged along the direction of rotation, which is controlled by the properties of a neutron star, such as rotational velocity and mass, this additional term imposes a self-consistent condition on the stellar structure of the neutron stars.

For slowly rotating neutron stars, Hartle and Thorne have provided a methodology to solve the structural equations in Refs. Hartle and Thorne 1968; Hartle 1967. Their methodology works fine for the neutron stars, which have a rotating velocity much smaller than their mass shedding velocity. Therefore, the same methodology is considered in this study. The structural

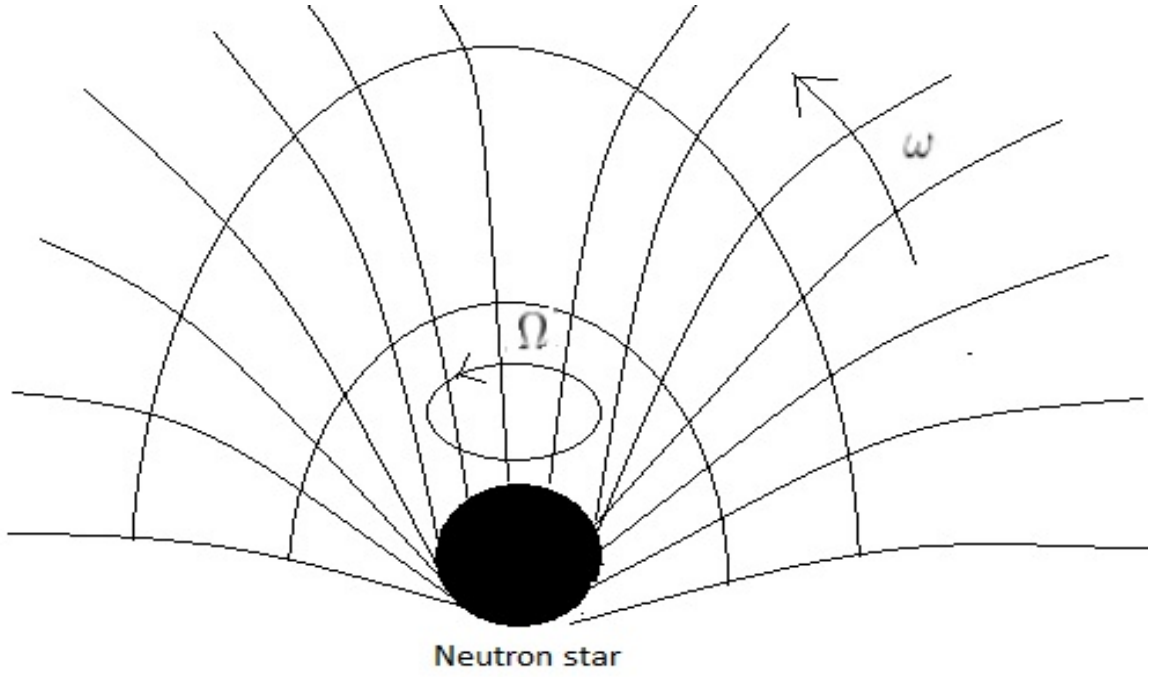

FIGURE 7.1: The curved spacetime around a rotating neutron star with the rotating velocity Ω in general relativity framework and position dependent local frame dragging angular velocity $\omega(r, \theta, \phi)$.

equations are solved step by step using the general relativistic framework by introducing perturbative metric. That involves

(1) Solve the TOV equations for a neutron star, assuming it is non-rotating.
(2) Now introduce the rotational perturbation expressions for determining the rotational velocity of the neutron star.
(3) Determine the angular moment of the neutron star using the expression given in equation (7.69).
(4) Use the expression given in equation (7.39).
(5) If one is interested, one can solve the quadrupole perturbation function to determine the shape of the star, and solving mono-pole equations to determine the extra mass a neutron star can have due to its rotation.

The first step, which is the methodology for the non-rotating neutron stars (TOV equations), has been provided above. The methodology for the second step is provided here.

7.2.1 Rotational pertubation

As the neutron stars rotate, their energy density and pressure get perturbed. Therefore, the perturbed line element for the axially symmetric rotating neutron star can be given by

$$ds^2 = -e^{2\nu(r,\theta,\Omega)}(dt)^2+e^{2\psi(r,\theta,\Omega)}(d\phi-\omega(r,\theta,\Omega)dt)^2+e^{2\mu(r,\theta,\Omega)}(d\theta)^2+e^{2\lambda(r,\theta,\Omega)}(dr)^2+\mathcal{O}(\Omega^3), \tag{7.40}$$

where θ and r are polar coordinates and ν, μ, λ, and ψ are the perturbed metric functions. The neutron star's uniform rotational velocity is represented by Ω and ω is the rotation speed of the local inertial frame of reference dragged along the direction of rotational of the neutron star. The dragging velocity, ω, depends on the polar coordinates r, θ. The velocity of local dragging of the inertial frame of reference depends on the mass and the energy density of the neutron star, which vary with Ω. Moreover, ω must be given as a function of Ω. Therefore, the relative angular velocity, $\bar{\omega}$, which can be given as,

$$\bar{\omega} = \Omega - \omega(r,\theta,\Omega). \tag{7.41}$$

Above equation (7.41) is useful when one wants to find the rotational flow of the fluid inside the neutron stars.

Since the neutron stars are expected to be axially symmetric and stationary, and they are assumed not to be radiating any rotational energy in the form of gravitational radiation. Otherwise, we would have a time dependent moment of inertia, which means the star could not remain in equilibrium over time. Therefore, the metric function must be independent of time and azimuthal angle (ϕ). Let us expand the metric functions in terms of second order of Ω as

$$e^{2\nu(r,\theta,\Omega)} = e^{2\Phi(r)}[1 + 2(h_0(r,\Omega)) + h_2(r,\Omega)P_2(\cos\theta)], \tag{7.42}$$

$$e^{2\psi(r,\theta,\Omega)} = r^2\sin^2\theta[1 + 2(\nu_2(r,\Omega)) - h_2(r,\Omega)P_2(\cos\theta)], \tag{7.43}$$

$$e^{2\mu(r,\theta,\Omega)} = r^2[1 + 2(\nu_2(r,\Omega)) - h_2(r,\Omega)P_2(\cos\theta)], \tag{7.44}$$

$$e^{2\lambda(r,\theta,\Omega)} = e^{2\Lambda(r)}[1 + \frac{2}{r}\frac{m_0(r,\Omega) + m_2(r,\Omega)P_2(\cos\theta)}{1-2m(r)/r}], \tag{7.45}$$

where the second order terms are defined as

$$h(r,\theta,\Omega) = h_0(r,\Omega) + h_2(r,\Omega)P_2(\cos\theta) + ... \tag{7.46}$$

$$\nu(r,\theta,\Omega) = \nu_0(r,\Omega) + \nu_2(r,\Omega)P_2(\cos\theta) + ... \tag{7.47}$$

$$m(r,\theta,\Omega) = m_0(r,\Omega) + m_2(r,\Omega)P_2(\cos\theta,\Omega). \tag{7.48}$$

Assuming that due to the rotational perturbation of the neutron star, the change in pressure is ΔP, the change in energy density is $\Delta\epsilon$ and the change in baryon number density is $\Delta\rho$. Let ΔT denotes the change in stress-energy tensor. Therefore, the new stress-energy tensor is

$$T_{\mu\nu} = T^0_{\mu\nu} + \Delta T_{\mu\nu}. \tag{7.49}$$

Here $T^0_{\mu\nu}$ is the stress-energy for a non-rotating neutron star

$$T^0_{\mu\nu} = (\epsilon + P)u_\mu u_\nu + P g_{\mu\nu}, \tag{7.50}$$

$$\Delta T_{\mu\nu} = (\Delta\epsilon + \Delta P)u_\mu u_\nu + \Delta P g_{\mu\nu}. \tag{7.51}$$

Here, ϵ is the energy density, P is the pressure, and ρ is the baryon number density (using one fluid concept), which are measured in the co-moving local inertial frame. u_ν is the four fluid velocity of the fluid, given by $u_\nu u^\nu = -1$.

Individually, the changes in the interested physical quantities can be given as

$$\Delta P = (\epsilon + P)(p_0 + p_2 P_2(cos\theta)), \tag{7.52}$$

$$\Delta\epsilon = \Delta P \frac{\partial\epsilon}{\partial P}, \tag{7.53}$$

$$\Delta\rho = \Delta P \frac{\partial\rho}{\partial P}, \tag{7.54}$$

where p_0 and p_2 are the monopole and quadrupole pressure perturbation functions, respectively. The monopole equations need to be solved if one is interested in calculating the extra mass a neutron star can have due to its rotation, and $P_2(\cos\theta)$ is the Legendre polynomial function, given by

$$P_2(z) = \frac{3z^2 - 1}{2}. \tag{7.55}$$

Now let us move on to finding the rotational equations that need to be solved under Hartle's framework. The frame dragging function ($\omega(r,\theta)$) is determined by Einstein's field equations

$$G^t_\phi = R^t_\phi = 8\pi T^t_\phi, \tag{7.56}$$

$$T^t_\phi = (\epsilon + P)\overline{\omega} r^2 \sin^2\theta e^{-2\nu}, \tag{7.57}$$

(See Appendix B)

$$\frac{1}{r^4}\frac{\partial}{\partial r}(r^4 e^{(\nu+\lambda)}\frac{\partial\overline{\omega}}{\partial r}) + \frac{e^{\lambda-\nu}}{r^2\sin^3\theta}\frac{\partial}{\partial\theta}\Big(\sin^3\theta\frac{\partial\overline{\omega}}{\partial\theta}\Big) - 16\pi(\epsilon+P)\overline{\omega}e^{\lambda-\nu} = 0, \tag{7.58}$$

where the following functions are set as

$$\frac{\partial\lambda}{\partial\theta} = \frac{\partial\nu}{\partial\theta} = \frac{\partial\nu}{\partial\theta} = 0. \tag{7.59}$$

Assuming

$$j(r) = e^{-(\Phi+\Lambda)} = e^{-\Phi(r)}\sqrt{1-\gamma(r)}, \tag{7.60}$$

where $\gamma(r)$ is given by

$$\gamma(r) = 1 - \frac{2m(r)}{r}. \tag{7.61}$$

To determine the coefficient of $\overline{\omega}$ as a function of the unperturbed metric function, differentiating equation (7.60) with respect to r gives

$$\frac{dj(r)}{dr} = -4\pi r\frac{[\epsilon(r)+P(r)]}{\sqrt{1-\gamma(r)}}e^{\Phi(r)}, \tag{7.62}$$

where equation (7.35) is used and $d\Phi/dr$ is plugged as follows

$$\frac{d\Phi}{dr} = -\frac{1}{\epsilon(r)+P(r)}\frac{dP(r)}{dr}. \tag{7.63}$$

Now, following algebraic manipulation in equation (7.58) and converting it into the form as

$$\frac{1}{r^4}\frac{\partial}{\partial r}(r^4 j\frac{\partial\overline{\omega}}{\partial r}) + \frac{4}{r}\frac{dj}{dr}\overline{\omega} + \frac{e^{\lambda-\nu}}{r^2\sin^3\theta}\frac{\partial}{\partial\theta}\Big(\sin^3\theta\frac{\partial\overline{\omega}}{\partial\theta}\Big) = 0. \tag{7.64}$$

Expanding ω in vector spherical harmonics

$$\overline{\omega}(r,\theta) = \Sigma_{l=1}^{\infty}\overline{\omega}_l(r)\Big(-\frac{1}{\sin\theta}\frac{dP_l}{\partial\theta}\Big), \tag{7.65}$$

$\overline{\omega}_l(r)$ satisfies

$$\frac{1}{r^4}\frac{\partial}{\partial r}\Big(r^4 j(r)\frac{d}{dr}\bar{\omega}(r)\Big) + \Big(\frac{4}{r}\frac{d}{dr}j(r) - e^{\lambda-\nu}\frac{l(l+1)-2}{r^2}\Big)\bar{\omega}_l(r) = 0. \tag{7.66}$$

For l = 1 and $r < R$, this yields

$$\frac{d}{dr}(r^4 j(r)\frac{d\overline{\omega}_l(r)}{dr}) + 4r^3\frac{dj(r)}{dr}\overline{\omega}(r) = 0. \tag{7.67}$$

The equation (7.67) is the equation we aimed to drive. The integration of this equation right from the center to the surface of the neutron star following the boundary conditions given as

(1) $\bar{\omega}$ must be regular at the center of the neutron when r = 0.

(2) The function $\frac{d\bar{\omega}}{dr}$ moves to 0 when r = 0.

For numerical calculations, one must select an arbitrary value for ω at the center of the neutron star and integrate towards the surface, where P = 0, and ϵ = 0. Outside the neutron star, $\overline{\omega}$ is given by

$$\overline{\omega}(r,\Omega) = \Omega - \frac{2}{r^3}J(\Omega), \tag{7.68}$$

Here, $J(\Omega)$ represents the angular momentum of the neutron star, which can be found using the expression

$$J(\Omega) = \frac{R^4}{6}\Big(\frac{d\overline{\omega}}{dr}\Big)_R. \tag{7.69}$$

where R is the radius of the neutron star. Once $d\overline{\omega}/dr$ is calculated, the angular momentum can be determined, and the moment of inertia can be found by using the expression given in the equation (7.39).

7.3 Tidal Love number and tidal deformability

Tidal deformability and tidal Love numbers are important quantities of the neutron star to know because they are related to the internal structure of the neutron star, and the discovery of gravitational waves using the neutron star binary system has put a very strict constraint on the tidal deformability of the neutron star. To calculate the tidal deformability and the tidal Love number, the method suggested in Refs. Hinderer 2008; Hinderer et al. 2010;

Flanagan and Hinderer 2008 is considered. If a spherically symmetric static neutron star is placed in an external tidal quadrupole field, given by ϵ_{ij}, and in response to the external quadrupole field, the neutron star develops a tidal quadrupole moment, given by Q_{ij}, then the tidal deformability, λ, can be given as

$$Q_{ij} = -\lambda \epsilon_{ij}. \tag{7.70}$$

The tidal Love number and tidal deformability are connected as

$$\lambda = \frac{2}{3} k_2 R^5, \tag{7.71}$$

where k_2 is the tidal Love number.

The developed quadrupole moment due to the presence of an external tidal field is the coefficient of the asymptotic expansion of the total metric at a large distance from the star

$$-\left(\frac{1+g_{tt}}{2}\right) = -\frac{m}{r} - \frac{3Q_{ij}}{2r^3} n^i n^j + ... + \frac{\epsilon_{ij}}{2} r^2 n^i n^j + ..., \tag{7.72}$$

where $n^i = x^i/r$ and Q_{ij} & ϵ_{ij} are symmetric and traceless. Following Ref. Hinderer et al. 2010 to calculate the tidal Love number using the Regge-Wheeler gauge, as suggested in Regge and Wheeler 1957, the perturbation metric of a spherically symmetric star in a tidal field in Regge Wheeler gauge (Regge and Wheeler 1957; Hinderer 2008) can be written as

$$\begin{aligned} ds^2 = -e^{2\Phi(r)}[1 + H(r)Y_{20}(\theta,\phi)]dt^2 + e^{2\Lambda(r)}[1 - H(r)Y_{20}(\theta,\phi)]dr^2 \\ + r^2[1 - K(r)Y_{20}(\theta,\phi)](d\theta^2 + \sin^2\theta d\phi^2), \end{aligned} \tag{7.73}$$

where H and Y_{20} are the factors originated from the Regge-Wheeler gauge transformation and K and H share the relationship

$$\frac{dK}{dr} = \frac{dH}{dr} + 2H\frac{d\Phi'}{dr}. \tag{7.74}$$

The tidal deformation of the neutron star will be symmetric around the axis that connects the two neutron stars, which is also the axis of spherical harmonic decomposition. Therefore, the azimuthal number, m, is set to zero in the equation (7.73)

Let $\delta\epsilon$ and δp be the changes in the energy density and pressure. Introducing the perturbation

in stress-energy tensor components as

$$\begin{aligned} \delta T^0_0 &= -\delta\epsilon(r) Y_{20}(\theta,\phi), \\ \delta T^i_i &= \delta p(r) Y_{20}(\theta,\phi). \end{aligned} \tag{7.75}$$

The function $H(r)$ is the solution of the differential equation

$$\Big[-\frac{6e^{2\Lambda}}{r^2} - 2(\Phi')^2 + 2\Phi'' + \frac{3}{r}\Lambda' + \frac{7}{r}\Phi' - 2\Phi'\Lambda' + \frac{f}{r}(\Phi'+\Lambda')\Big]H + \Big[\frac{2}{r} + \Phi' - \Lambda'\Big]H' + H'' = 0, \tag{7.76}$$

where $f = \delta\epsilon/\delta p$ when the change in the fluid flow is slow, f is

$$f = \frac{d\epsilon}{dp}. \tag{7.77}$$

The stress-energy tensor of the perfect fluid is

$$T^{\mu}_{\nu;\mu} = (\epsilon + P)\Phi' + P', \tag{7.78}$$

using the equations (7.30), (7.31), (7.32), (7.36), in the equation (7.76), gives two first order differential equations

$$\frac{dH}{dr} = \beta, \tag{7.79}$$

$$\begin{aligned} \frac{d\beta}{dr} = 2(1-2\frac{m}{r})^{-1}H[-2\pi(5\epsilon + 9p + (\epsilon+p)f) + \frac{3}{r^2} + 2(1-2\frac{m}{r})^{-1}(\frac{m}{r^2} + 4\pi r p)^2] \\ +2\frac{\beta}{r}(1-2\frac{m}{r})^{-1}[-1 + \frac{m}{r} + 2\pi r^2(\epsilon - p)]. \end{aligned} \tag{7.80}$$

The equations (7.79) and (7.80) are to be integrated from just outside the center of the neutron star to the surface with the ordinary TOV equations (differential equations of the pressure and the mass). The behaviour of function H near the center can be given as an expansion in terms of infinitesimal distance from the center: $H(r) = a_0 r^2$. Therefore, β function can be given as $\beta(r) = 2a_0 r$, having r infinity small, such as $r \to 0$, where a_0 is an arbitrary expansion factor that can have any selected value. The selected value of a_0 does not affect the value of the tidal Love number or tidal deformability because it cancels out at the end expression. Outside the neutron star, the general solution of $H(r)$ can be given in terms of the second order Legendre

function, for the large value of r

$$H = C_1 Q_2^2(r/M - 1) + C_2 P_2^2(r/M - 1), \tag{7.81}$$

and the values of C_1 and C_2 can be found by comparing its asymptotic expansion with equation (7.72) using equation (7.70) in terms of λ

$$C_1 = \frac{15}{8M^3}\lambda\epsilon, C_2 = \frac{M^2\epsilon}{3}. \tag{7.82}$$

Plugging the values of C_1 and C_2 in equation (7.81) gives the exterior solution. To solve for λ, at the surface where $r = R$ (radius), one has to match the interior solution (equation (7.76)) with the exterior solution (equation (7.81)) and their first derivatives. For simplicity, assuming, $C = M/R$ and $y = R\beta(R)/H(R)$, the equation for the tidal Love number takes the form

$$\begin{aligned} k_2 = \frac{8C^5}{5}(1-2C)^2[2 + 2C(y-1) - y] \times [2C(6 - 3y + 3C(5y-8)) + \\ 4C^3(13 - 11y + C(3y-2) + 2C^2(1+y)) + 3(1-2C)^2(2 - y + 2C(y-1)) \\ \times \log(1-2C)]^{-1}. \end{aligned} \tag{7.83}$$

Using the above expression, the tidal Love number can be calculated, and once the tidal Love number is known, the tidal deformability (λ) can be determined by using the expression given in equation (7.71).

CHAPTER 8

Results

In this chapter, the consequences of dark matter on the properties of neutron stars are presented. In section 8.1, the consequences of fermionic and bosonic dark matter are presented when the neutron stars capture dark matter from their surroundings. In sections 8.2, the consequences of neutrons decaying into dark matter are presented.

8.1 Dark matter captured inside neutron stars

For modelling the neutron star matter, three different equations of state are considered, namely, N-QMC700 represents nucleons only, F-QMC700 allows the development of hyperons at higher energy densities, and the strange matter equation of state represents deconfined quarks at the core of the neutron stars. Figure 8.1 shows the pressure and energy density of nuclear matter inside the neutron stars. The equation of state based on nucleons only at the core of neutron stars is the stiffest. The presence of hyperons or strange matter at the higher energy densities at the core of the neutron stars makes the equation of state softer, but the strange matter equation of state is stiffer than the equation of state based on hyperons at the higher energy densities.

For the case of dark matter captured inside the neutron star, the mass of the dark matter particle is considered to be m_χ = 1 GeV regardless of the nature of dark matter, whether it is fermionic or bosonic dark matter, which is similar to what is considered in Refs. Li et al. 2012b; Kouvaris 2012; Ellis et al. 2018; Mukhopadhyay et al. 2017. As shown above, the equation of state of self-interaction bosonic dark matter involves scattering length, which is considered to be l_χ = 1 fm. The equation of state of self-interacting fermionic dark matter

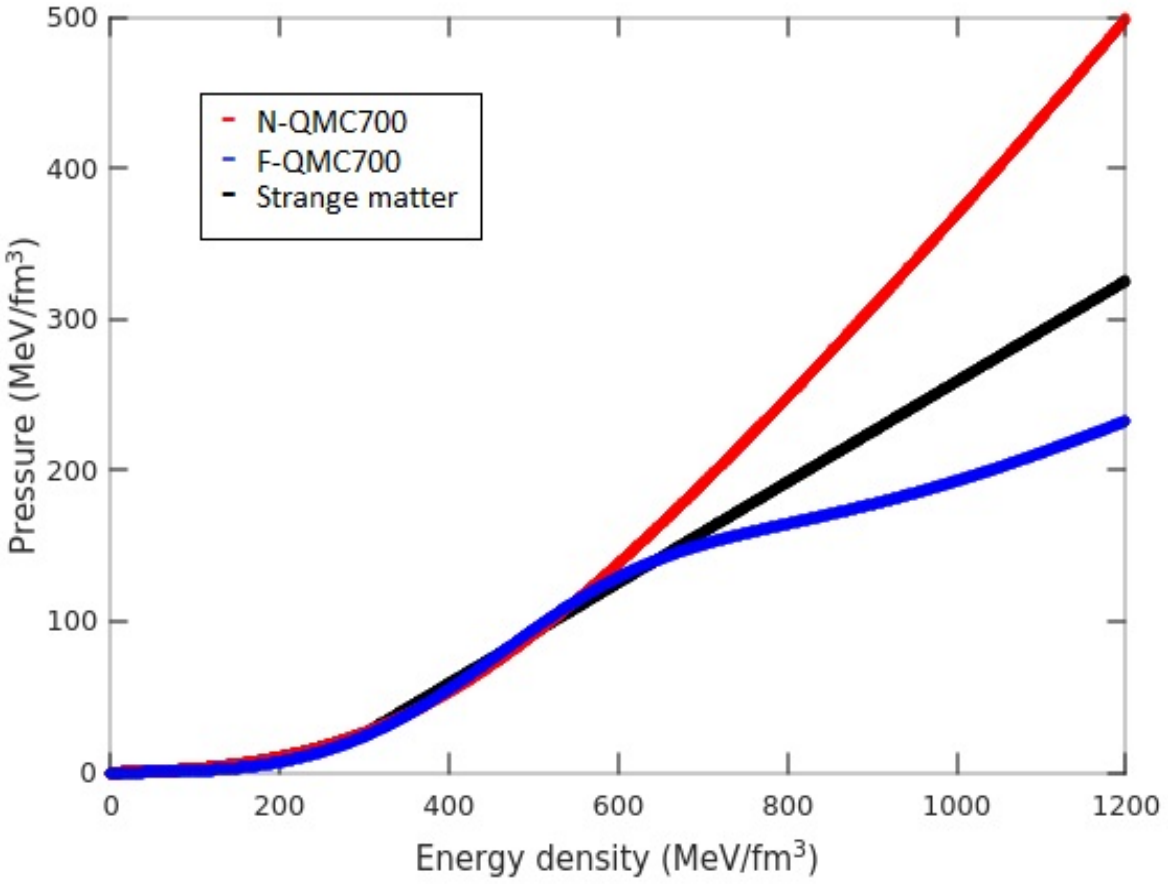

FIGURE 8.1: The relationship between energy and pressure is depicted for selected models of nuclear matter in neutron stars.

involves the mass of the dark photon (or self-interacting exchange particle), which is selected to be m_I = 100 MeV. In the following figures, the contribution of mass by the nuclear matter is kept fixed, and the contribution of dark matter is increased inside the neutron star. The plots displayed in Figs. 8.2 and 8.3 are constructed assuming that the neutron star contains only nucleons at the core. Figure 8.2 is constructed using the N-QMC700 equation of state with bosonic dark matter, and Figure 8.3 is constructed for the N-QMC700 equation of state with fermionic dark matter. Figs. 8.2 and 8.3 show the relation between the radius and the mass of the neutron stars at different % contributions of bosonic and fermionic dark matter to the total mass of the neutron stars.

The total mass and radius of the neutron star reduce when they capture more dark matter inside them. As discussed above, the observational constraint for the total (maximum) neutron

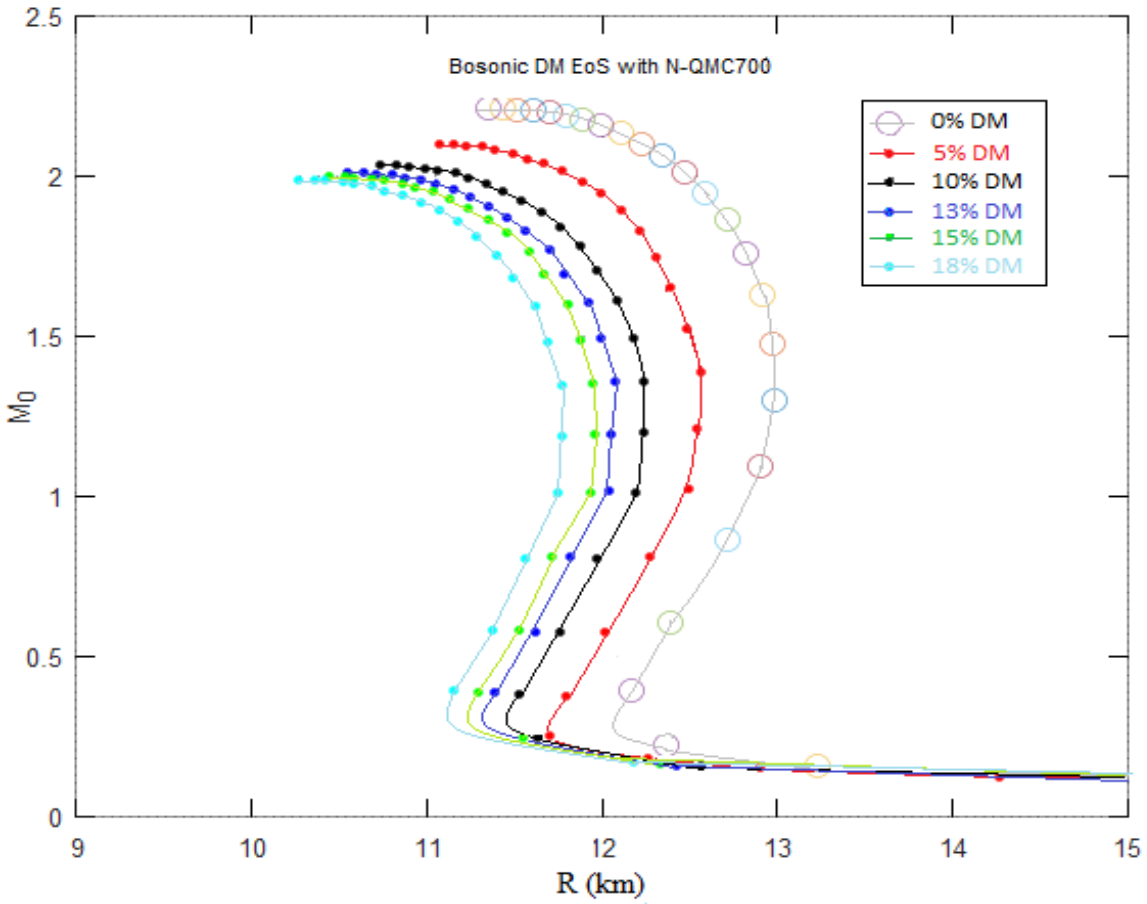

FIGURE 8.2: Total mass (given in solar masses) against the radius of the neutron stars, which contain nucleons only at the core. The bosonic dark matter is captured from the surroundings, and the plot is given for different % contributions of bosonic dark matter mass to the total mass of the neutron star, where m_χ = 1 GeV and l_χ = 1 fm.

star mass suggests that a neutron star should have a maximum mass of at least two solar masses. As shown in Figure 8.2, the constraint on the maximum mass is satisfied if the bosonic dark matter contribution to the total mass of the neutron star is less than 15%. As shown in Figure 8.3, when the fermionic dark matter contribution is less than 10% of the total mass of the neutron star, its maximum mass remains above 2 solar masses, and as the dark matter mass increases more than that, the maximum mass of the neutron star falls below 2 solar masses. Moreover, there is a significant difference in the radii of bosonic and fermionic dark matter neutron stars, when dark matter contribution is 15% of the total neutron star mass.

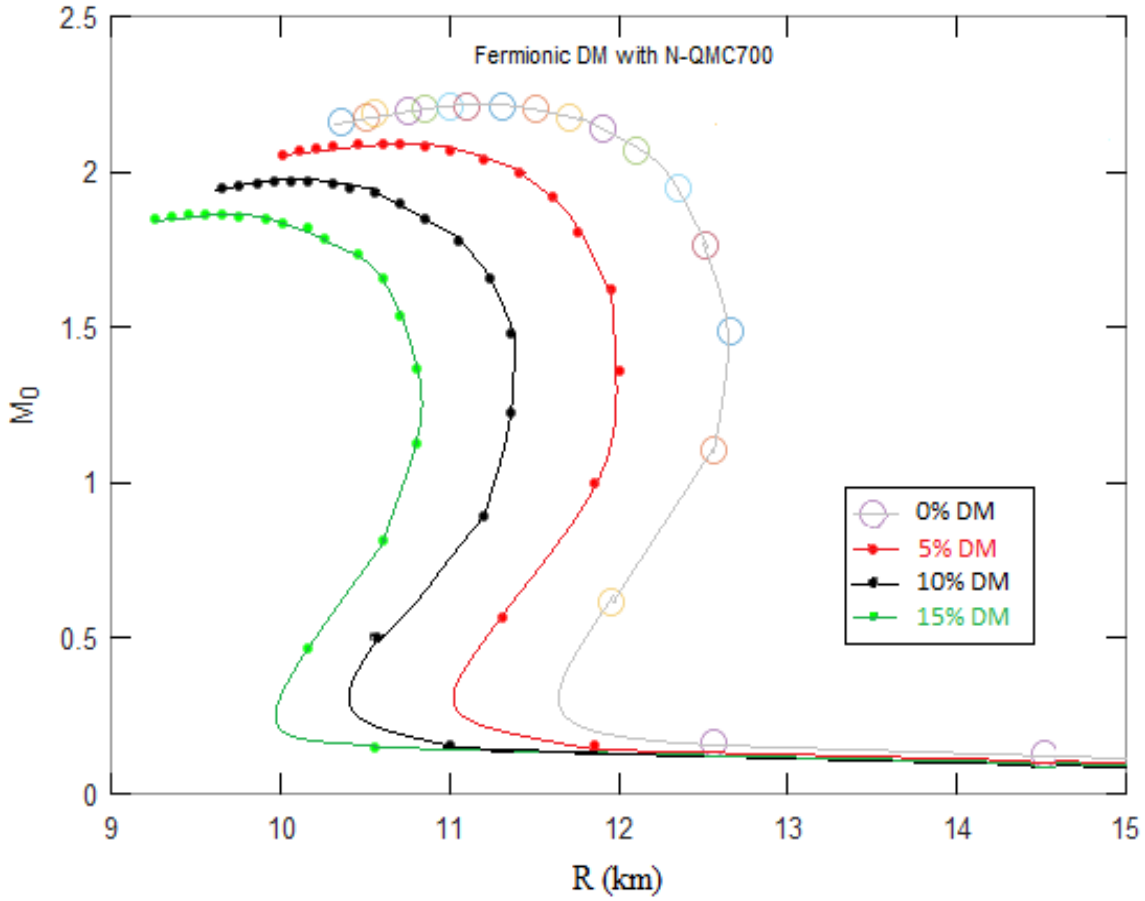

FIGURE 8.3: Total mass (given in solar masses) is plotted against the radius of neutron stars with nucleons only at the core, where fermionic dark matter is captured from the surroundings. The plot shows different % contributions of fermionic dark matter mass to the total mass of the neutron star, where m_I = 100 MeV and m_χ = 1 GeV.

The neutron stars with N-QMC700 and bosonic dark matter at the core are relatively heavier and bigger in size than their fermionic counterparts.

Figures 8.4 and 8.5 depict the effects of dark matter on neutron stars containing hyperons at higher energy densities of nuclear matter. Specifically, Figure 8.5 shows the total mass vs. radius for bosonic dark matter captured at the core of F-QMC700, while Figure 8.4 represents fermionic dark matter. Both figures (8.4 and 8.5) reveal that the presence of dark matter causes the neutron stars to become smaller in size and less massive. The neutron stars with hyperons at the core have a maximum mass smaller than 2 solar masses when the dark matter contribution to the total neutron star mass reaches 5%. The radii of hyperons included neutron

stars with bosonic and fermionic dark matter at the core, are significantly different for the same percentage of dark matter mass inside the core.

In general, fermionic dark matter neutron stars are smaller compared to bosonic dark matter neutron stars when they have the same % contribution of dark matter mass due to the larger effective mass of fermionic particles. While the presence of hyperons at the core does make the neutron stars lighter compared to the nucleons only equation of state. It also makes the equation of state softer, which does not allow the neutron stars to reach higher masses. However, the capture of dark matter makes the neutron stars collapse faster and prevents them from reaching masses of 2 solar masses.

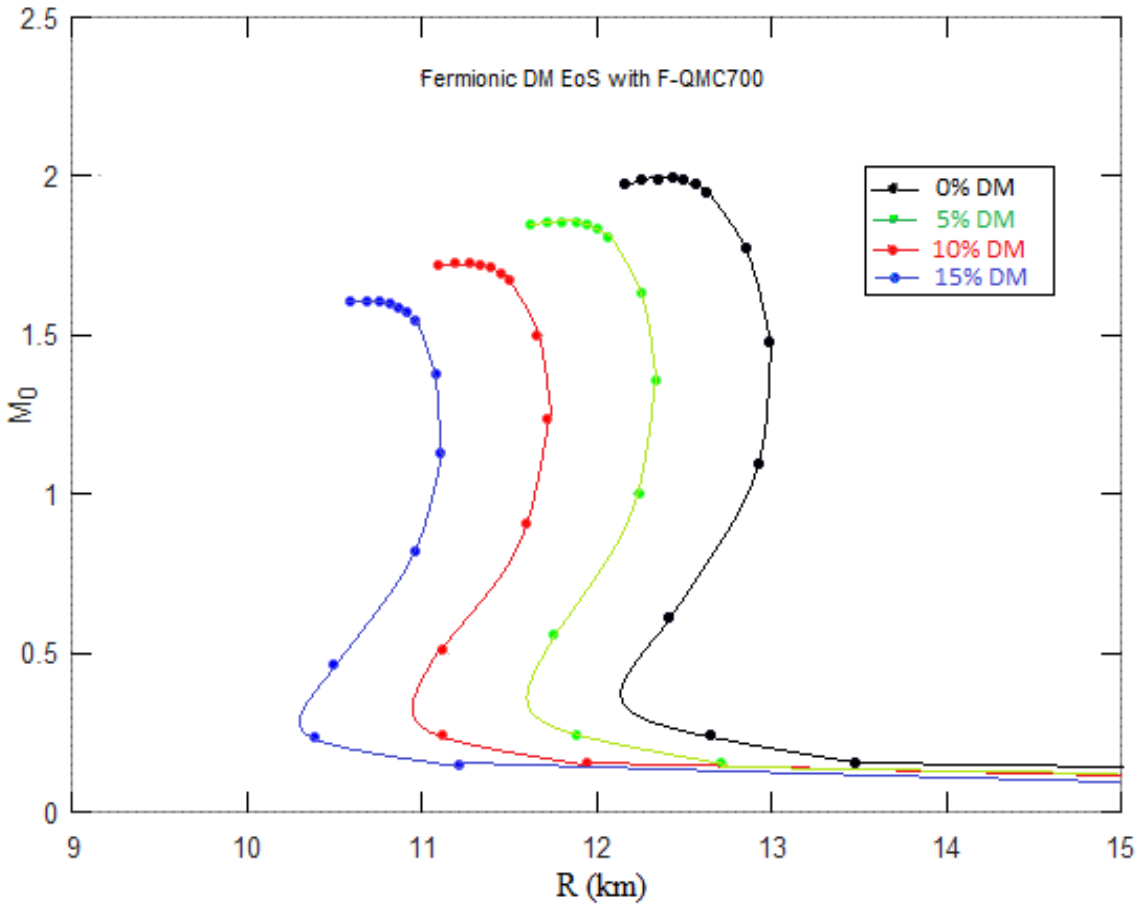

FIGURE 8.4: Total mass (given in solar masses) against the radius of the neutron stars, which contain hyperons with fermionic dark matter at the core. The plot is given for different % contributions of fermionic dark matter mass to the total mass of the neutron star, where m_I = 100 MeV and m_χ = 1 GeV.

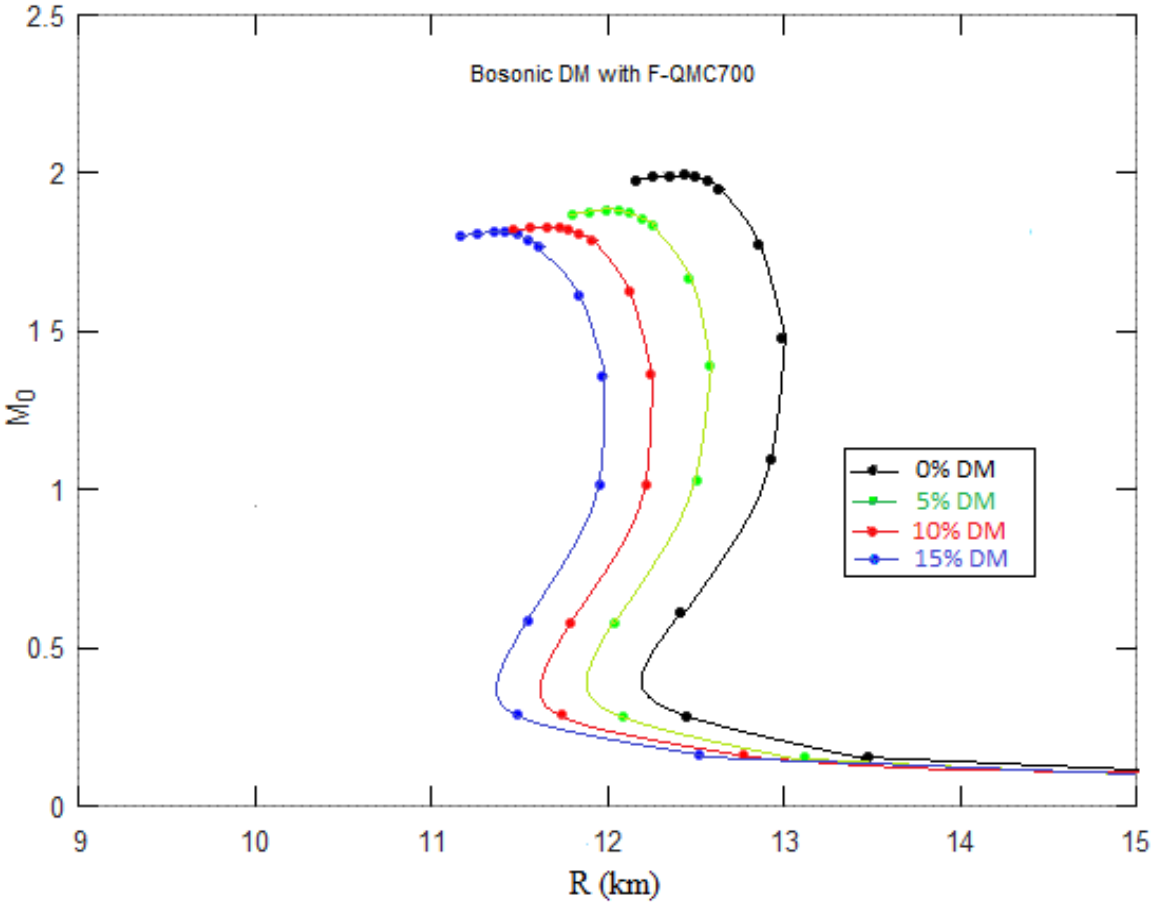

FIGURE 8.5: Total mass (given in solar masses) against the radius of the neutron stars, which contain hyperons with bosonic dark matter at the core. The plot is given for different % contributions of bosonic dark matter mass to the total mass of the neutron star, where l_χ = 1 fm and m_χ = 1 GeV.

Figures 8.6 and 8.7 are constructed to display the relationship between the mass and the radius for neutron stars containing deconfined quark matter at the core, also called strange matter at the core with dark matter. Figure 8.6 represents the strange matter equation of state with bosonic dark matter, and Figure 8.7 displays the results for a strange matter equation of state with fermionic dark matter at the core. Strange matter stars are slightly heavier than F-QMC700 neutron stars when they do not have dark matter trapped inside them. Without dark matter, they produce neutron stars of maximum mass close to 2 $M_\odot$. However, similar to F-QMC700 neutron stars, strange matter equation of state neutron stars with dark matter have a maximum mass of less than 2 $M_\odot$ when dark matter particles contribute just 5% of the total mass of the neutron stars. The behaviour of fermionic and bosonic dark matter with

strange matter equation of state neutron star is similar in terms of the impact on the mass and radius of the neutron star. Both types of dark matter cause a reduction in the maximum mass that the neutron star can have, with the presence of dark matter resulting in neutron stars with maximum masses less than 2 $M_{\odot}$. Additionally, the neutron stars become slightly smaller in size when dark matter is present. There is no significant difference in the total mass and radius of strange matter neutron stars when they have a same % of dark matter compared to F-QMC700 neutron stars.

From the mass vs. radius plots, it is evident that the contribution of 5% of the mass by dark matter is enough to make significant changes in the properties of the neutron stars.

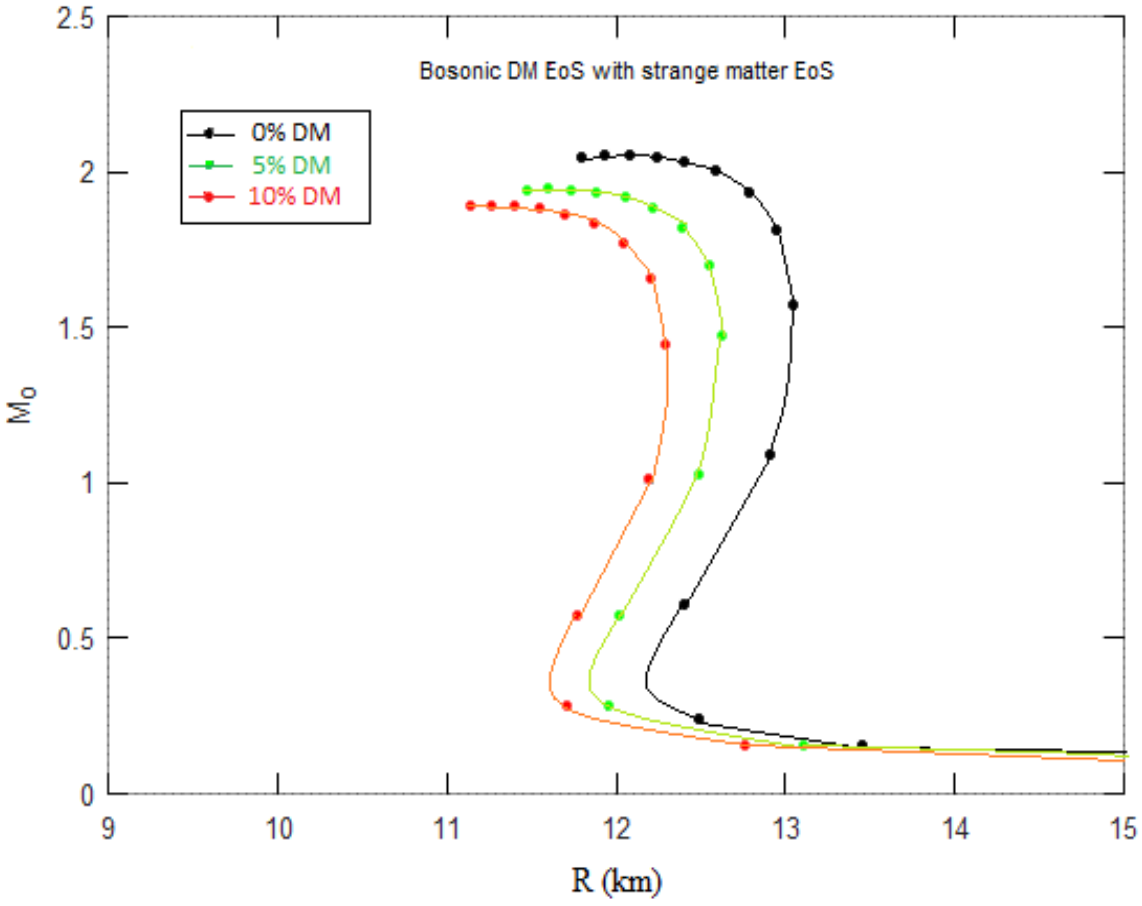

FIGURE 8.6: Total mass (given in solar masses) against the radius of the neutron stars, which contain strange matter with bosonic dark matter at the core. The plot is given for different % contributions of bosonic dark matter mass to the total mass of the neutron star, where l_{χ} = 1 fm and m_{χ} = 1 GeV.

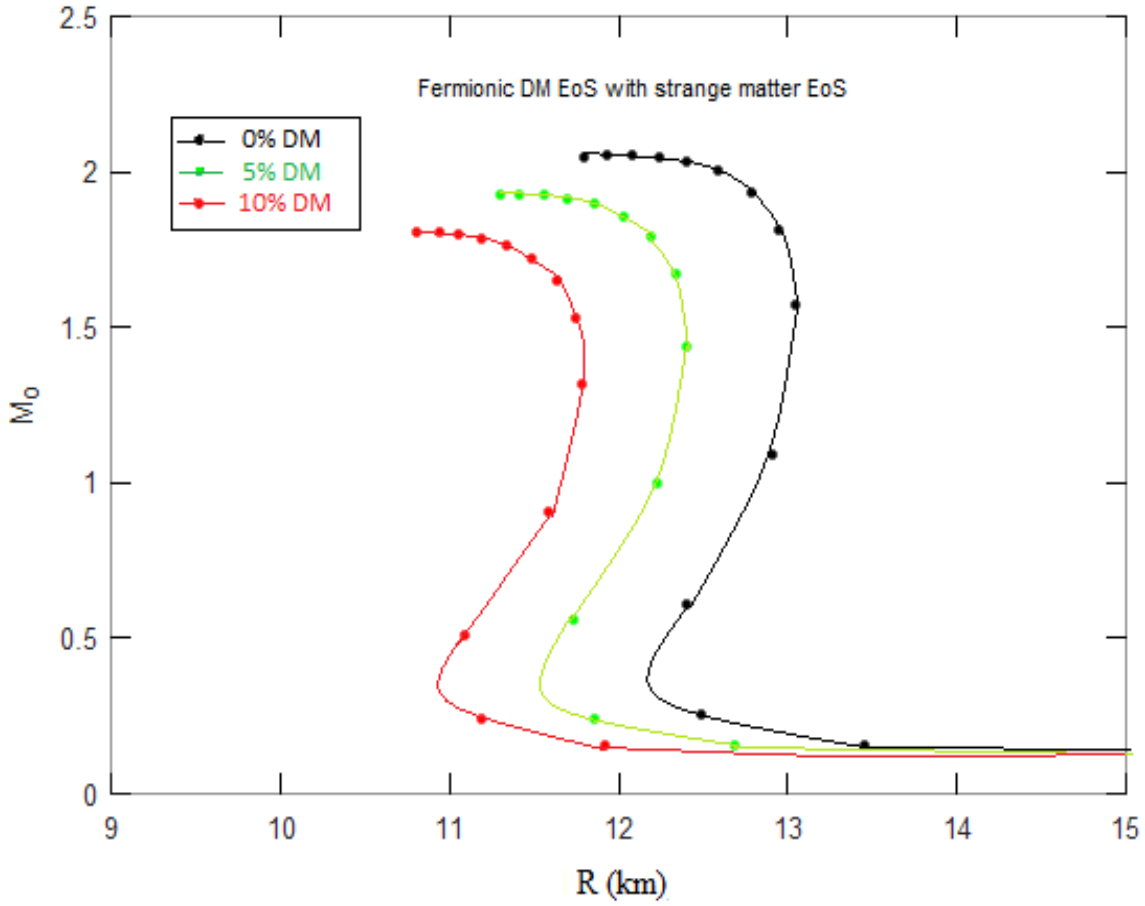

FIGURE 8.7: Total mass (given in solar masses) against the radius of the neutron stars, which contain strange matter with fermionic dark matter at the core. The plot is given for different % contributions of fermionic dark matter mass to the total mass of the neutron star, where m_I = 100 MeV and m_χ = 1 GeV.

Figures 8.8 to 8.13 are given to show the distribution of dark matter and the nuclear matter inside the neutron star. We can obtain some insight (Nelson et al. 2019) into the structure of neutron stars containing dark matter, which contributes 5% of the total mass. These figures (8.8 to 8.13) display the distribution of energy densities of dark matter and nuclear matter inside the neutron star, from the center to the surface. Figures 8.8, 8.9, and 8.10 show the distribution of energy density of the nuclear matter and the fermionic dark matter inside the neutron stars with the F-QMC700 equation of state, the N-QMC700 equation of state, and the strange matter equation of state, from the center towards the surface. Figures 8.11, 8.12, and 8.13 display the distribution of energy density of the bosonic dark matter inside the neutron stars for the N-QMC700 equation of state, F-QMC700 equation of state, and strange matter

equation of state energy density, respectively. The distribution of the energy density of dark matter suggests that bosonic dark matter remains inside the neutron star, irrespective of the nuclear matter the neutron stars contain at the core (hyperons, nucleons, or strange matter). Whereas, the distribution of fermionic dark matter is very different inside the neutron stars; in fact, fermionic dark matter envelops the neutron stars, irrespective of the nuclear matter the neutron stars contain at the core (hyperons, nucleons, or strange matter). The bosonic dark matter condenses and remains trapped inside the surface of the neutron star within a radius of a few kilometers. Whereas, fermionic dark matter covers the whole neutron star, right from the center of the neutron star to outside its surface. The pressure of fermionic dark matter does not vanish before that of nuclear matter pressure, as shown in Figs. 8.8, 8.9, and 8.10. For instance, the distances from the centre of the neutron star to the points where fermionic dark matter vanishes are: N-QMC700 has a radius of 220.3 km, F-QMC700 has a radius of 223.47 km, and strange matter has the largest radius of 225.9 km. A similar phenomenon that forms a dark matter halo around the neutron star is reported in Ref. Nelson et al. 2019. Compared to bosonic dark matter, fermionic dark matter requires a smaller energy density at the center to contribute 5% of the total mass of the neutron star.

Figures 8.14 to 8.19 have been produced to show the tidal deformability of neutron stars containing dark matter inside the core, against the mass of the neutron stars. Figures 8.14 to 8.16 display the tidal deformability of neutron stars against their radius with condensed bosonic dark matter at the core. Figures 8.17, 8.18, and 8.19 show the tidal deformability of neutron stars containing fermionic dark matter inside them. As the dark matter contribution inside the neutron star increases, its tidal deformability decreases, because the neutron star becomes smaller in size and they tend to become more compact, which can also be seen in mass vs. radius plots. The equation of state based on the QMC model shows that neutron stars have higher tidal deformability, while the strange matter neutron stars show lower values of tidal deformability when they do not have dark matter inside them, while QMC700 and strange matter equations of state satisfy the tidal deformability constraint if they contain a certain amount of dark matter inside them. The dark matter contribution to neutron star mass that satisfy the tidal deformability constraint is as follows. For a neutron star of mass 1.4 $M_{\odot}$, having a dark matter mass between 5% to 18% (Husain and Thomas 2021b) of the

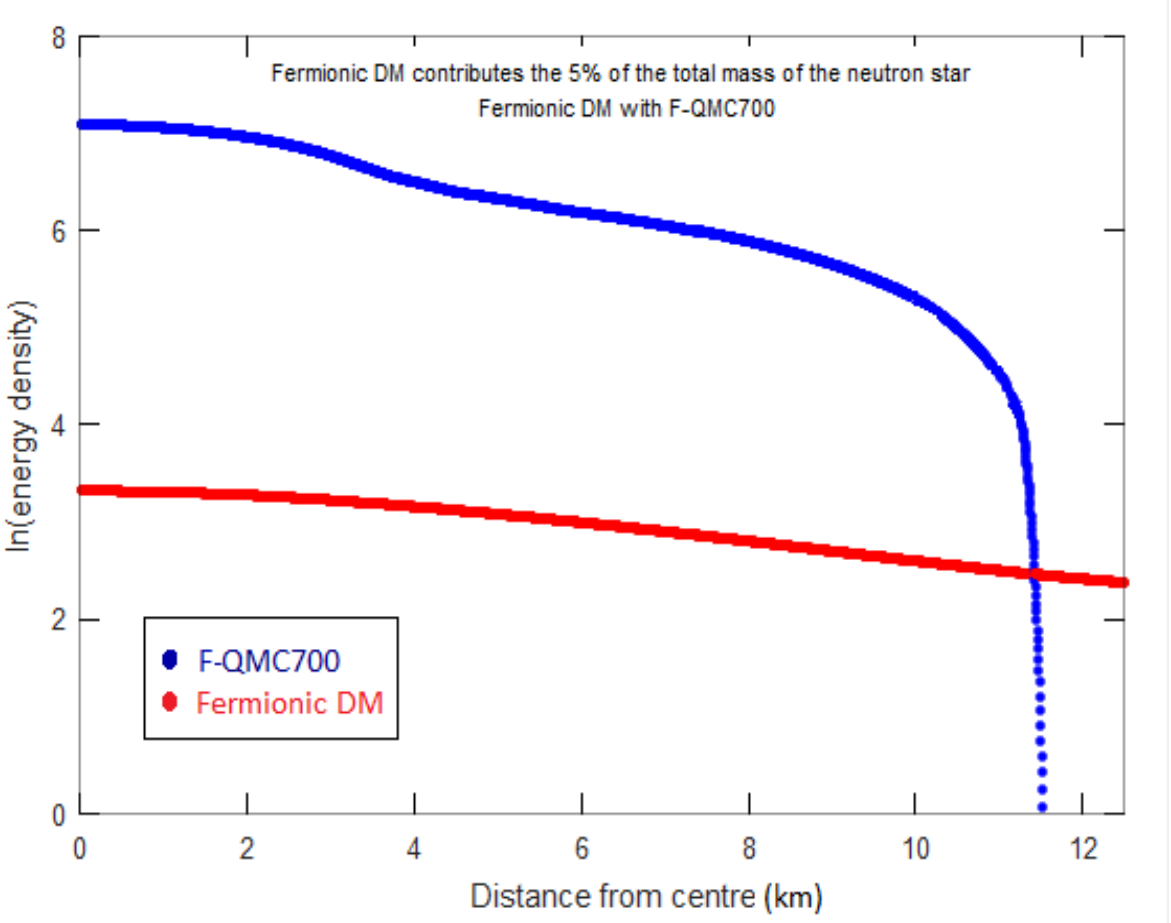

FIGURE 8.8: Distribution of fermionic dark matter and hadronic matter energy density (MeV/fm^3) inside the neutron star (from the center towards the surface), which contains hyperons (F-QMC700) at the core. The dark matter mass contribution is 5% of the total mass of the neutron star.

total mass satisfies the tidal deformability constraint imposed by gravitational wave detection Abbott et al. 2017b; Abbott et al. 2019. As shown in Figure 8.15, for neutron stars with F-QMC700 and bosonic dark matter the tidal deformability decreases with increasing dark matter content inside the neutron star. The bosonic dark matter contribution between 5% to 15% for a neutron star of 1.4 $M_\odot$ satisfies the tidal deformability constraint. Figure 8.16 shows a neutron star having strange matter at the core with bosonic dark matter. The tidal deformability constraint is followed by a neutron star of mass 1.4 $M_\odot$ only when the bosonic dark matter mass contribution to the total mass is less than 5%.

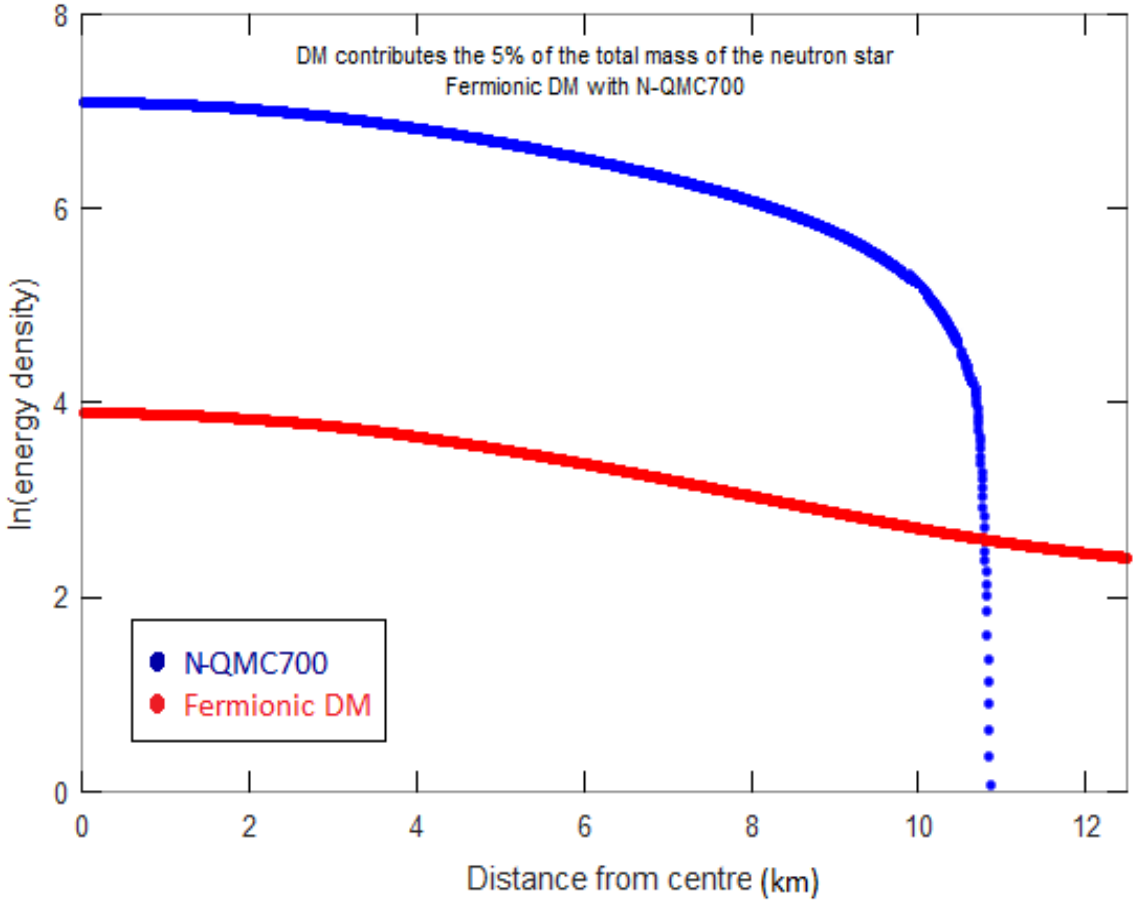

FIGURE 8.9: Distribution of fermionic dark matter and nuclear matter energy density (MeV/fm^3) inside the neutron star (from the center towards the surface), which contains nucleons only (N-QMC700) at the core, and the dark matter mass contribution is 5% of the total mass of the neutron star.

Figure 8.17, 8.18, and 8.19 are plotted for fermionic dark matter with N-QMC700, F-QMC700, and strange matter equations of state, respectively. Figure 8.17 suggests that for a neutron star of mass 1.4 $M_\odot$, the constraint on tidal deformability is only satisfied when fermionic dark matter contribution to the total mass is between 5% and 10% while for bosonic dark matter cases, it is satisfied up to 18%. Figure 8.18 indicates that for a neutron star of mass 1.4 $M_\odot$, the constraint on tidal deformability is satisfied when fermionic dark matter contribution to the total mass is between 5% and 10%, while for bosonic dark matter it is satisfied up to 15%. As suggested in Figure 8.19, a neutron star of mass 1.4 $M_\odot$, the constraint on tidal deformability is only followed when fermionic dark matter contribution to the total mass is less than 5%. The properties of neutron stars are quite different with bosonic and fermionic

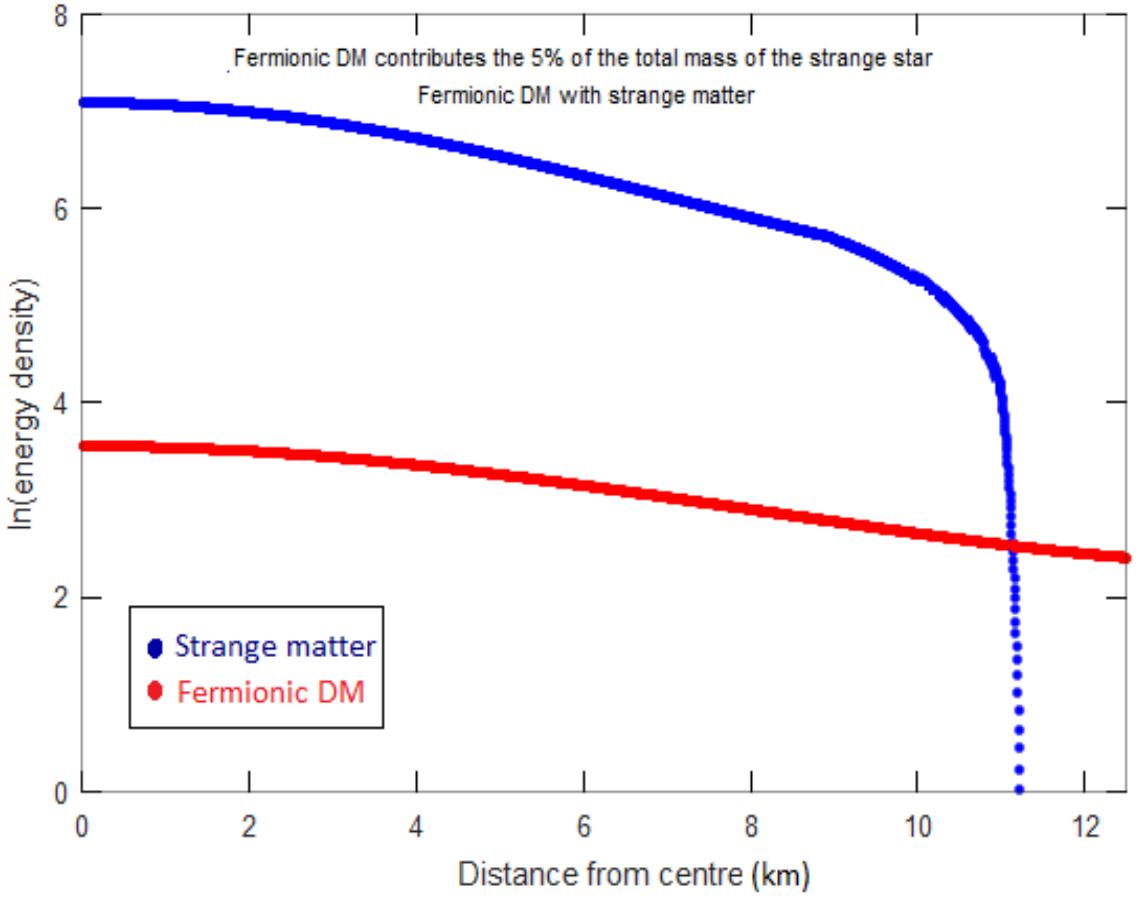

FIGURE 8.10: Distribution of fermionic dark matter and strange matter energy density (MeV/fm^3) inside the neutron star (from the center towards the surface), which contains deconfined quarks at the core. The dark matter mass contribution is 5% of the total mass of the neutron star.

dark matter, particularly the distribution of dark matter energy density, which in turn affects other properties of the neutron star, such as its total mass and radius.

In next section, the effects of neutron decay have been explored. The consequences of the decay on the properties of the neutron stars are tested against the observational constraints. In this study, a strong focus is kept on the total baryon number and conservation of energy. There are two hypothesis that are given above, namely, the Fornal and Grinstein hypothesis, and the Strumia hypothesis for neutron decay, that are taken into consideration.

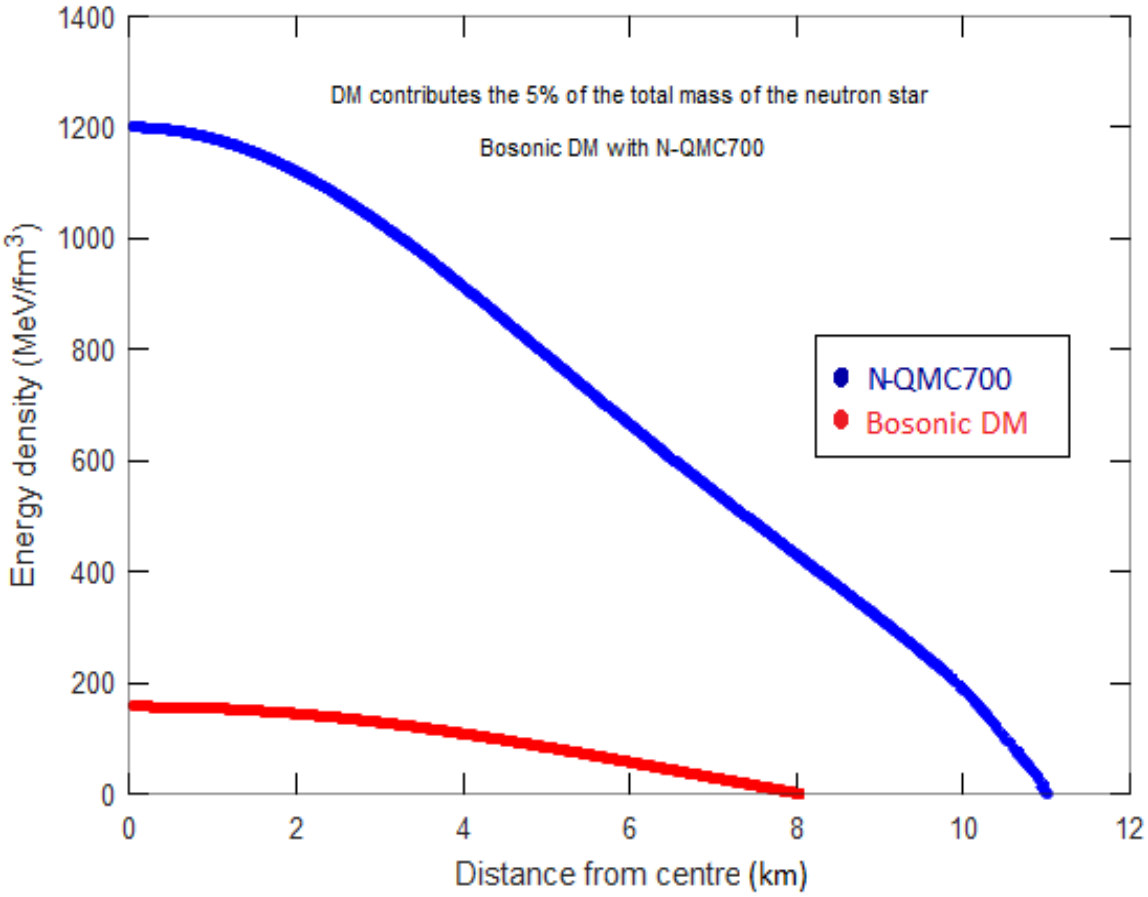

FIGURE 8.11: Distribution of bosonic dark matter and nuclear matter energy density inside the neutron star (from the center towards the surface), which contains nucleons only (N-QMC700) at the core. The dark matter mass contribution is 5% of the total mass of the neutron star.

8.2 Consequences of the Fornal and Grinstein hypothesis of neutron decay into dark matter

The equation of state of neutrons decaying into dark matter according to the Fornal and Grinstein hypothesis given above is integrated with the nuclear matter equation of state and two fluid structural equations, and the properties of the neutron stars are calculated as follows:

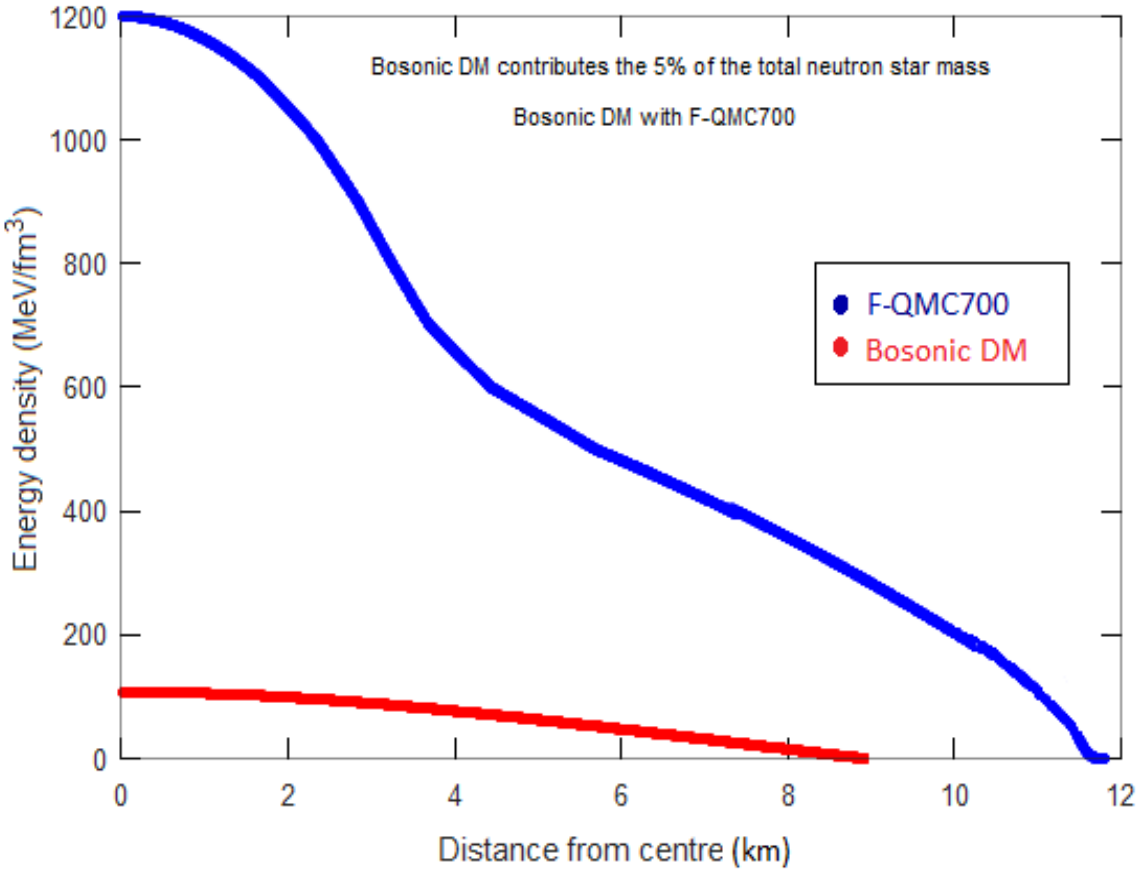

FIGURE 8.12: Distribution of bosonic dark matter and nuclear matter energy density inside the neutron star (from the center towards the surface), which contains hyperons (F-QMC700) at the core. The dark matter mass contribution is 5% of the total mass of the neutron star.

8.2.1 Mass and tidal deformability of the neutron star and the population of dark matter

Figure 8.20 displays the relationship between pressure and the energy density of matter inside the neutron star. Before neutrons decay into dark matter, the equation of state is stiff and produces neutron stars with a maximum mass above 2 $M_{\odot}$. As neutrons decay into dark matter, following the Fornal and Grinstein hypothesis, the pressure reduces significantly when dark matter is assumed to be non-self-interacting and produces neutron stars of maximum mass of 0.7 $M_{\odot}$. To produce heavier neutron stars, the equation of state must be stiff. Therefore, dark matter self interaction is introduced and increased until it produces the neutron star of 2 $M_{\odot}$.

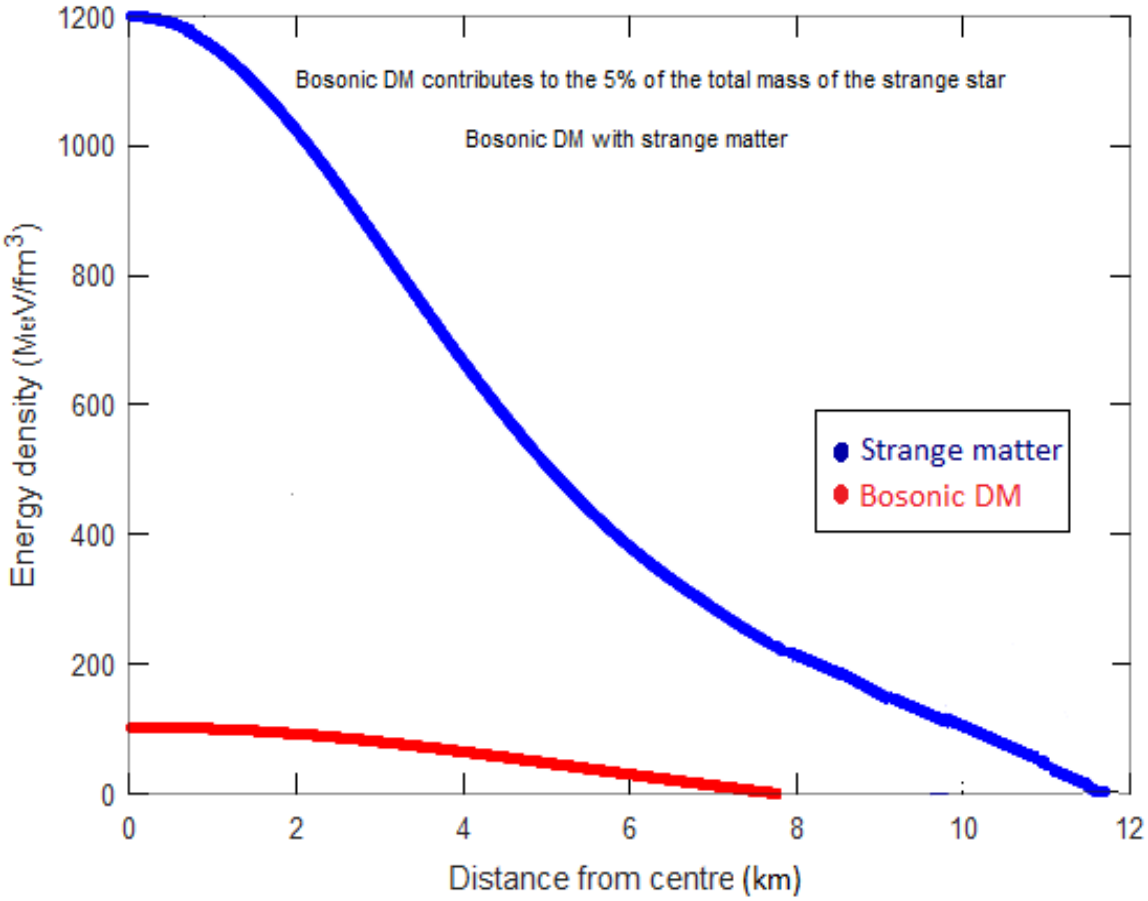

FIGURE 8.13: Distribution of bosonic dark matter and strange matter energy density inside the neutron star (from the center towards the surface), which contains deconfined quarks at the core. The dark matter mass contribution is 5% of the total mass of the neutron star.

The self-interaction of dark matter is considered similar to the neutron-ω coupling, which is given by G, which is defined as

$$G = \left(\frac{g_{int}}{m_{int}}\right)^2, \tag{8.1}$$

where g_{int} is the coupling constant and m_{int} is the mass of the interchange particle. Figure 8.21 is plotted to display the relation between the mass and the radius of neutron stars. From Figure 8.21, it is evident that as the neutrons decay into dark matter, if the dark matter is non-self-interacting ($G = 0$ fm^2), the maximum mass of the neutron star falls from 2.23 $M_\odot$ to 0.7 $M_\odot$, which is consistent with what is shown in Ref. Motta et al. 2018b. Therefore, the dark matter repulsive self-interaction must be strong to sustain the neutron star against gravity and produce a neutron star of maximum mass of at least 2 $M_\odot$. Indeed, as shown in

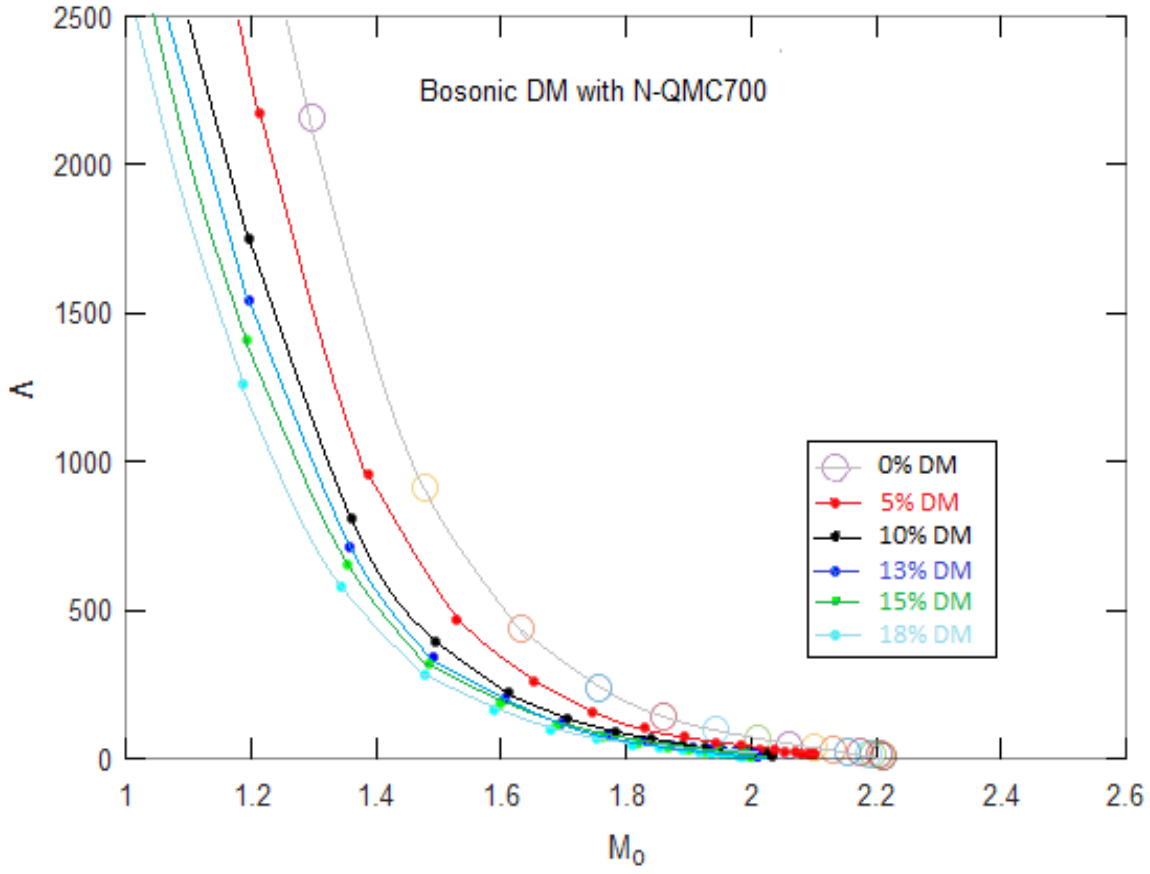

FIGURE 8.14: Tidal deformability against the mass (given in solar masses) of the neutron star, which contains nucleons only matter (N-QMC700) and different amounts of bosonic dark matter mass contribution to the total mass of the neutron stars.

Fig. 8.21, to get a neutron star of 2 $M_\odot$, the dark matter self-repulsion must have a strength of at least $G = 26$ fm^2, which agrees with the findings proposed in Ref. Cline and Cornell 2018. Figure 8.22 shows the tidal deformability of a neutron star against its mass. The discovery of gravitational waves (Abbott et al. 2017b; Abbott et al. 2019; Bramante et al. 2018) from the binary neutron star merger GW170817 puts a constraint on the tidal deformability that is the first analysis Abbott et al. 2017b shows that a neutron star of mass 1.4 $M_\odot$ must have tidal deformability in the range, $70 \leq \Lambda \leq 580$, at 90% confidence level. Fig. 8.22 shows that this constraint on tidal deformability is satisfied when neutrons decay into dark matter inside the neutron stars.

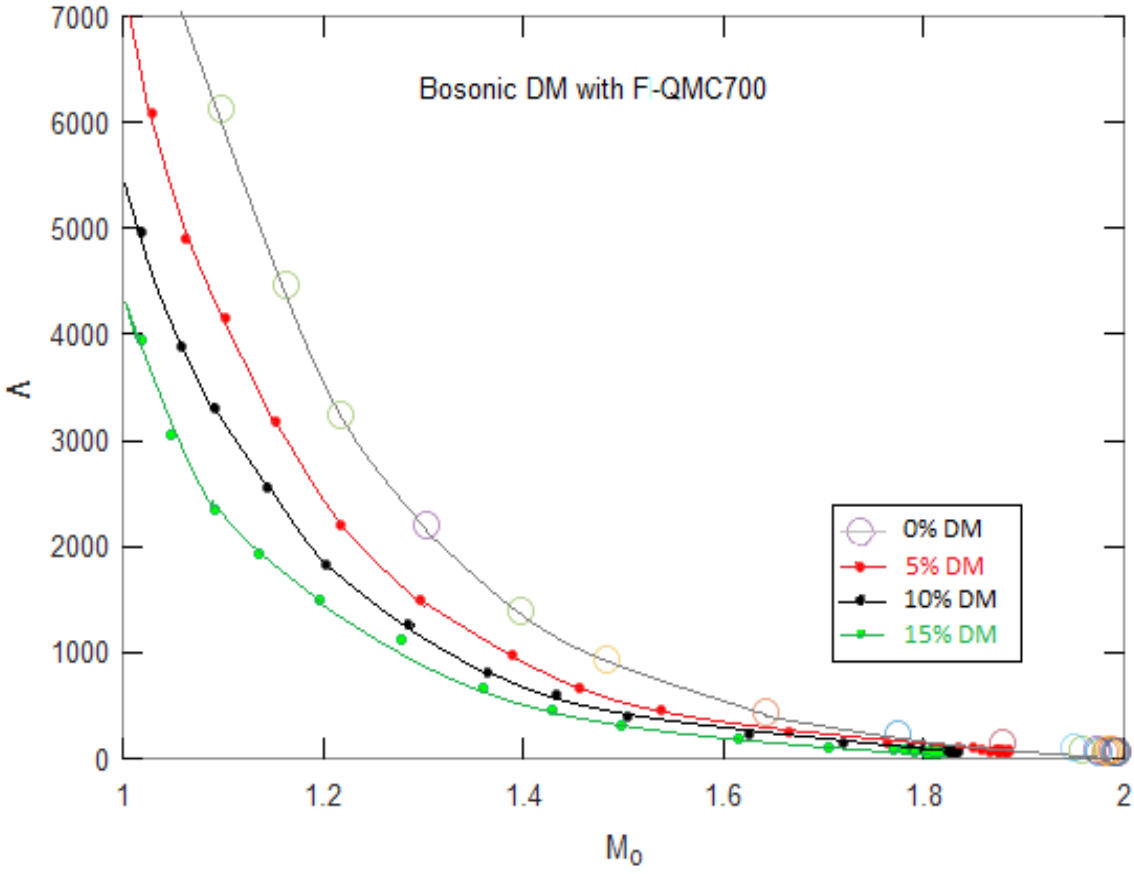

FIGURE 8.15: Tidal deformability against the mass (given in solar masses) of the neutron star, which contains hyperons (F-QMC700) and different amounts of bosonic dark matter mass contribution to the total mass of the neutron stars.

In the process of neutron decay, described in Eq. (6.5), it is not expected that the energetics permit the baryonic matter to be lost or emitted from the neutron star. Therefore, we expect that in the process of neutron decay into dark matter, the total number of baryons inside the neutron star must remain constant. The total energy of the system must not increase, but some of the energy is expected to be lost via ϕ bosons that will leave the neutron star immediately. Figures 8.23 and 8.24 display the population of different kinds of baryons against the different self-repulsive strengths of dark matter. Figure 8.23 is given for a heavier neutron star, which contains 2.4×10^{57} baryons while Figure 8.24 is plotted for a lighter neutron star, which contains only 2.4×10^{57} baryons inside it. As shown in both figures (8.23 and 8.24), the population of dark matter particles reduces significantly with the increment of dark matter self-repulsion. As indicated in Figure 8.21 for the sake of satisfying the constraint on the

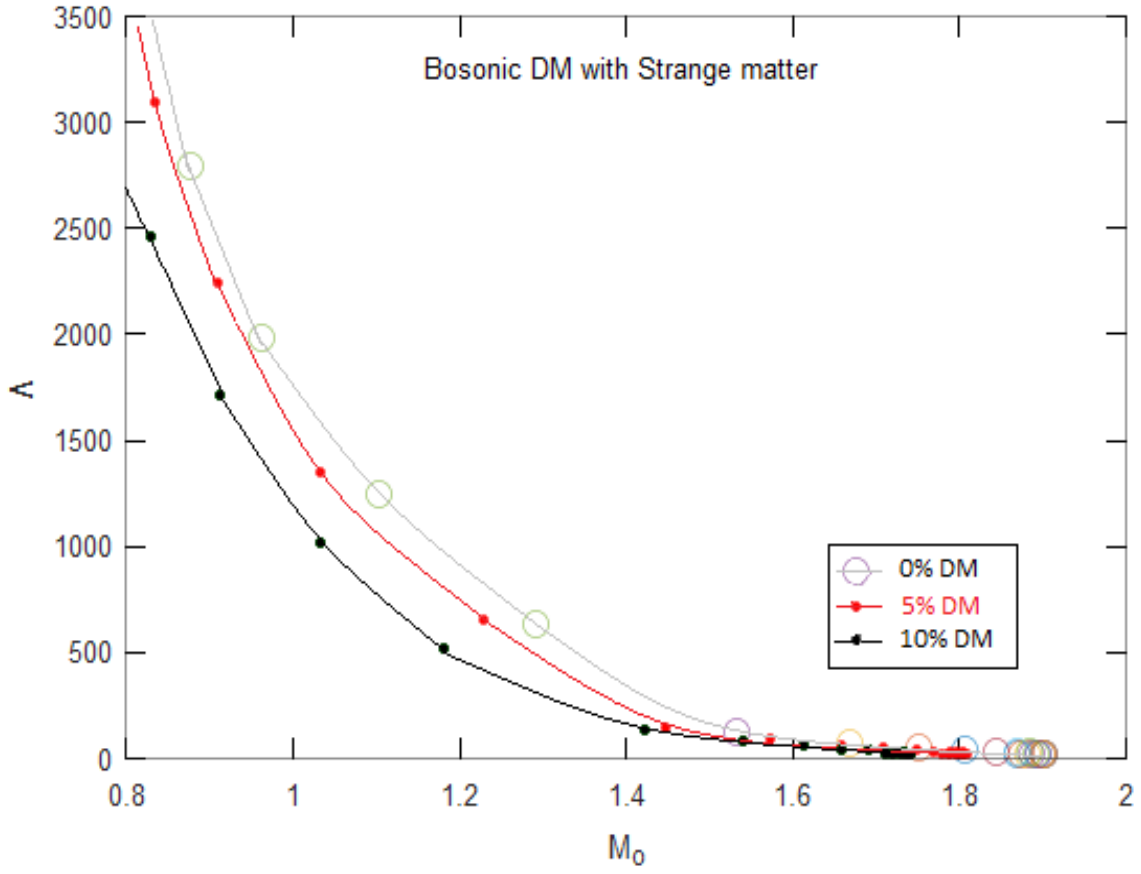

FIGURE 8.16: Tidal deformability against the mass (given in solar masses) of the neutron star, which contains strange matter and different amounts of bosonic dark matter mass contribution to the total mass of the neutron stars.

maximum mass of the neutron stars, the dark matter must be strongly self-interacting with $G \geq 26$ fm^2, so we are only interested in the dark matter self interaction, $G \geq 26$ fm^2, and at those values of dark matter self-interaction, the population of dark matter inside the neutron stars is much smaller compared to the number of protons and neutrons they contain.

8.2.2 Conservation of baryon number

In this section, focus is kept on the conservation of baryons, total energy, and momentum. During the process of neutron decay, the total energy-momentum, and the number of baryons must be conserved. Therefore, Figure 8.25 is plotted to show the number of particles (baryons)

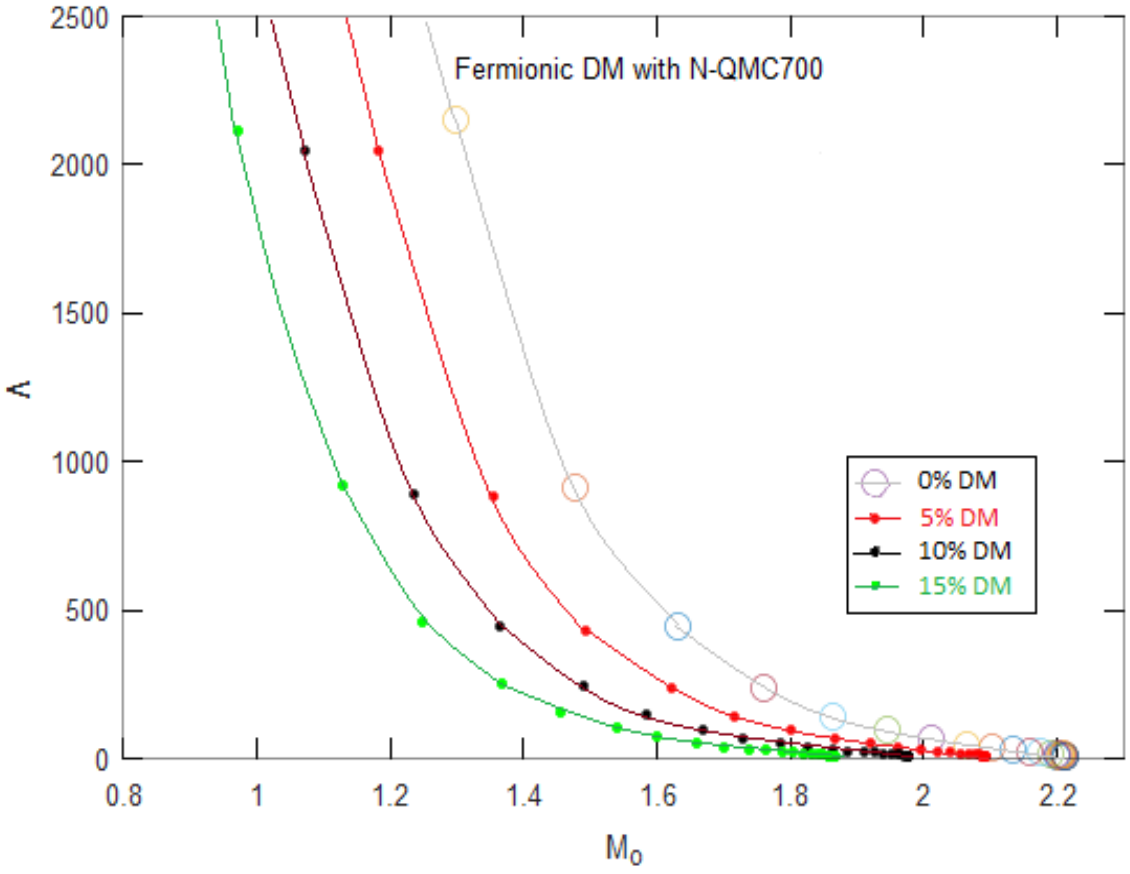

FIGURE 8.17: Tidal deformability against the mass (given in solar masses) of the neutron star, which contains nucleons only (N-QMC700) and different amounts of fermionic dark matter mass contribution to the total mass of the neutron stars.

inside the neutron star of mass 1.8 $M_\odot$ as a function of the strength of the dark matter self-repulsion. This naively suggests that the number of baryons inside the neutron star will not be conserved, which agrees with the study given in Baym et al. 2018. The plot in Figure 8.25 indicates that if decay takes place inside the neutron star, keeping the mass of the star fixed, the number of particles (baryons) inside the neutron star must increase, which is not possible, and as remarked earlier, we expect that the total number of baryons must be conserved. It is shown in Fig. 8.25 that for lower strength of dark matter self-interactions, the increment in the number of particles (baryons) is sharp. As mentioned above, we are interested in the strength of dark matter self-repulsion only in the region where $G \geq 26$ fm^2. It is found that at $G = 26$

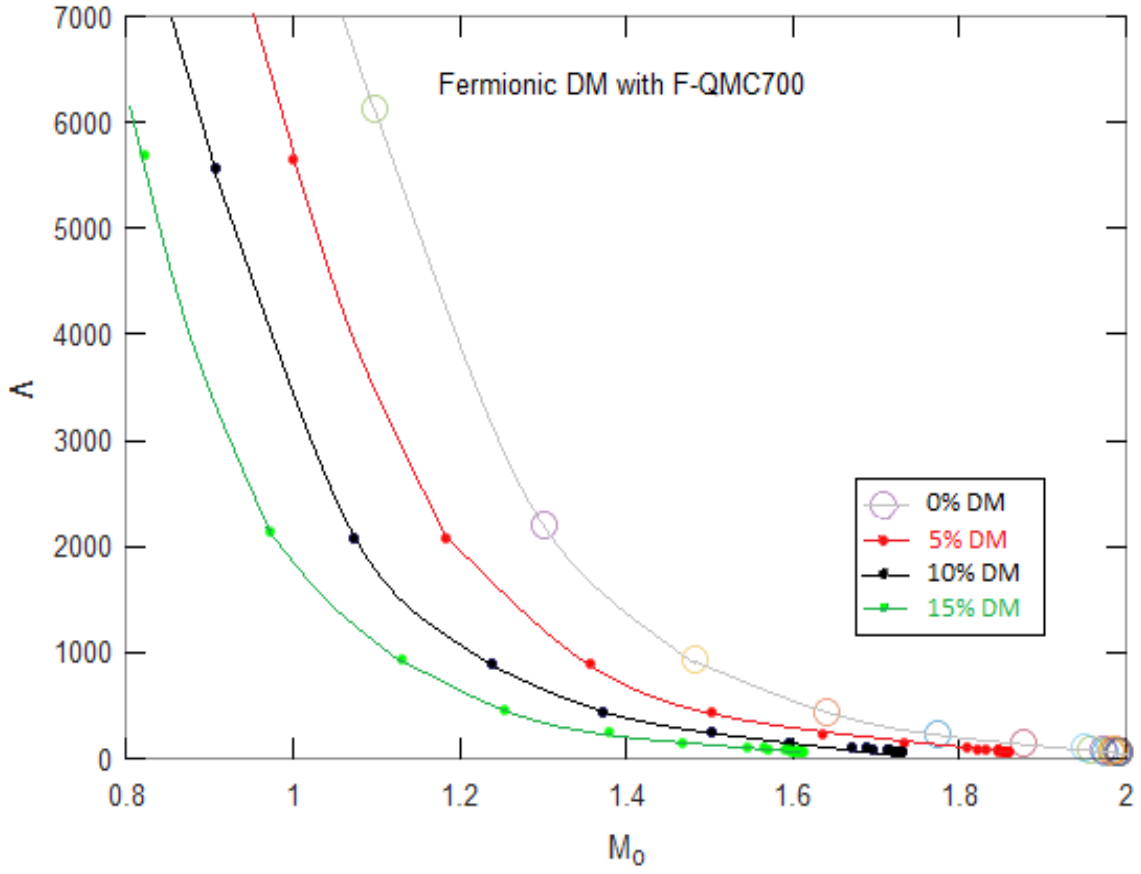

FIGURE 8.18: Tidal deformability against the mass (given in solar masses) of the neutron star, which contains hyperons (F-QMC700) and different amounts of fermionic dark matter mass contribution to the total mass of the neutron stars.

fm^2, the total number of baryons inside the neutron star after the decay is approximately 2.5 $\times$ 10^{55}, or 1% more than the initial number, where the mass of the neutron star is held fixed.

To explore this phenomenon, further plots are presented in Figs. 8.26 and 8.27, where the mass of the neutron star is plotted against the strength of self-repulsion of the dark matter. The total number of particles (baryons) inside the neutron star is kept fixed at 2.4 $\times$ 10^{57} in one plot and 2 $\times$ 10^{57} baryons in the other plot, respectively. In both figures, the mass of the neutron star is smaller than the mass of the neutron star before the decay. Indeed, the plots indicate that as the process of neutron decay takes place for a fixed total number of baryons, the mass of the neutron star reduces rapidly when the strength of the dark matter self-interaction is smaller than 26 fm^2. Both the figures (8.26 and 8.27), indicate that at G

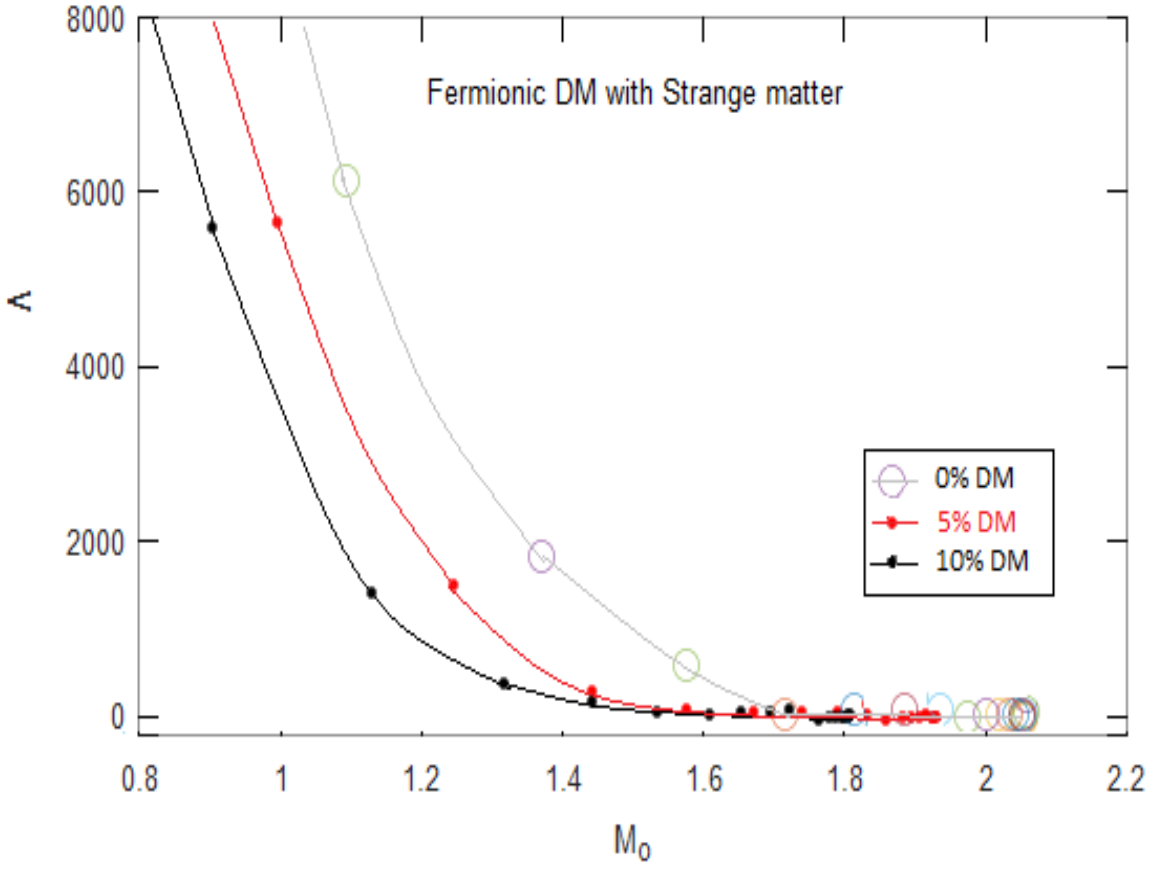

FIGURE 8.19: Tidal deformability against the mass (given in solar masses) of the neutron star, which contains strange matter and different amounts of fermionic dark matter mass contribution to the total mass of the neutron stars.

= 26 fm^2 the change in the mass of the neutron star is approximately 0.002 $M_\odot$ or 0.14%, which is quite large. Figure 8.28 displays the mass of the neutron star before and after the neutron decay, at G = 26 fm^2, for the fixed number of baryons inside the neutron star. The plot clearly shows the difference in mass of the neutron star after the neutron decay, while the number of baryons remains fixed. Clearly, this cannot happen unless we either heat the neutron star, emit this amount of energy, or do both.

8.2.3 Change in temperature of the neutron star

It is worth exploring the consequences for the star when all of the required decrease in mass is not carried by ϕ bosons. Neutron stars cool down very quickly. In fact, the nuclear matter

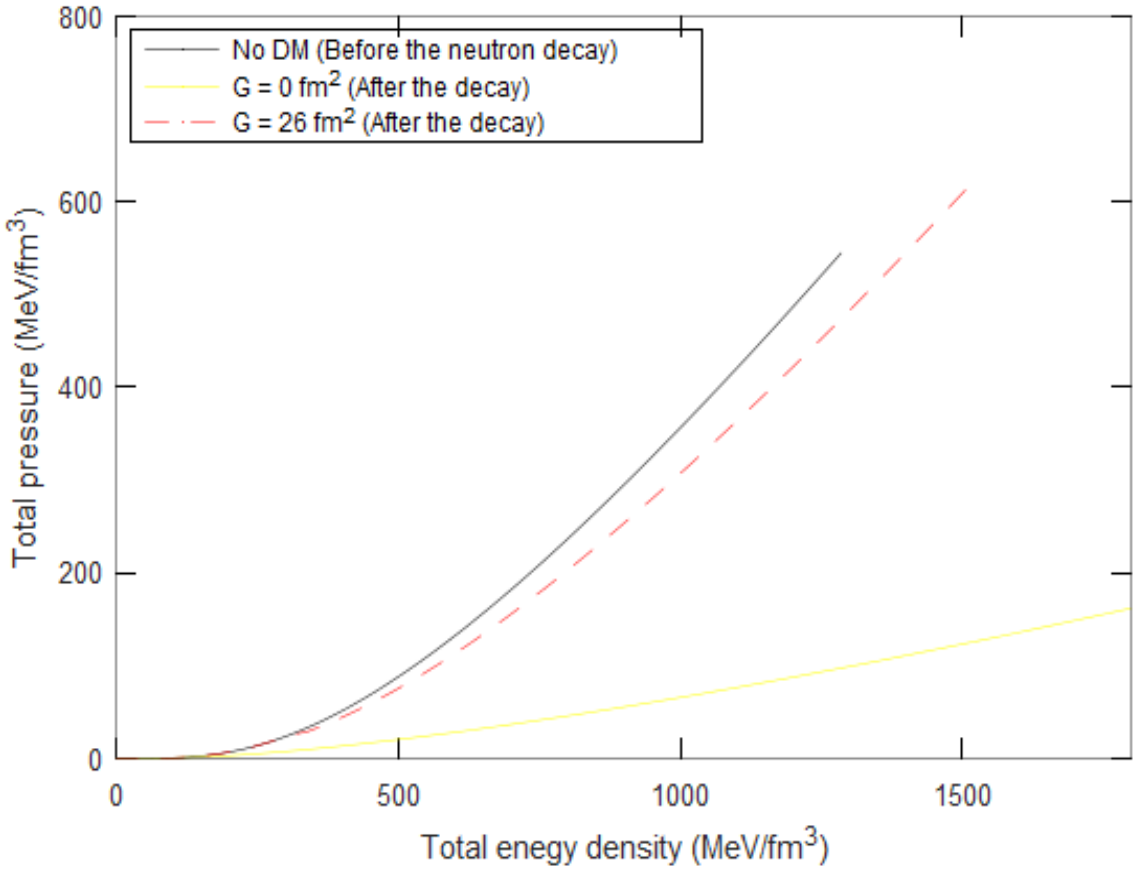

FIGURE 8.20: Equation of state for neutrons decaying into dark matter inside a neutron star according to the Fornal and Grinstein hypothesis.

of the neutron stars cools down before reaching the temperature of 1 MeV within the order of seconds. The cooling process and time scale of cooling the nuclear matter are much shorter than the time scale of neutron decay into dark matter (of the order 10^5 seconds). Thus, we may treat the neutrons as a degenerate Fermi gas while considering the effect of dark matter on the properties of the neutron star having a finite temperature. We expect the temperature of dark matter to be significantly higher than that of nuclear matter. Generally, we expect objects to expand when heated, and if the neutron star heats up during the decay, then we naively expect it to expand, which must lead to a reduction in its rotational speed. The plot shown in Fig. 8.21 for a neutron star of fixed mass at a temperature of $0\,^{\circ}K$, indicates that the radius of the neutron star is expected to reduce after the neutron decays into dark matter, or that the neutron stars have smaller radii after the decay than before. Therefore, it is a matter

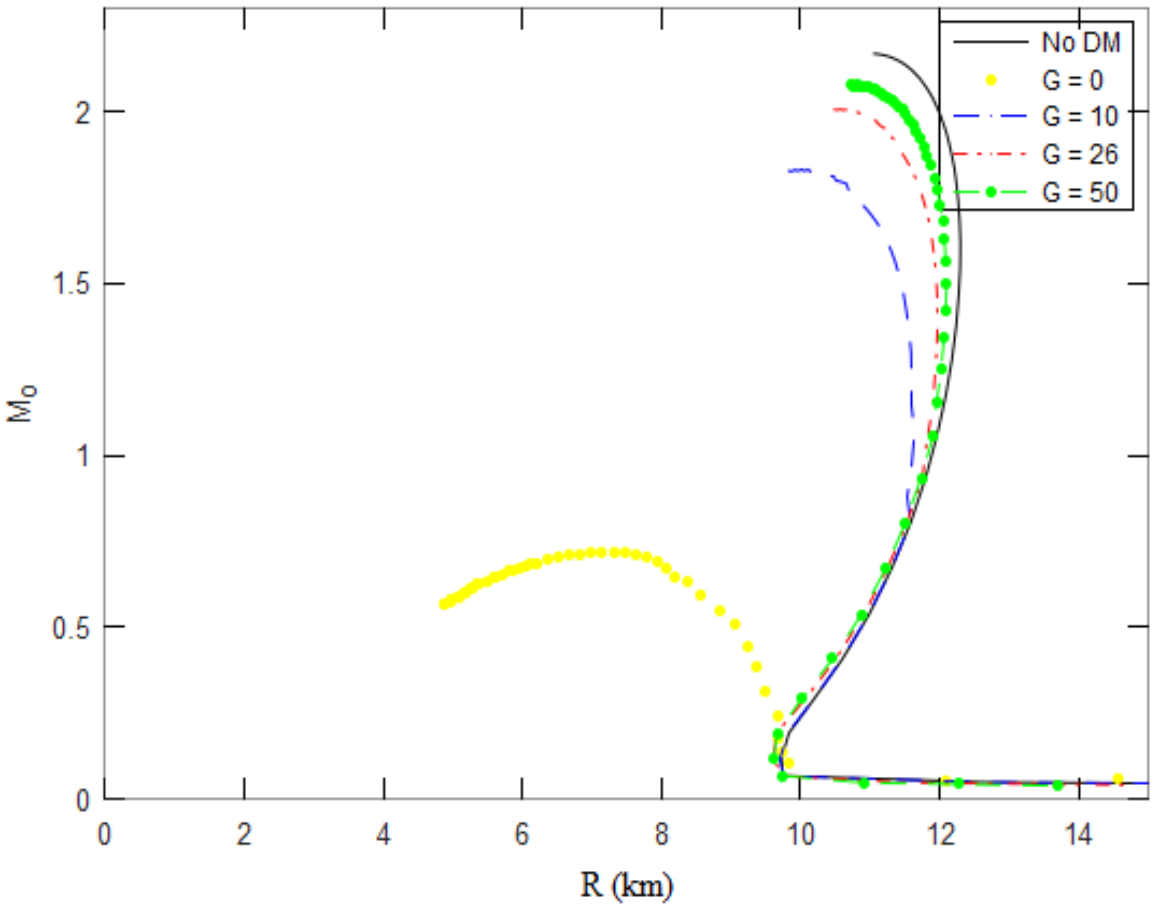

FIGURE 8.21: Total mass (given in solar masses) against the radius of the neutron star at $T = 0\ ^{\circ}K$, before and after the neutrons decay into dark matter at different dark matter self-interaction (G) strengths.

of investigation whether the neutron star expands or shrinks due to neutron decay into dark matter. To resolve the question, we compare the neutron star radius at T = $0^{\circ}K$ before the neutron decay for a neutron star that contains nucleons only, against the radius of a neutron star that contains nucleons and dark matter after the neutron decay with the same total number of baryons and the dark matter is heated by the energy equivalent of 0.001 $M_{\odot}$ (assuming energy equivalent to the rest of the mass is carried by ϕ bosons), which is a conservative upper limit (corresponding to the 1.4 $M_{\odot}$ case).

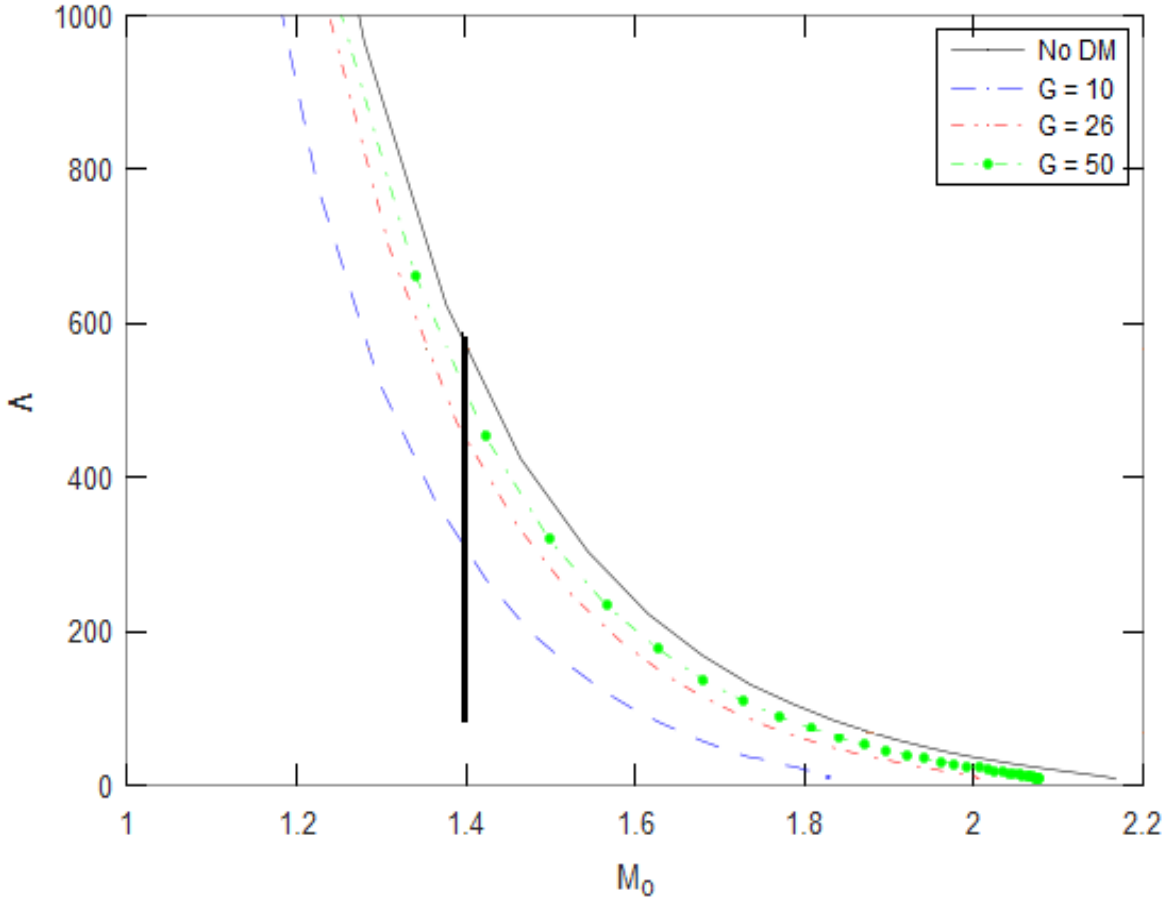

FIGURE 8.22: Tidal deformability versus mass (given in solar masses) of the neutron star at different dark matter self-interactions (G). The dark, bold vertical line gives the range of values acceptable for tidal deformability for a neutron star of 1.4 $M_{\odot}$.

	NS Mass	T (MeV)	R (km)	I (kg.m^2)
1	1.4 $M_{\odot}$ (Nuclear matter before decay)	0	12.25	1.62×10^{38}
2	1.4 $M_{\odot}$ (Nuclear matter + DM after decay)	0	11.60	1.38×10^{38}

TABLE 8.1: The properties of the neutron star are given at T = $0°K$ before and after the neutrons decay into dark matter, where T is the temperature, M is the mass of the neutron star, R stands for the radius, and I represents the moment of inertia of the neutron star.

Table 8.1 is given for the properties of the neutron stars at temperature $0°K$ before and after the neutron decay into dark matter and the total number of baryons remain conserved. From Table 8.1, it is evident that there is a significant change in the radius and moment of inertia of the neutron star after the decay at $0°K$. While Table 8.2 is presented for the properties of the

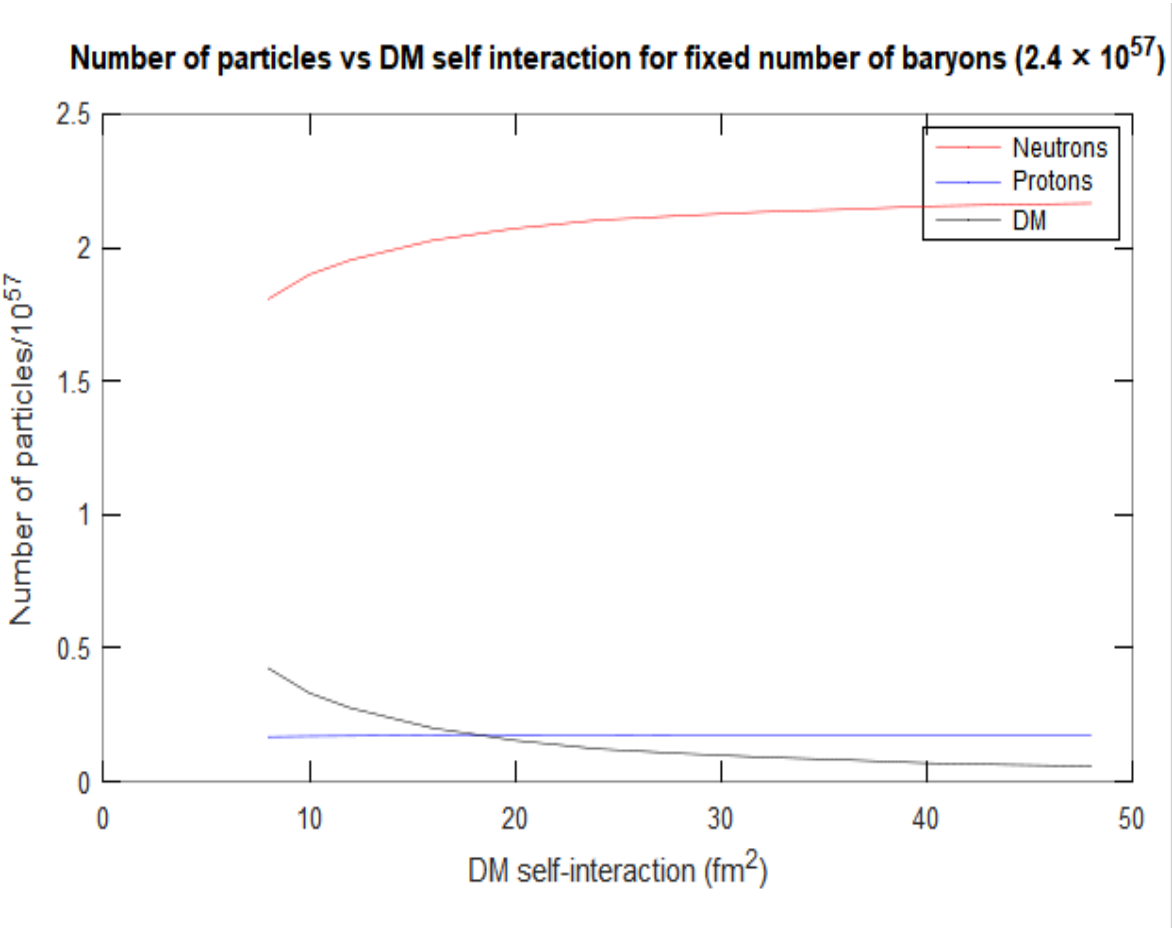

FIGURE 8.23: The population of baryons against the dark matter self-interaction G for a neutron star of a fixed total number of baryons at 2.4 $\times$ 10^{57}.

NS Mass	T (MeV)	Δ M ($M_\odot$)	Δ R (m)	% Δ R	Δ I (kg.m^2)	% Δ I
1.4 $M_\odot$	0.25 (Nuclear matter)	0.001	450 (decrease)	3.673%	0.1653$\times$ 10^{38}	10.21%
1.4 $M_\odot$	2 (DM)	0.001	620 (decrease)	5.06 %	2.28 $\times$ 10^{37}	14.11 %

TABLE 8.2: The properties of the neutron star associated with a rise in its temperature. Here, T is the rise in temperature following the decay, ΔM stands for the equivalent changes in mass associated with the decay, ΔR is the change in radius, and ΔI gives the change in moment of inertia due to the change in temperature. The radius of the neutron star after the decay is smaller compared to the radius of the neutron star before the decay. The changes in the values are given with respect to the first entry in Table 8.1.

neutron star at a certain temperature of nuclear matter and dark matter having a total number of baryons conserved. For a neutron star of mass 1.4 $M_\odot$, if only nuclear matter heats up, it will require a rise of 0.25 MeV in temperature corresponding to an energy equivalent of

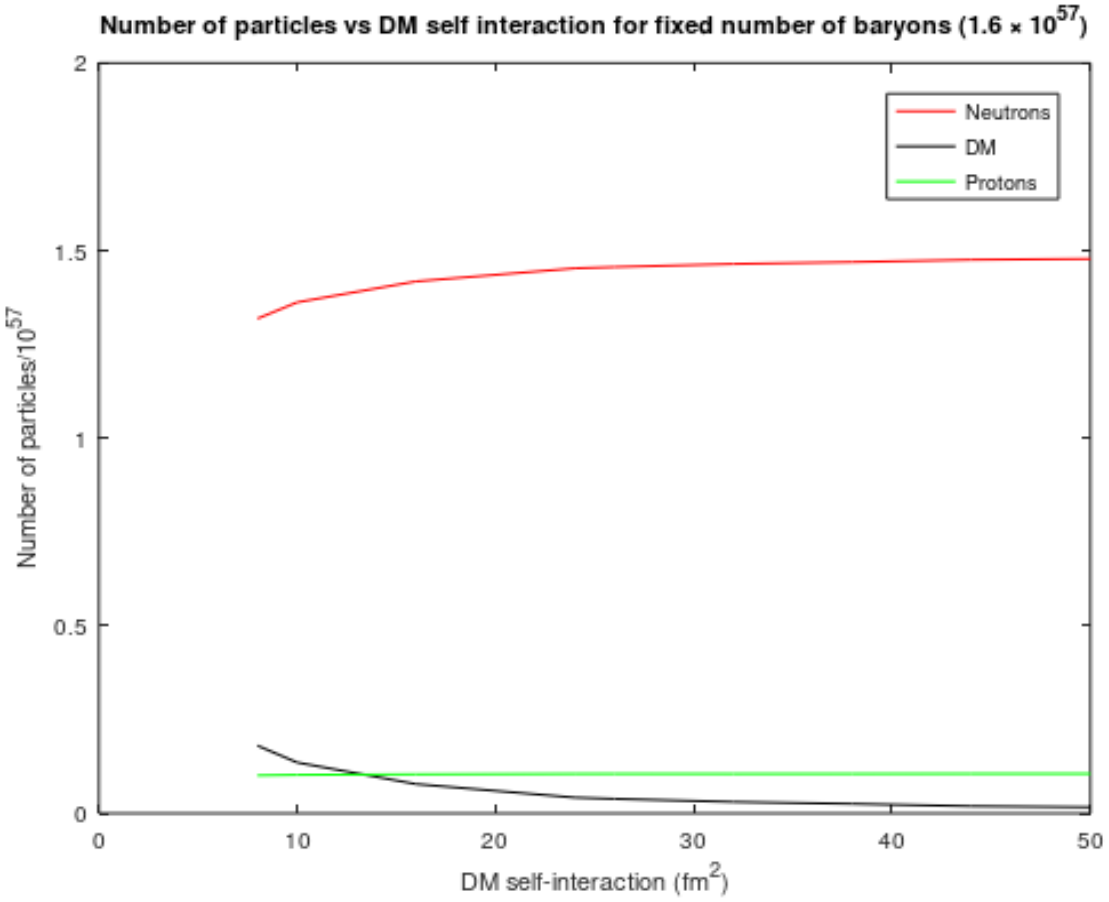

FIGURE 8.24: The population of baryons against the dark matter self-interaction G for a neutron star of a fixed total number of baryons at 1.6 $\times$ 10^{57}.

0.001 $M_{\odot}$. This rise in temperature leads to a reduction in the radius of the neutron star by 450 meters, or approximately 3.673 % . On the other hand, if only dark matter heats up by the same amount of energy, it requires a rise of 2 MeV in temperature, which leads to a reduction in the radius of the neutron star by approximately 5.061 %. The reduction of radii in both cases, whether dark matter heats up or nuclear matter heats up, leads to a significant decrease in the radius and the moment of inertia of the neutron star, which must cause the neutron star to spin up. The decrease in moment of inertia corresponding to the reduction in radius by 450 m corresponding to the case where the nuclear matter is heated to 0.25 MeV, is 0.1653 kg.m^2 $\times 10^{38}$ or 10.2103%, while the reduction in the moment of inertia is 0.2277$\times 10^{38}$ kg.m^2 or 14.067 % when the radius decreases by 620 m, with the dark matter heated to 2 MeV. Thus,

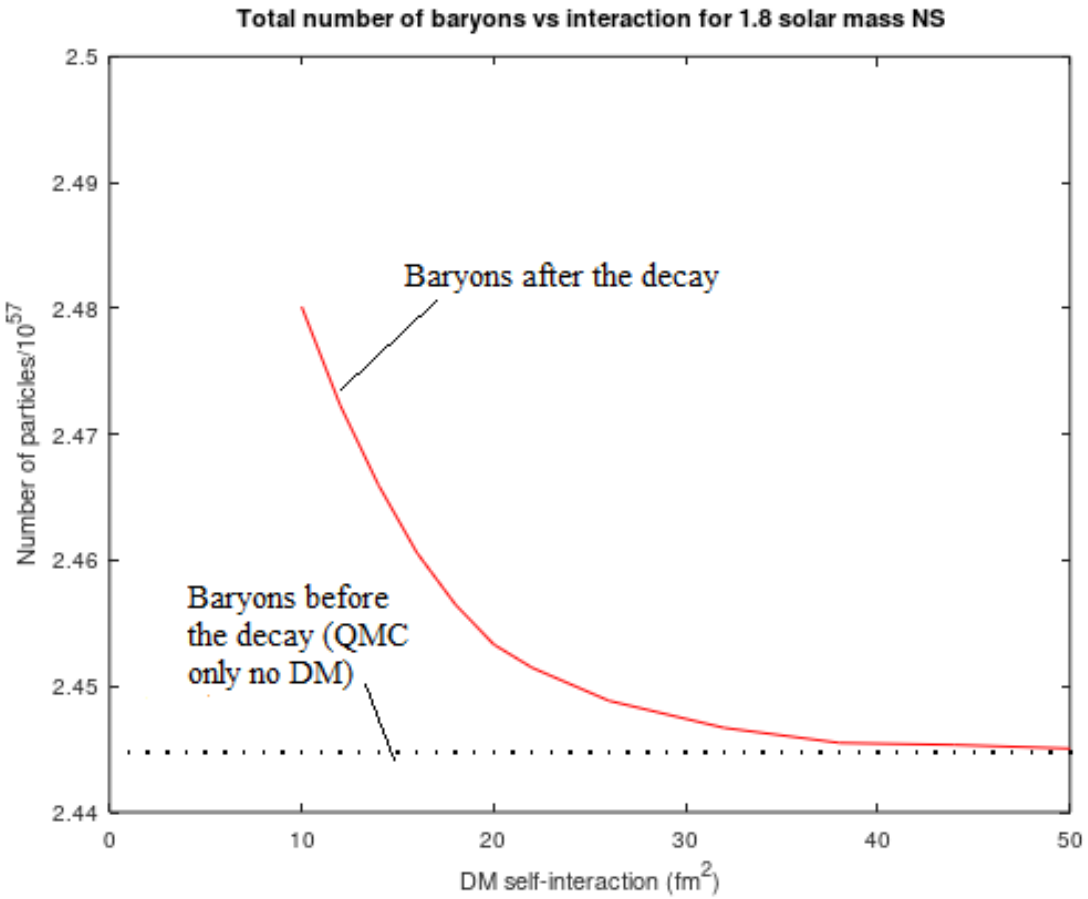

FIGURE 8.25: For a neutron star of fixed mass 1.8 $M_{\odot}$, the plot is given for the total number of baryons inside the neutron star before and after the neutrons decay into dark matter versus different dark matter self-interaction strengths (G).

it is evident that the radius of the neutron star reduces after the neutrons decay into dark matter, even though the process involves the neutron star heating up. It seems surprising at first glance, but to understand the shrinking of the neutron star point, one may consider three cases. In the first case, let us consider a neutron star, which contains nucleons only before the neutron decays at the temperature $T = 0^{\circ}K$. In the second case, let us consider the neutron star, which contains nucleons and dark matter after decay, but the temperature of the neutron star is $T = 0^{\circ}K$. In the third case, the neutron star contains nucleons and dark matter at some non-zero temperature, T. If one compares cases 2 and 3, then the neutron star radius clearly expands as the neutron star heats up. However, case 2 is not possible because it violates energy-momentum conservation. Therefore, one must compare cases 1 and 3. From Figure

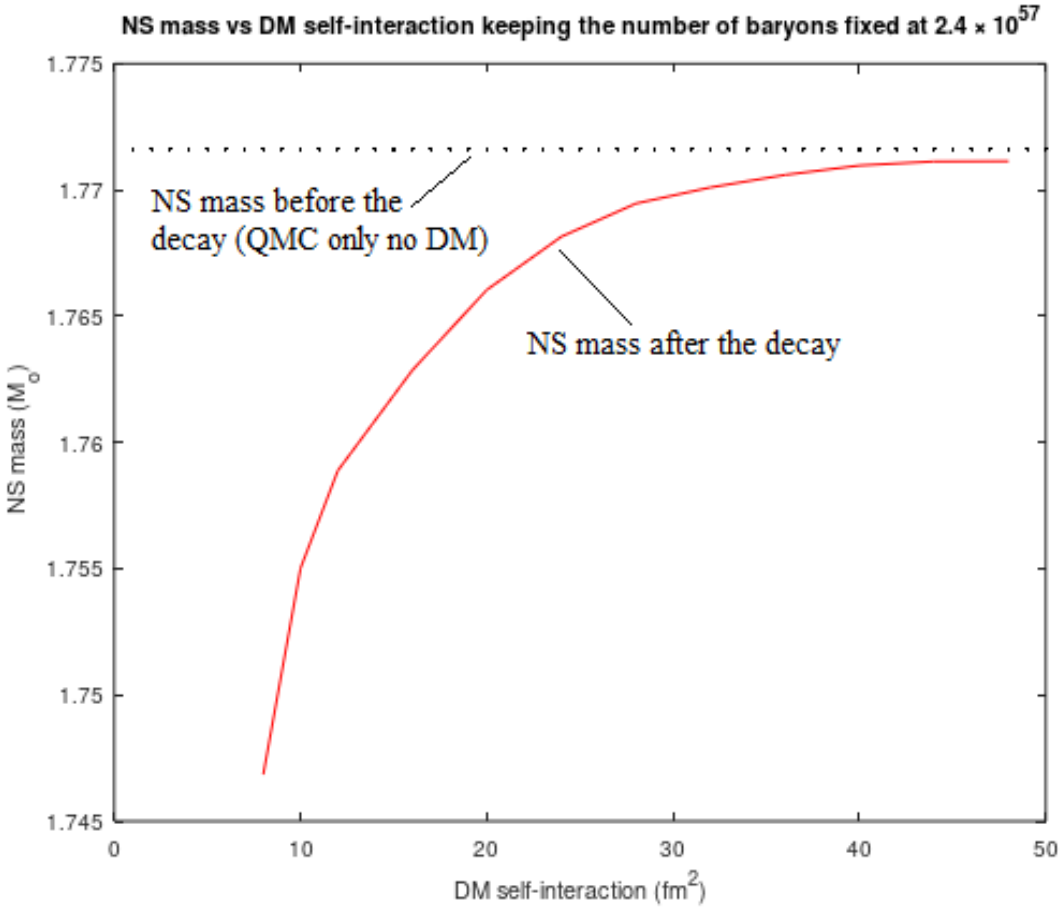

FIGURE 8.26: The mass (given in solar masses) of the neutron star is plotted against the dark matter self-interaction strength (G in fm^2) when the total number of baryons inside the neutron star is fixed at 2.4×10^{57}.

8.21 the radius of the neutron stars shrinks a lot following the neutrons decay. Ultimately, the temperature required to provide the necessary mass is not enough to outweigh the reduction in the radius of the neutron star caused by the conversion of neutrons to dark matter at $T = 0^{\circ}K$. This is why the final radius (after the decay) is smaller than the radius before the decay, even though the neutron star heats up.

8.3 Consequence of neutron decay: Strumia hypothesis

In this section, the effects of Strumia's hypothesis that neutrons decay into three identical dark matter particles inside neutron stars are explored. Figure 8.29 shows the equations of

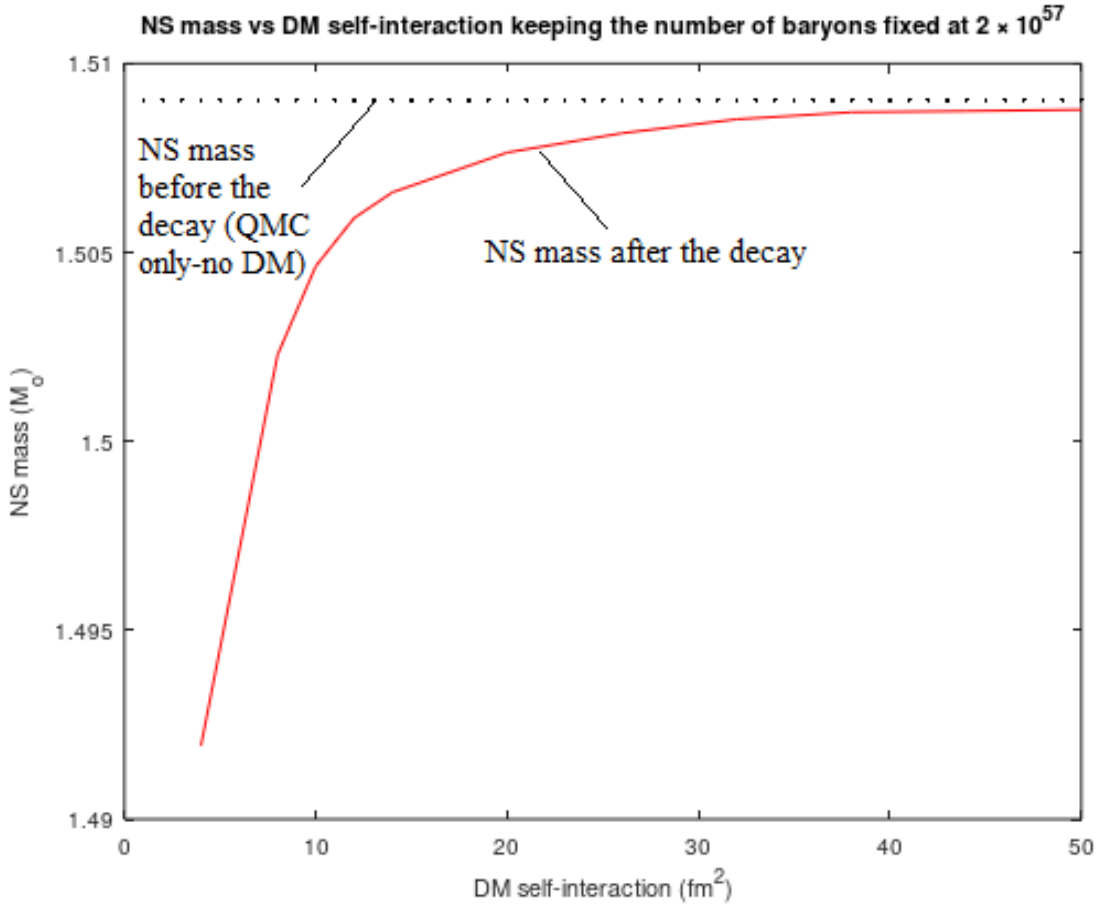

FIGURE 8.27: The mass (given in solar masses) of the neutron star is plotted against the dark matter self-interaction strength (G in fm^2) when the total number of baryons inside the neutron star is fixed at 2×10^{57}.

state of a neutron star following Strumia's hypothesis of neutrons decaying into dark matter. There are two equations of state considered. The equations of state are derived for nucleons only, and hyperons included at the higher energy densities of the nuclear matter at the core of the neutron stars. Figure 8.29 clearly shows that if neutrons decay into three identical dark matter particles, as suggested by Strumia, the equations of state after the neutrons decay get softer a little yet remain quite stiff. The equation of state that includes hyperons remains almost identical after the neutrons decay into dark matter, while the equation of state that only includes nucleons gets softer. Figure 8.30 shows the relation between mass and radius of neutron stars at a temperature $T = 0^{\circ}K$. Here, two equations of state are presented before the neutron decays into dark matter. One is based on nucleons only, and the other equation of

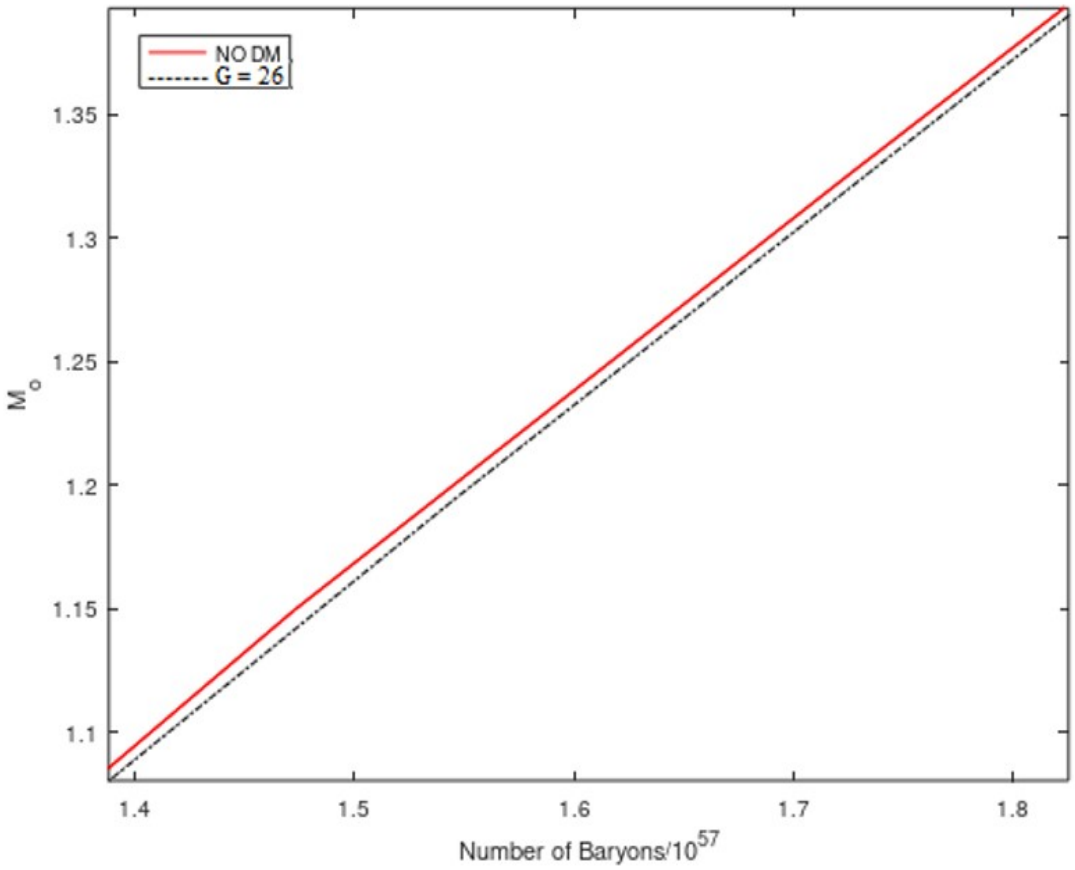

FIGURE 8.28: The mass (given in solar masses) of the neutron star is plotted against the total number of baryons before and after the neutron decay, where dark matter interaction strength is $G = 26$ fm^2.

state allows the development of hyperons at higher energy densities. As shown in Fig. 8.30 both the equations of state predict neutron stars of maximum mass of close to 2 $M_\odot$ before the neutrons decay into dark matter, although the hyperons included equation of state is softer compared to the nucleons only equation of state because in that equation of state, as the energy density increases, the high momentum nucleons get replaced by the low momentum hyperons, which is why the nucleons only equation of state predicts a neutron star of maximum mass of 2.25 $M_\odot$ while hyperons included equation of state gives neutron stars of maximum mass close to 2 $M_\odot$ only. After the neutrons decay into dark matter, the mass of the neutron star decreases, but even after the neutrons decay, both equations of state are stiff enough to predict neutron stars with a maximum mass close to 2 $M_\odot$. Therefore, the Strumia hypothesis of

neutrons decaying into three identical dark matter particles does not require the dark matter particles to be self-interactive at all in order to produce the neutron stars of 2 $M_{\odot}$. The radius of the neutron stars shrinks after the neutrons decay into dark matter for both equations of state, but remains well within the observational values of the radius. Fig. 8.31 presents the

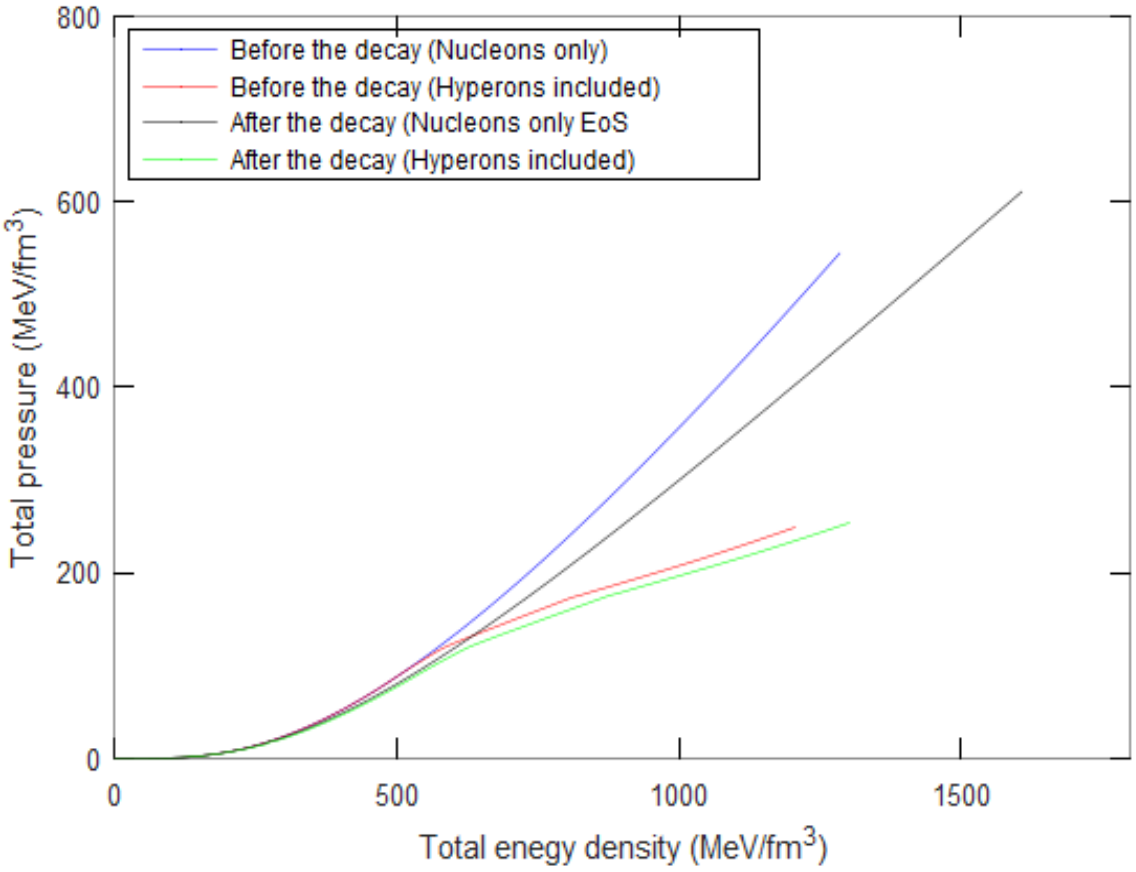

FIGURE 8.29: Relationship between pressure and energy density of matter inside the neutron star following Strumia's hypothesis of neutrons decaying into dark matter.

tidal deformability against the mass of the neutron star. The bold dark vertical line represents the range of values of tidal deformability that a neutron star of mass 1.4 $M_{\odot}$ should have in order to be consistent with the finding of gravitational waves observational as indicated in Abbott et al. 2017b; Abbott et al. 2019; Bramante et al. 2018. As it can be seen in Fig. 8.31, that the value of the tidal deformability of the neutron star produced by nucleons only and hyperons included in the equation of state follows the constraint on the tidal deformability

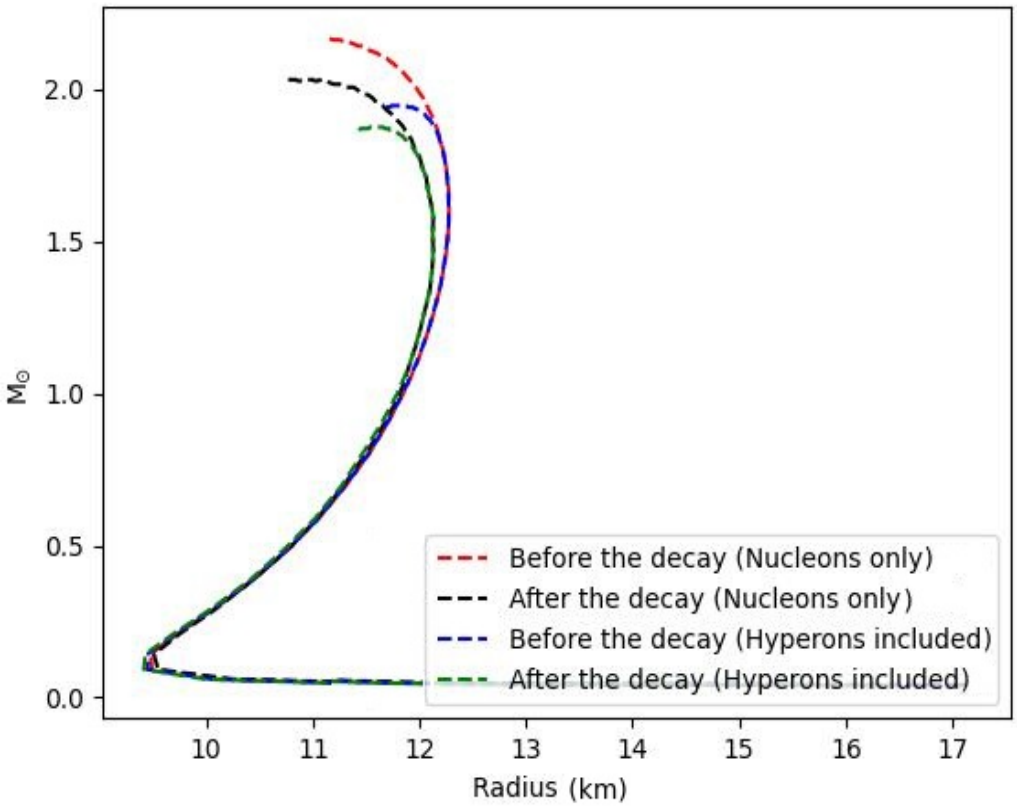

FIGURE 8.30: Total mass (given in solar masses) vs. radius of the neutron stars for nucleons only and hyperons included equation of state at $T = 0\,^{\circ}K$, before and after the neutrons decay into dark matter.

before and after the neutrons decay into dark matter. Therefore, Strumia's hypothesis that neutrons decay into dark matter survives. Figure 8.32 shows the relationship between the mass and the moment of inertia of the neutron stars produced by nucleons only and hyperons included in the equation of state. As shown in Figure 8.32, the moment of inertia of the neutron star decreases after the neutrons decay into dark matter, which is consistent with the finding in Fig. 8.30, which suggests that the radius of the neutron star of the same mass decreases following the neutrons decay into dark matter. The reduction of the moment of inertia should lead to an increment in the spin of the neutron star, which may play a vital role in detecting the observational signal of the neutron decay hypothesis.

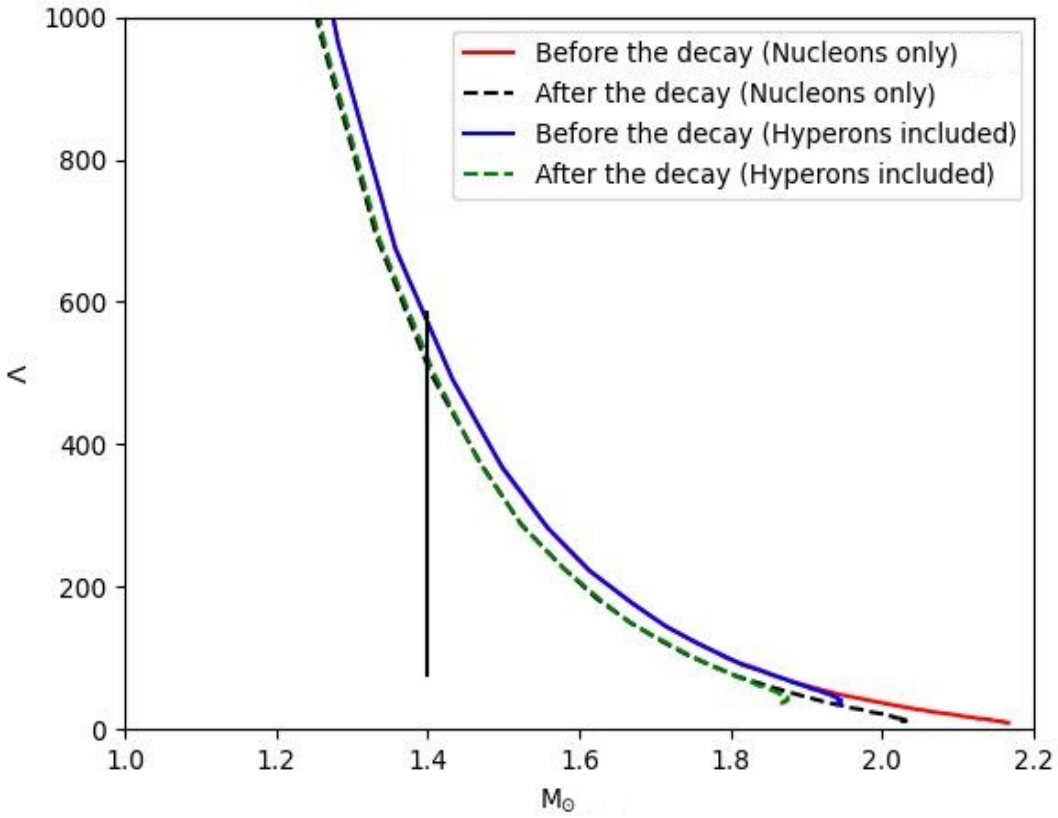

FIGURE 8.31: Tidal deformability against the mass (given in solar masses) of the neutron star before and after neutrons decay into dark matter for the nucleons only and hyperons included in the equation of states.

Figure 8.33 shows the distribution of energy density of the nuclear matter and the dark matter inside the neutron star from the centre to the surface. Although, the plot is given for the nucleons only equation of state, the plot for the hyperons equation of state is essentially identical. Be it the nucleons only equation of state or the hyperons included equation of state, the degenerated dark matter remains inside the neutron star and does not shield the surface, and the dark matter remains inside the core.

Figure 8.34 displays the relative population of dark matter inside the neutron stars, and Figure 8.35 gives the contribution of the dark matter mass to the total mass of the neutron stars. The Figures 8.34 and 8.35 suggest that the fraction of conversion from neutrons to dark matter particles inside the lighter neutron stars is quite small. The lighter neutron star does not

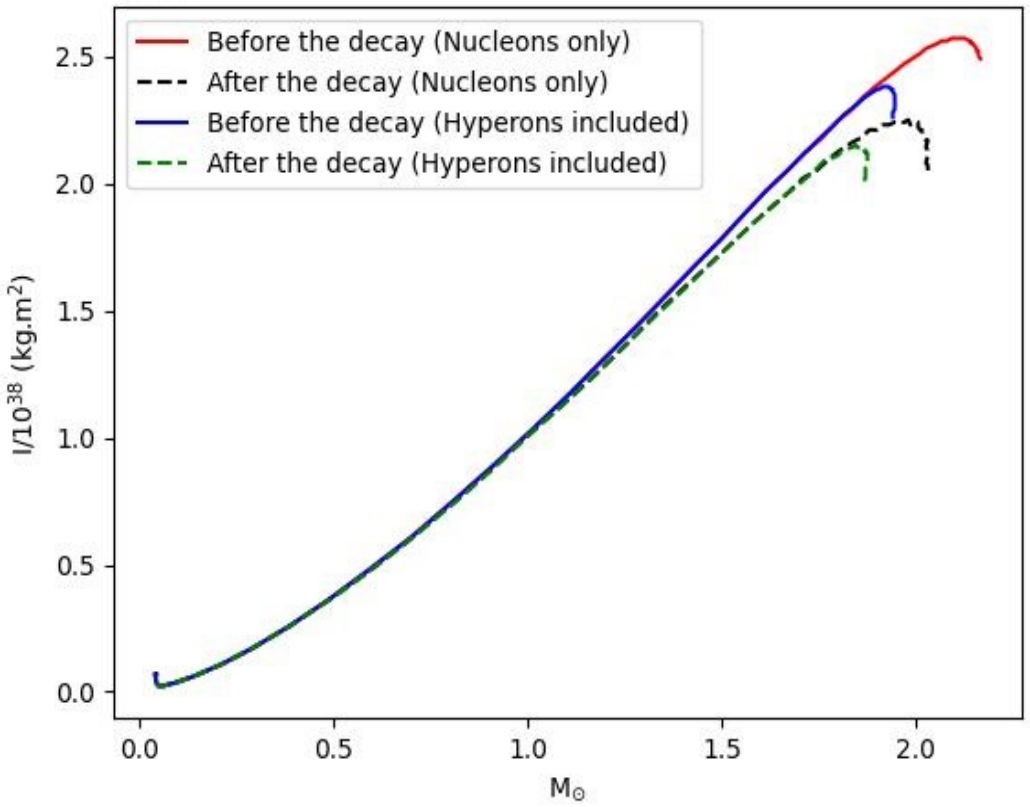

FIGURE 8.32: The moment of inertia versus the mass (given in solar masses) of the neutron star for nucleons only and hyperons included in the equation of state is given at $T = 0^{\circ}K$ before the neutrons decay into dark matter.

contain much dark matter, although the population of dark matter particles increases rapidly in heavier neutron stars. In the neutron star of maximum mass produced by nucleons only and hyperons included in the equation of state, dark matter can have mass as much as 4% of the total mass of the neutron star. The total number of dark matter particles is about 12% of the total number of particles. The 12% contribution of dark matter particles to the total number of particles is enough to generate enough repulsion to sustain it against gravity and satisfy the constraints on maximum mass and tidal deformability of the neutron star.

During the decay of neutrons into dark matter, it is expected that the total energy and the total baryon number inside the neutron star must remain conserved. Therefore, to explore the neutron decay hypothesis further, the properties of the neutron star of mass 1.8 $M_{\odot}$ are given

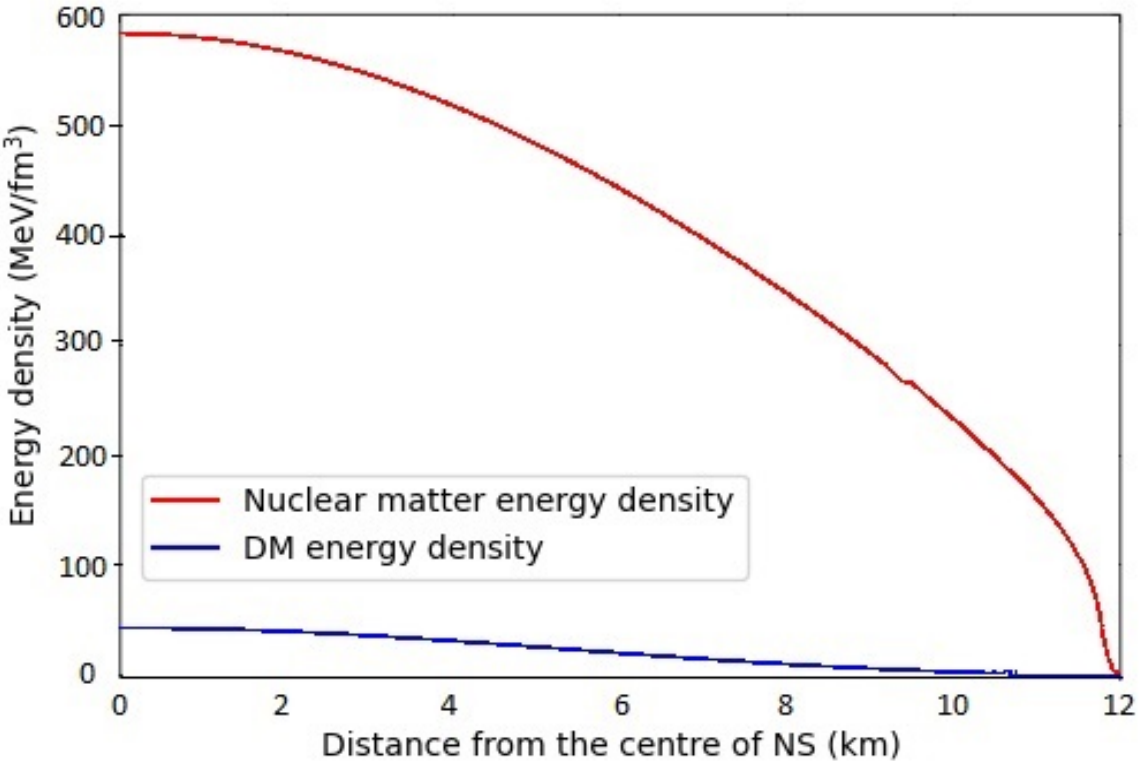

FIGURE 8.33: The distribution of nuclear matter and the dark matter energy density inside the neutron star from the centre to the surface.

in Table 8.3 which displays that, be it nucleons only or hyperons included in the equation of state, if the total baryon number is kept fixed, then after the decay, the neutron star mass is lighter than before the decay, by approximately 0.007 $M_\odot$. Since neutron stars are extremely compact objects with an escape velocity comparable to the velocity of light. Virtually, nothing but light can escape from the neutron star. Therefore, following the neutron decay into dark matter, there is no known mechanism that suggests that particles can have enough velocity to escape the neutron star. The problem can be solved by having dark matter that is not completely degenerate but is effectively at a finite temperature. The energy equivalent to the difference in the mass of the neutron star before and after the decay, i.e., 0.007 $M_\odot$ may be used to heat up the dark matter inside the neutron star. Here, the properties of the neutron stars produced by both equations of state are given, with hot dark matter having a heat

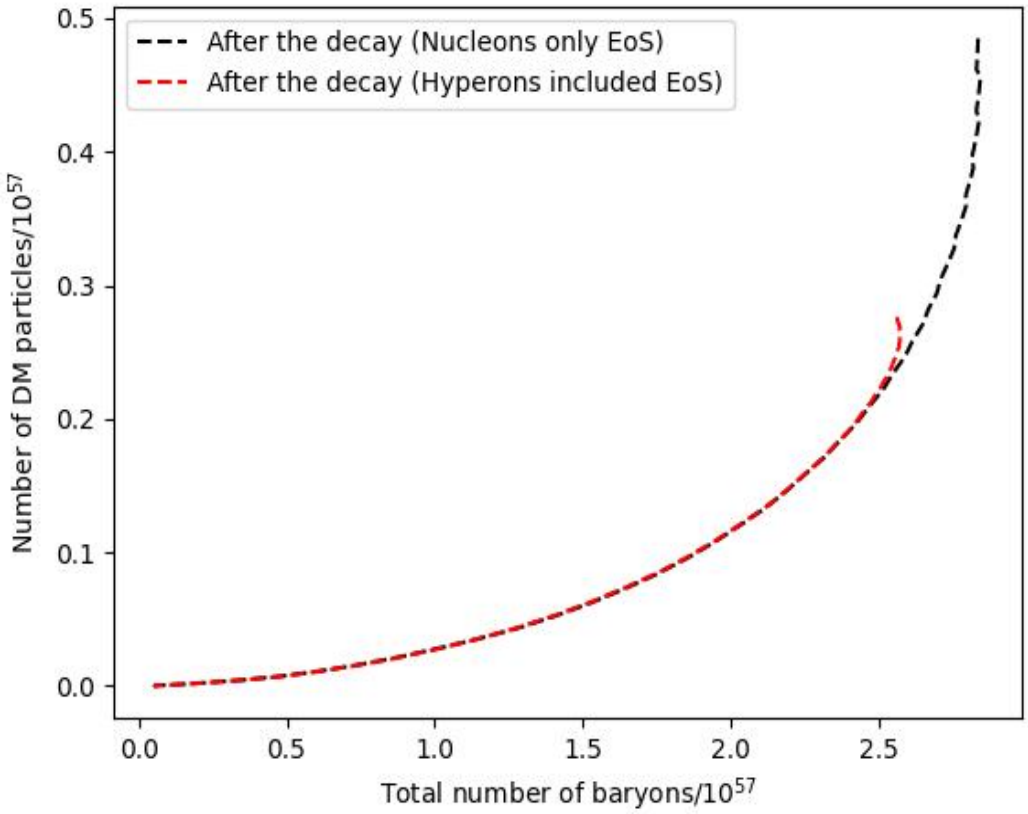

FIGURE 8.34: The population of dark matter particles against the total number of baryons inside the neutron star for nucleons only and hyperons included in the equation of state.

energy equivalent to 0.007 $M_{\odot}$ as given in Table 8.4. Table 8.4 suggests that, for nucleons only equation of state the dark matter inside the neutron must heat up to a temperature of approximately 6.5 MeV, whereas for hyperons included equation of state, the dark matter must heat up to a temperature of approximately 6 MeV. As given in Table 8.4, the radius of the neutron star is almost unchanged with hot dark matter at the temperatures given above, and the moment of inertia of the neutron star having hot dark matter at the temperature of 6 MeV or 6.5 MeV remains almost unchanged as of the moment of inertia at $0°K$. Therefore, the heating of dark matter inside the neutron stars produced by the Strumia hypothesis does not change the effective radius. The radius remains the same as the radius of a neutron star with dark matter at a temperature $0°K$. However, the decay of neutrons into dark matter

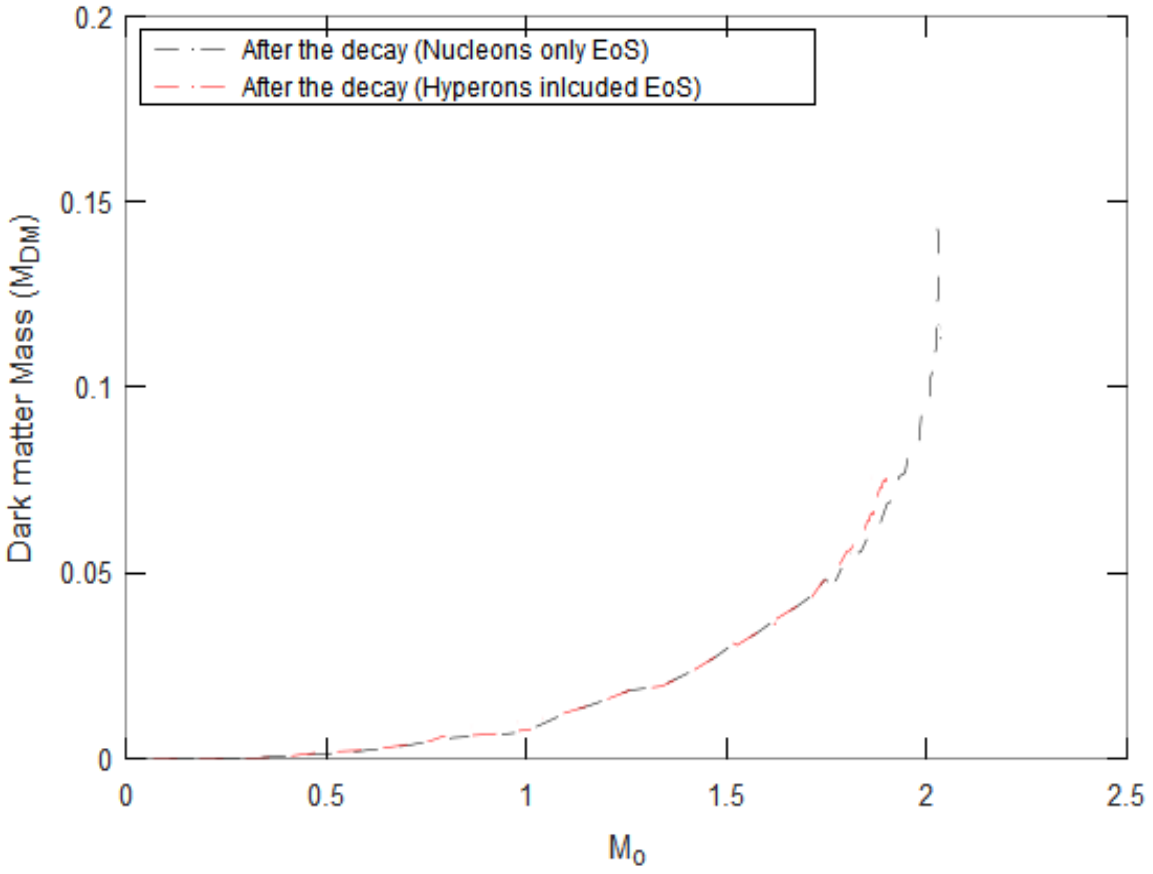

FIGURE 8.35: The contribution of the dark matter mass (given in solar masses) is given against the total mass (given in solar masses) of the neutron star, with nucleons only and hyperons included in the equation of state.

	NS Mass	T (MeV)	R (km)	I (kg.m^2)
1	1.8 $M_\odot$ (Nucleon only EoS before decay)	0	12.25	2.25×10^{38}
2	1.793644 $M_\odot$ (Nucleon only EoS + DM after decay)	0	11.96	2.12×10^{38}
3	1.8 $M_\odot$ (Hyperons included EoS before decay)	0	12.20	2.24×10^{38}
4	1.793577 $M_\odot$ (Hyperons included EoS + DM after decay)	0	11.96	2.11×10^{38}

TABLE 8.3: The properties of a 1.8 $M_\odot$ neutron star containing 2.4445 $\times 10^{57}$ total baryon number at $0^\circ K$ before and after the neutrons decay. Here, T is the temperature, M is the mass, R is the radius, and I is the moment of inertia of the neutron star.

shrinks the radius of the neutron star, which is significant and effectively reduces the moment of inertia by approximately 5.75%. As a result, the neutron star must spin up during the decay.

$M_\odot$	T (MeV) of DM	R (km)	I (kg.m^2)
1.8 $M_\odot$ (Nucleon only EoS before decay)	0	12.25	2.25×10^{38}
1.7936 $M_\odot$ (Nucleon only EoS + DM after decay)	6.5	11.96	2.124×10^{38}
1.8 $M_\odot$ (Hyperons included EoS before decay)	0	12.20	2.24×10^{38}
1.7935 $M_\odot$ (Hyperons included EoS + DM after decay)	6	11.96	2.115×10^{38}

TABLE 8.4: The properties of a 1.8 $M_\odot$ neutron star containing 2.4445 $\times 10^{57}$ total baryon numbers with dark matter heated by the energy equivalent to the 0.007 $M_\odot$.

8.4 Fornal and Grinstein hypothesis with heavier ϕ boson

As shown above, the decay of neutrons into dark matter does not necessarily result in the massless ϕ bosons. In fact, for stable nuclei to remain stable, the masses of m_χ and m_ϕ must satisfy the condition 937.906 MeV < $m_\chi + m_\phi$ < 938.79. Most of the studies have selected the mass of ϕ boson very close to zero, which makes the calculation easier, and one does not have to bother about ϕ boson because, being massless, it escapes the neutron star immediately. In this section on Fornal and Grinstein decay, it is assumed that the ϕ boson is not massless but has a mass of 1 MeV and will not escape the neutron star but remain trapped inside it like χ fermions. Since ϕ's are bosons, if they remain inside the neutron stars, they must condensate. Hence, a neutron star must have nuclear matter, χ fermions, and ϕ bosons inside it.

Below the critical temperature, the ϕ bosons must condense. Since the mass of the ϕ bosons is very small, their contribution is far too small to make any significant changes in the existing properties of the neutron stars even after their condensation. Therefore, for the sake of ease of calculation, the condensation of the ϕ bosons has not been considered. Since the ϕ bosons are present in the neutron star, the chemical composition of the neutron star has changed, and the following chemical equilibrium conditions must hold true:

$$\mu_n = \mu_\chi + m_\phi \qquad \mu_n = \mu_p + \mu_e \qquad \mu_\mu = \mu_e \qquad n_p = n_e + n_\mu \tag{8.2}$$

where m_ϕ is the mass of the ϕ boson, which is 1 MeV, and m_χ is selected to be 937.79 MeV. Following these conditions, the equation of state constructed using the Fornal and Grinstein

hypothesis has been solved, and the following results have been produced. Figure 8.36 shows the equation of state of the neutron star when neutrons decay into dark matter according to the Fornal and Grinstein hypothesis, and one of the decay products, m_ϕ has a mass of 1 MeV and remains trapped inside the neutron star. Since the mass of the ϕ boson is very small, it does not affect the equation of state much, and the Figure 8.36 remains almost similar to the Figure 8.20, which has been calculated for a massless ϕ boson. The dark matter has to be self-interacting with a self-interaction strength of at least G = 26 fm^2 to produce a neutron star of 2 M$_\odot$. Figure 8.37 is the relationship between the mass and radius of the neutron star, which contains dark fermions and dark bosons. Similar to section 8.2, the vector repulsion of dark fermions is increased until the maximum mass of the neutron star is produced to be 2 M$_\odot$. The result is very similar to the earlier one, where ϕ is assumed to be massless because the mass contribution of the ϕ boson is about 1/10^6 M$_\odot$ which is insignificant to impact the properties of the neutron star such as mass and radius. It is evident from Figure 8.37 that the mass and the radius of neutron stars decrease following the neutron decay hypothesis, even when the bosons are considered to be heavy. The constraint on the maximum mass of the neutron star is satisfied when the dark fermions vector interaction strength is G = 26 fm^2. In the plot shown in Figure 8.38 the tidal deformability of the neutron decreases after the neutron decays into dark matter. Similar to mass and radius, tidal deformability also remains almost unchanged with the presence of the 1 MeV ϕ boson. m_ϕ = 1 MeV and G = 26 fm^2 satisfy the constraint on tidal deformability. The moment of inertia of the neutron star is presented against its mass. Having a heavier dark boson ϕ also suggests that the moment of inertia decreases after the neutron decay. We are only interested when $G \geq 26$ fm^2. Therefore, at G = 26 fm^2 the change in moment of inertia is significant after the neutron decay into dark matter, which indicates that neutron star must spin up following the neutron decay. But compared to the case of massless ϕ bosons, the moment of inertia remains unchanged when m_ϕ = 1 MeV. Although the contribution of ϕ bosons with m_ϕ = 1 MeV, to the total mass of the neutron star is very small to change the properties of the neutron star compared to the case of a massless ϕ boson. But if ϕ bosons decay into photons, they may play a significant role in neutron star heating. Most of the studies show that neutron stars cool down rapidly following the standard Urca process. After a million years, the neutron stars have a luminosity of order $10^{31.5}$ erg/sec.

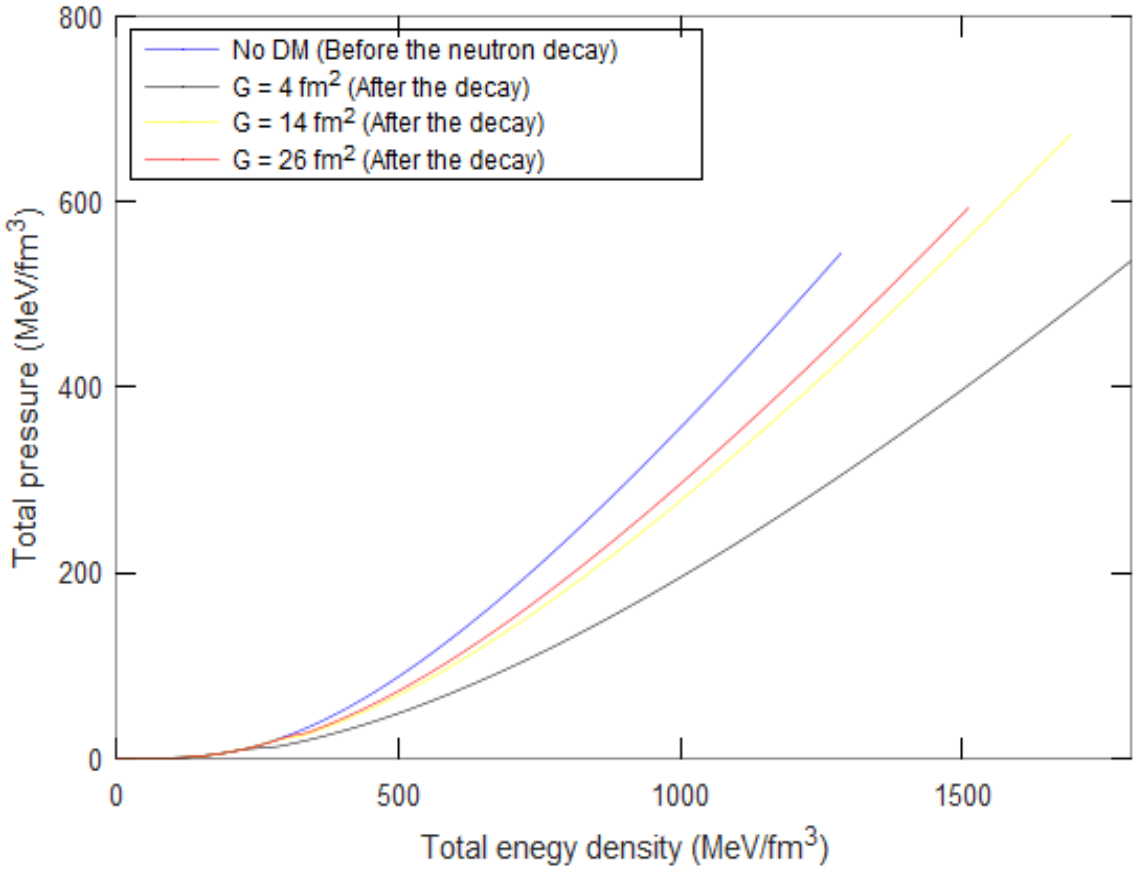

FIGURE 8.36: Relationship between pressure and energy density of matter following the Fornal and Grinstein hypothesis when m_ϕ = 1 MeV.

So, if ϕ bosons decay into photons, then after a million years they must not contribute to luminosity $\geq 10^{31.5}$ erg/sec. Based on the luminosity after 10^6 years, the lifetime of the dark ϕ bosons is calculated to be 1.85×10^{11} years.

8.5 Decay modes of ϕ bosons

The decay products of the neutron, the χ and ϕ are BSM particles (beyond Standard Model particles) that can originate from some UV-complete theory or be considered within some low-energy effective theory. The physics of their existence remain unknown, but we can still constrain them from various sources. The massive fermion, χ, is an ideal dark matter candidate and can make up the bulk or all of the observed relic density today. The other

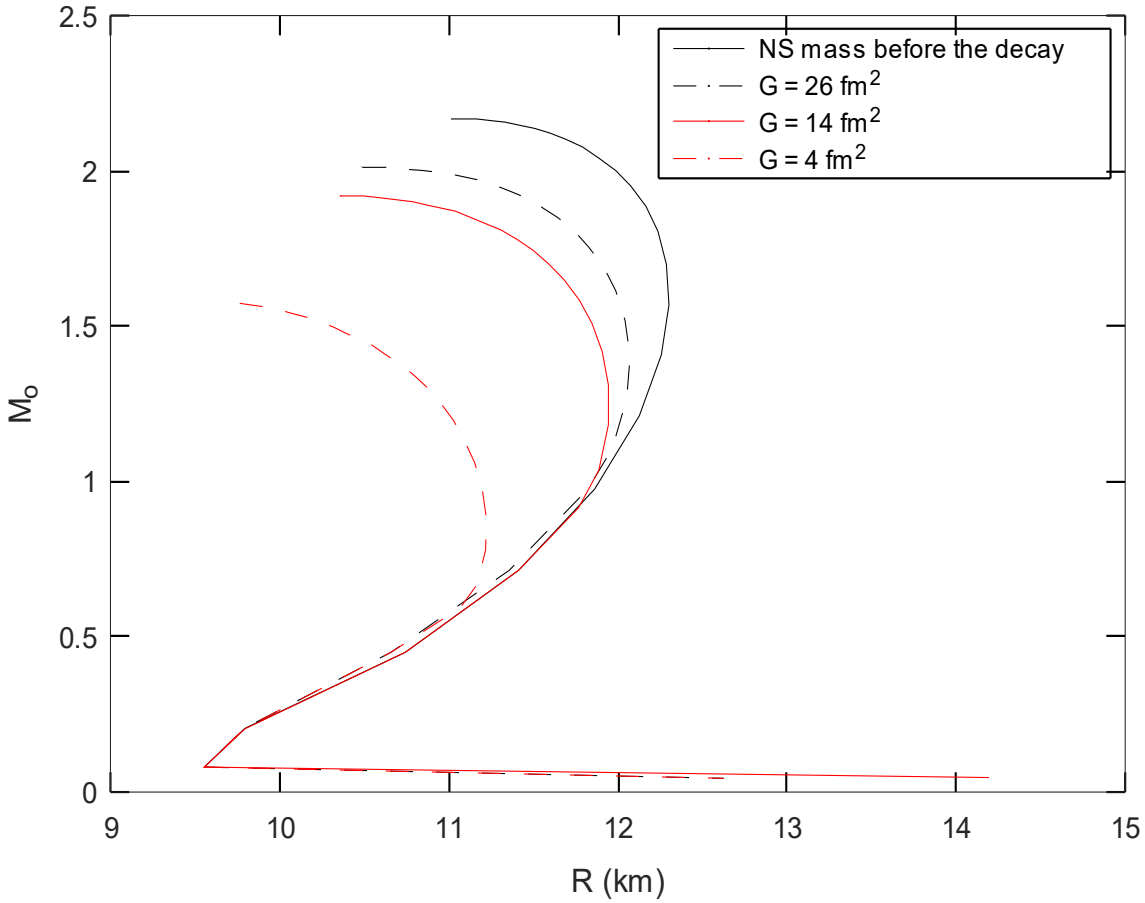

FIGURE 8.37: Mass (given in solar masses) vs. radius plot for neutron stars with dark fermions and dark bosons inside the core with different χ-χ interactions.

product of decay, the boson, can originate from a BSM source. On general grounds and experimental considerations, the possibility that the boson is a photon has been ruled out. Here, some possibilities of ϕ bosons to couple the Standard Model particles have been considered, as have constraints based on the findings in the previous section.

8.5.1 Scalars and pseudoscalars

In the last few years, light scalar and pseudo-scalar particles have emerged as leading new physics candidates that can be constrained from a variety of sources. While the primary motivation is derived from axions, simplified models with light scalars or pseudo-scalars have triggered a lot of attention. Here, we assess their viability given our findings above.

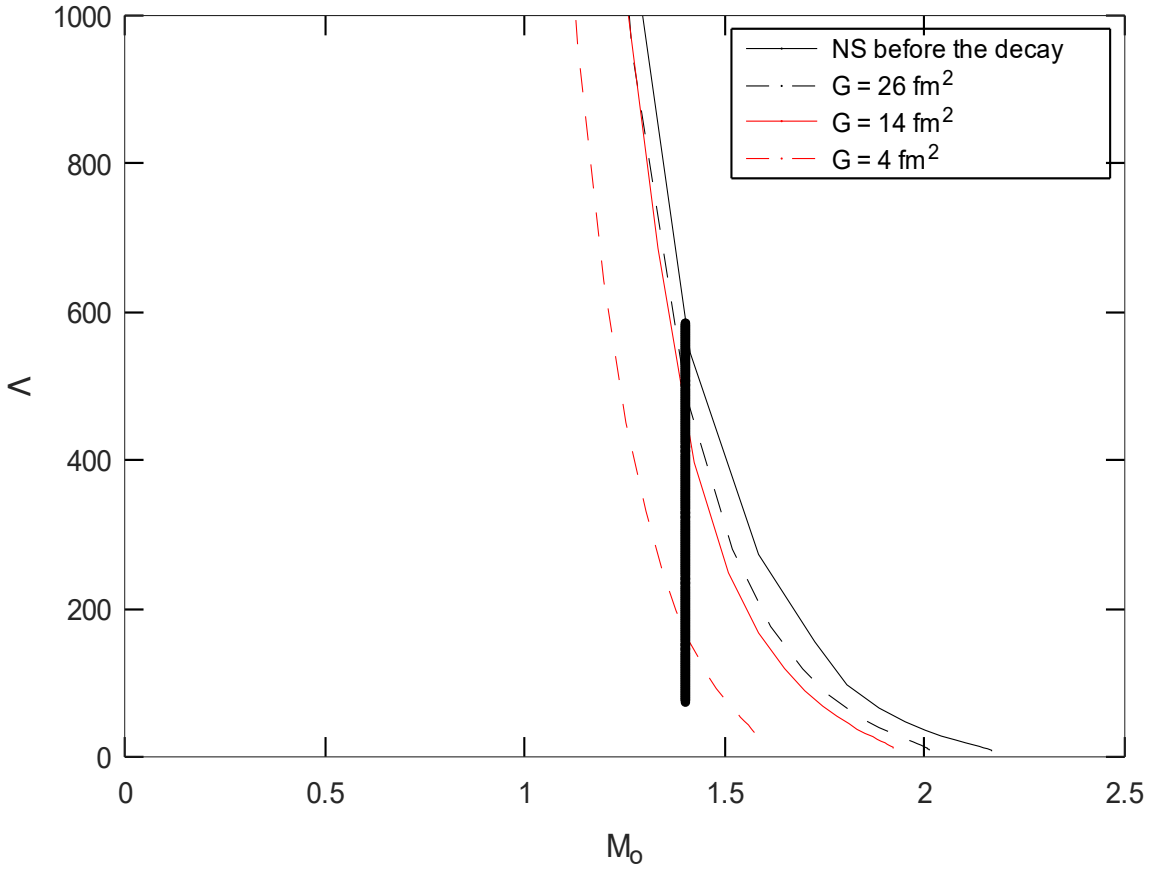

FIGURE 8.38: Tidal deformability against the mass (given in solar masses) of the neutron star before and after the neutron decays into dark matter. The bold, black, vertical line indicates the acceptable range of values for tidal deformability.

The first bosonic candidate is a scalar coupled to the electromagnetic field strength,

$$\mathcal{L}_{int} = \frac{C_s}{\Lambda}\phi F_{\mu\nu}F^{\mu\nu} + \frac{m_f}{\Lambda}\phi \bar{f} f + \cdots \tag{8.3}$$

where ϕ is the scalar field, $F_{\mu\nu}$ the electromagnetic field strength, and f is the Dirac spinor for the leptons. The overall normalization $\frac{C_s}{\Lambda}$ is model dependent, while m_l is the mass of the lepton. The linear couplings can be generated by the scalar coupling to Higgs as $\phi H^\dagger H$. A quadratic coupling can also be generated if ϕ carries a Z_2 symmetry,

$$\mathcal{L} = \frac{C_q}{\Lambda_q^2}\phi^2 F_{\mu\nu}F^{\mu\nu} + \sum_f \frac{m_f}{\Lambda_q^2}\phi^2 \bar{f} f + \cdots \tag{8.4}$$

In both cases, the dots indicate any other couplings that may be induced.

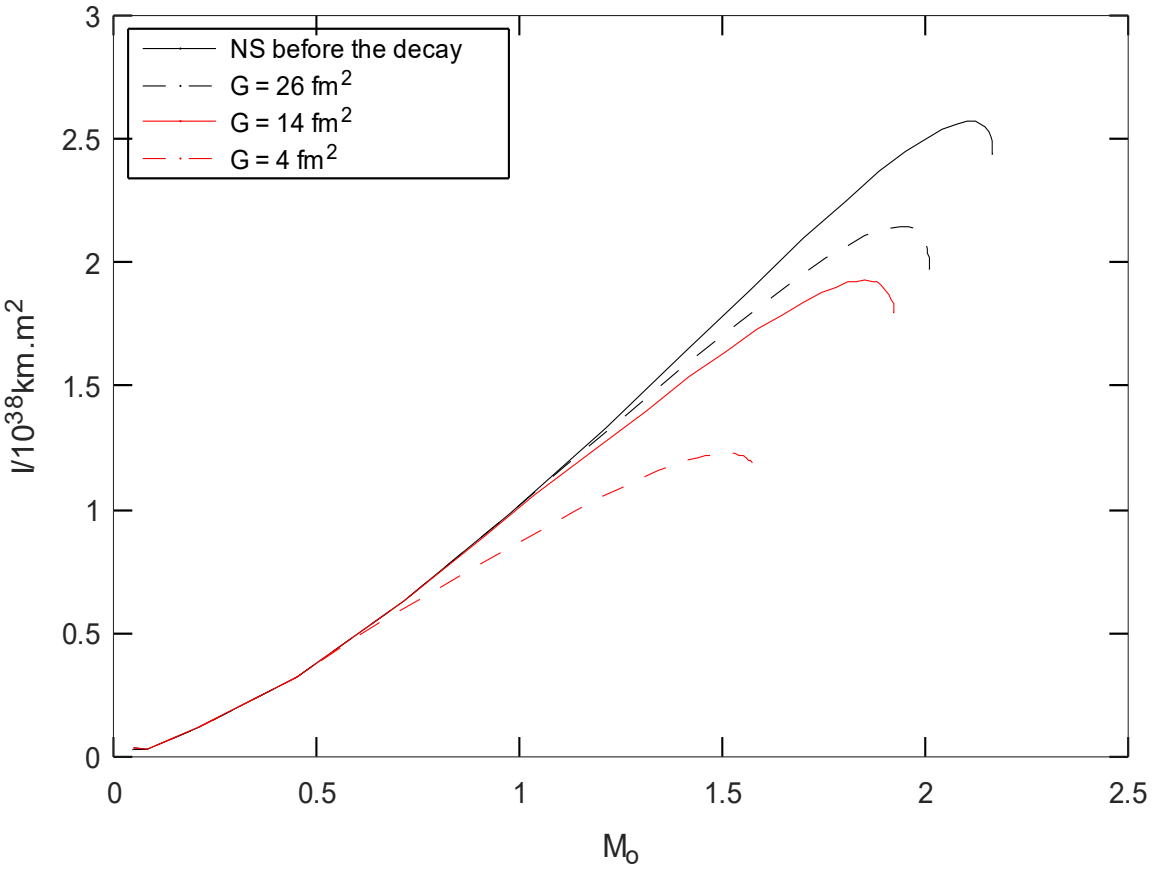

FIGURE 8.39: Moment of inertia of the neutron star against its mass (given in solar masses) when m_ϕ = 1 MeV remains trapped inside the core.

Couplings to the neutron can be obtained by integrating out, for example, heavy fermions yielding dimension 6 operators, such that the effective neutron coupling can be written as,

$$\mathcal{L} \in L_{kin} + \lambda_{eff} n \chi \phi \,. \tag{8.5}$$

The linear (and quadratic) couplings induce a shift in the electromagnetic couplings that can be constrained by a variety of sources. A summary of these can be found in Ref. Antypas et al. 2022.

The next possibility is that of a pseudoscalar that couples like an axion (like particle) to photons, and derivatively to electrons,

$$\mathcal{L}_{int} = \frac{C_{s\gamma}}{\Lambda} \phi F_{\mu\nu} \tilde{F}^{\mu\nu} + \frac{C_f}{2\Lambda} (\partial_\mu \phi) \bar{f} \gamma^\mu \gamma^5 f + \cdots \,. \tag{8.6}$$

For axion-like particles in Equation 8.6, the effective ALP coupling to leptons generates a coupling,

$$\frac{C_f}{2\Lambda}(\partial_\mu\phi)\bar{f}\gamma^\mu\gamma^5 f = -\frac{C_f m_f}{\Lambda} i\bar{f}\gamma^\mu\gamma^5 f + \cdots \tag{8.7}$$

where the dots indicate terms proportional to $F\tilde{F}$. The decay widths of charged fermions are given by,

$$\Gamma(a \to f\bar{f}) = \frac{m_f^2 m_a |C_f^2|}{4\pi\Lambda^2}\sqrt{1 - \frac{4m_f^2}{m_a^2}}\,. \tag{8.8}$$

Analogous to scalars the effective ALP coupling to neutrons can be written as,

$$\mathcal{L} \in L_{kin} + \lambda_{eff} n\chi\gamma^5\phi\,. \tag{8.9}$$

A comprehensive account of UV complete models and their phenomenological consequences is left for future work. In principle, since the bosons in our case are heavy, the most general Lagrangian will contain interaction terms involving not only photons and leptons but hadrons as well.

The decay widths for pseudoscalars to diphotons are given by,

$$\Gamma(a \to \gamma\gamma) = \frac{|C_\gamma^2|}{4\pi\Lambda^2} m_a^3\,. \tag{8.10}$$

The lifetime is

$$\tau(a \to \gamma\gamma) = 1/\Gamma(a \to \gamma\gamma \times f) \tag{8.11}$$

where f is the conversion factor from GeV^{-1} to seconds. From the estimates derived above, for a boson mass of 1 MeV, a lifetime of $\tau \geq\simeq 10^{11}$ years, and if this is only decay channel relevant, the effective coupling, $g_{eff} = C_\gamma/\Lambda \leq 10^{-17}$. Note that a lifetime of 10^{11} years is about 10^{18} seconds. The lifetime of the universe is about 10^{18} seconds, and therefore this boson is cosmologically stable and should add to the total relic density of the universe. For scalars and pseudoscalars, one of the strongest constraints at this mass originates from the consideration that photons produced during ALP decays when the universe is transparent should not exceed the total extragalactic background light (EBL) Cadamuro and Redondo 2012. For pseudoscalar ALPs, this limits lifetimes to $\tau \geq 10^{23}$ seconds, such that the effective ALP coupling is restricted to $g_{eff} \leq 10^{-19}$. Furthermore, X-rays produced from ALP decays

in galaxies must not exceed the known backgrounds. This limits $\tau \geq 10^{25}$ seconds, leading to an effective coupling $g_{eff} \leq 10^{-20}$ Cadamuro and Redondo 2012.

8.5.2 Spin-1

While the decay to a photon has been ruled out, a possible solution is that the spin-1 boson can be a dark (kinetically) mixed photon. The massless part of the most general theory of two $U(1)_{a,b}$ Abelian gauge bosons can be written as,

$$\mathcal{L} = -\frac{1}{4}F_{a\mu\nu}F_a^{\mu\nu} - \frac{1}{4}F_{b\mu\nu}F_b^{\mu\nu} - \frac{\varepsilon}{2}F_{a\mu\nu}F_b^{\mu\nu} \tag{8.12}$$

The masses of these can be obtained via a Stuckelberg mechanism or via spontaneously broken gauge symmetry

$$\mathcal{L}_m = \frac{1}{2}M_a^2 A_\mu^a A^{a\mu} + \frac{1}{2}M_b^2 A_\mu^b A^{b\mu} + M_a M_b A_\mu^a A_b^\mu \tag{8.13}$$

Consider a hypercharge mixing with the usual photon,

$$\mathcal{L} = \frac{\epsilon}{2\cos\theta_W}\tilde{F}'_{\mu\nu}B^{\mu\nu}\,. \tag{8.14}$$

Then, the effective Lagrangian becomes,

$$\mathcal{L} \in e\epsilon J_\mu A'_\mu + e'\epsilon\tan\theta_W J'_\mu Z_\mu + e' J'_\mu A'_\mu\,, \tag{8.15}$$

where J'_μ and e' are the dark sector current and the dark photon coupling to the dark sector. Once the Z boson is integrated out, we can see that the coupling of the dark photon to SM fermions is proportional to $e\epsilon$, i.e., millicharged dark photons, which are constrained from various sources. The effective coupling to neutrons can be written as,

$$\mathcal{L} \in e\epsilon(n\sigma^{\mu\nu}\chi F'_{\mu\nu})\,. \tag{8.16}$$

Below the two electron threshold, the constraints on dark photons originate from stellar cooling bounds and from the Xenon-1T experiments Caputo et al. 2021; Aprile et al. 2022. The constraints on the kinetic mixing parameter is $\epsilon \leq 10^{-13}$ for $m_{A'} \simeq 1$ MeV.

CHAPTER 9

Conclusion

The presence of dark matter inside neutron stars has serious implications. With the existence of dark matter inside the neutron star, whether it is captured from the surroundings or comes from neutron decay, the properties of the neutron star change significantly.

9.1 Dark matter capture

In section 8.1, the effects of different dark matter candidates (bosonic and fermionic dark matter) on the properties of neutron stars are presented when the neutron stars capture the dark matter particles from their surroundings. The comparative study has been conducted using three models of neutron stars with dark matter having a mass of m_χ = 1 GeV for fermionic and bosonic dark matter, both (assuming l_χ= 1 fm for bosonic dark matter and mass m_I = 100 MeV for fermionic dark matter). The available models suggested by Li et al. 2012b; Bell et al. 2020; Kouvaris and Tinyakov 2010 that explain the capture of dark matter inside a neutron star indicate that neutron stars take billions of years or maybe more to accumulate dark matter mass that contributes 5% of the total mass. Figs. 8.2 and 8.3 show that if the neutron stars are produced by the nucleons only equation of state (N-QMC700), they can accumulate up to 15% mass of the total mass of the neutron star if the dark matter is bosonic and 10% mass of the total mass of the neutron star if the dark matter is fermionic, and still produce massive neutron stars of 2 $M_\odot$. The fermionic dark matter tends to collapse the neutron star faster than the bosonic dark matter.

Figs. 8.4 and 8.5 show the effect of fermionic and bosonic dark matter on the neutron stars produced by F-QMC700, containing hyperons at the core. The maximum mass of a neutron

star produced by F-QMC700 is close to 2 $M_\odot$. The accumulation of dark matter inside the neutron star drops the maximum mass of the neutron star below 2 $M_\odot$. Even the 5% contribution of the dark matter mass to the total mass is large enough that the neutron stars cannot be massive enough to have a mass of 2 $M_\odot$. Therefore, the neutron stars must have a dark matter mass contribution smaller than 5% of the total mass of the neutron star. Figures 8.6 and 8.7 suggest that if the neutron stars contain strange matter at higher energy densities, they can produce neutron stars with a maximum mass of 2 $M_\odot$ and the accumulation of the dark matter drops the maximum mass of the neutron star close to 2 $M_\odot$ when the dark matter mass contribution is 5% of the total mass of the neutron star. The radius of the neutron star remains in the range of 9 to 13 km for all the cases explored of dark matter accumulation. Therefore, having 5% of the mass contributed by dark matter to the total mass of the neutron star seems to be enough to make significant changes in the properties of the neutron star. Having 5% or less dark matter mass in the core seems like a good and realistic approximation to see the changes in the neutron star's properties. The mass and radius analysis suggest that the presence of dark matter inside the neutron star reduces the maximum mass and radius of the neutron star. For the same contribution of dark matter mass to the total mass of the neutron star, the bosonic dark matter neutron stars are bigger and heavier compared to the fermionic dark matter neutron stars.

For all the cases considered, Figs. 8.8 to 8.13 show the distribution of the energy density of nuclear matter and dark matter inside the neutron stars (Nelson et al. 2019), which contain 5% dark matter mass to the total neutron star mass. In general, these figures suggest that regardless of the nuclear matter inside the neutron stars, the bosonic dark matter captured by the neutron star remains trapped inside the neutron star, while the captured fermionic dark matter covers the neutron star from the center to the surface, and in fact, fermionic dark matter envelops the neutron star. From Figures 8.14 to 8.19, the analysis of the constraint on tidal deformability indicates that, in general, neutron stars can contain a greater amount of bosonic dark matter compared to fermionic dark matter (Husain and Thomas 2021a). The fermionic dark matter mass contribution can be at most 10% of the total neutron star mass for nucleons only equation of state (N-QMC700) and hyperons included equation of state (F-QMC700),

while it can be 18% for bosonic dark matter with N-QMC700. Tidal deformability of the strange matter equation of state of the neutron star suggests that the dark matter contribution to the total mass of the neutron star cannot be greater than 5% regardless of whether dark matter is fermionic or bosonic in nature.

.

9.2 Fornal and Grinstein hypothesis

Apart from the effects of captured dark matter inside the neutron stars on its properties. In section 8.2, Fornal and Grinstein's hypothesis of neutrons decaying into χ (dark matter fermion) and ϕ (dark boson) is explored. Figure 8.20 shows that the presence of dark matter soften the equation of state and it has been displayed in Figure 8.21 that the dark matter has to be self-repulsive with vector coupling strength $G \geq 26$ fm^2 in order to produce the neutron stars of mass above 2 $M_\odot$ and to be consistent with the observations. Figure 8.22 shows that, at this coupling strength, the constraint on the tidal deformability, which is derived from the gravitational wave observation of GW170817, is also satisfied. As the coupling strength of the dark matter increases, the population of dark matter inside the neutron star decreases, as shown in Figs. 8.23 and 8.24. Therefore, when $G \geq 26$ fm^2 the population of dark matter inside the neutron star is relatively low, the relative population of dark matter particles is less than 5% even in heavier stars, with masses of order 1.8 $M_\odot$. Even though the amount of dark matter populated inside the neutron star is low, it is enough to make significant changes in the properties of the neutron star. Figs. 8.25, 8.26 and 8.27 demonstrate that it is not possible to conserve the number of baryons while keeping the total mass fixed inside the neutron star. Instead, the figures indicate that to keep the total number of baryons and total energy conserved, the neutron star must heat up during the decay process. The nuclear matter inside the neutron star will cool down by the standard mechanism, but the cooling of dark matter will take much longer. The primary mechanism of dark matter cooling will involve the collision of two dark matter particles, producing two neutrons, which will be partially Pauli blocked because of the rapid cooling of the nuclear matter. This mechanism will be

considerably slower than the rate of neutron decay to dark matter, but it will cool down the neutron star, eventually.

Table 8.3 shows that the decay of neutrons to dark matter causes a significant reduction in the radius of the neutron star, which leads to a reduction in the moment of inertia. Therefore, the rate of rotation of the star must change; in fact, the neutron stars must spin up during the decay. The dark matter populated inside the neutron star must be at a finite temperature and will cool down very slowly. Given the mechanism for the decay, the time scale for the neutron star to spin-up should be about 100,000 seconds. The neutron star spinning up and heating may provide signals of the neutron decay inside the neutron star.

Moreover, in section 8.4, the Fornal and Grinstein hypothesis is extended, and the ϕ boson is considered to have a mass of 1 MeV, with the ϕ bosons remaining trapped inside the neutron star. From Figures 8.36 to 8.39, it is clear that the presence of ϕ bosons of mass 1 MeV does not affect the properties of neutron stars. The properties of the neutron star remain very similar to those of the massless ϕ boson. Additionally, different scenarios for ϕ bosons to decay into Standard Model particles are considered, and based on the heating of the neutron stars, constraints on the couplings of ϕ bosons with Standard Model particles are deduced.

9.3 Strumia hypothesis

Similar to the Fornal and Grinstein hypothesis, the Strumia hypothesis leads to changes in neutron star properties. Figure 8.29 demonstrates that the equation of state following Strumia's hypothesis of neutron decay remains quite stiff. Figure 8.30 indicates that the neutrons decay into three identical dark matter particles, where dark matter particles are non-self-repulsive, which is consistent with the neutron star maximum mass constraint, regardless of the nuclear matter inside the neutron star, be it nucleons only or hyperons at the core. The Strumia's decay hypothesis suggests that the dark matter particles do not need to be necessarily self-interacting in order to produce neutron stars of above 2 $M_{\odot}$. Figure 8.31 suggests that the neutrons decay into three identical dark matter particles, which is also consistent with the constraint on the tidal deformability of the neutron star. It is evident from Figure 8.32 that the moment of

inertia of the neutron star decreases, followed by the neutron decay into dark matter similar to the Fornal and Grinstein decays. Following Strumia's decay hypothesis, it suggests that neutron stars must spin up during the decay. Figure 8.33 illustrates that the populated dark matter remains trapped inside the neutron star.

As illustrated by Figs. 8.34 and 8.35 that the population of dark matter is very low in lighter neutron stars but increases rapidly in heavier neutron stars, which suggests that heavier neutron stars with a considerable population of dark matter are ideal for studying this mode of neutron decay. Similar to Fornal and Grinstein decay, it is not possible to conserve the total number of baryons and keep the mass of the neutron star fixed. From the conservation of total baryon number and total energy, Tables 8.3 and 8.4 show that if neutrons decay into three identical dark matter particles inside a neutron star, then the neutron star must heat up by 6 MeV (nucleons only at the core) and 6.5 MeV (hyperons included at the core), approximately, depending on the nuclear matter considered at the core of the neutron star. The nuclear matter will cool down by the Urca process, while the dark matter will cool down by dark matter-dark matter collisions, the mechanism suggested above in Fornal and Grinstein section. As suggested in Tables 8.3 and 8.4, compared to the neutron star properties at $0^{\circ}K$ the heating of dark matter does not lead to a significant change in the radius or moment of inertia of the neutron star. Although, there is a significant change in the radius and the moment of inertia of the neutron star before and after the decay. Therefore, the Strumia hypothesis of neutron decay also leads to heating and spinning up the neutron star.

9.4 Future outlook

As shown above, the results of fermionic dark matter capture indicate that the fermionic dark matter envelops the neutron star while the bosonic dark matter remains inside the core. In the future, it will be interesting to look for the gravitational lensing effects around neutron stars can provide valuable information about the nature of the dark matter enveloping the neutron star. The gravitational lensing effects are influenced by the mass and distribution of the dark matter around the neutron star. Therefore, by measuring these effects, scientists

can infer the properties of the dark matter, such as its mass, density, and distribution. It is also possible that different types of dark matter, such as fermionic or bosonic, could produce different gravitational lensing effects, allowing scientists to distinguish between different dark matter models.

The observation of a supernova that results in a newly born neutron star will be interesting in the future. Indeed, the observation of a supernova resulting in a newly born neutron star that exhibits heating or spinning-up within 100,000 seconds after its birth would be a significant breakthrough in particle physics. This would provide strong evidence for the decay of neutrons into dark matter, as predicted by Fornal and Grinstein, and Strumia's hypothesis. Furthermore, it would open up new avenues for research and investigation into the properties of dark matter and its interactions with normal matter. The detection of such signals would also have implications for our understanding of the evolution and dynamics of supernovae and neutron stars, which are important astrophysical objects with a wide range of applications in various fields of physics.

In addition to the signals mentioned earlier, it would be worthwhile to calculate the frequency and amplitude of the gravitational signal for a binary system of neutron stars when the neutron stars are relatively close to each other and the distance between them is just a few times the radius of the neutron stars and they contain dark matter inside. At this point, the internal structure of the neutron stars becomes important, the tidal effects on nuclear matter and dark matter will be different, and the gravitational wave signal is expected to change dramatically if the neutron stars contain dark matter inside. The calculated values can be compared with observational constraints and findings.

Appendix A

Nuclear theory

The mass of baryons in the bag model

The mass of baryon of flavour f, containing quarks (n_{ud}, n_s) is given by

$$M_f = \frac{n_{ud}\Omega(m_{ud}) + n_s\Omega(m_s)}{R} - \frac{Z_0}{R} + \Delta E_M(f) + (4/3)\pi B R^3, \tag{9.1}$$

where B is the bag constant, R is the radius of the bag, and $\Omega(m)$ (quark mode) is calculated using the boundary condition

$$\frac{\sin x}{x} + \frac{\cos x - \frac{\sin x}{x}}{\Omega + mR} = 0, \qquad x = \sqrt{\Omega^2 - (mR)^2}, \tag{9.2}$$

where $\Omega^2 - (mR)^2 < 0$ in the presence of a scalar field. But the equation remains valid by analytical continuation. The radius of the bag is set to be constant for every baryon, regardless of its flavour. Therefore, using the stability condition $\frac{\delta M_f}{\delta R} = 0$. The masses of Up and the Down quarks are considered to be 0, and the zero point parameter. Z_0, is considered to be the same for all particles.

DeGrand et al. 1975 determined the Hyperfine color interaction for color singlet baryon

$$\Delta E_M = \Sigma_i^j E_{ij} \vec{\sigma_i}.\vec{\sigma_j}, i < j, \tag{9.3}$$

where σ_i stands for the Pauli matrix and E_{ij} is calculated in terms of magnetic moment μ_i as

$$E_{ij} = 8g_c \frac{\mu_i(R)\mu_j(R)I_{ij}}{R^3} \tag{9.4}$$

$$\mu_i(R) = \frac{4R\Omega(m_i) + 2R^2 m_j - 3R}{12\Omega(m_i)(\Omega(m_i) - 1) + 6Rm_i} \tag{9.5}$$

where g_c is the color coupling constant. It is noted that quark mass dependence produces a non-trivial flavour dependence of the coupling to the nuclear scalar field. The expression for the overlapping integral I_{ij} is:

$$I_{ij} = 1 + \frac{-3y_iy_j - 4x_ix_j \sin^2 x_i \sin^2 x_j + x_ix_jK_{ij}}{2(x_i \sin^2 x_j - (3/2)y_i)(x_j \sin^2 x_j - (3/2)y_j)} \tag{9.6}$$

$$K_{ij} = 2x_iS_i(2x_i) + 2x_jS_j(2x_j) - (x_i + x_j)S_i(2x_i + 2x_j) - (x_i - x_j)S_i(2x_i - 2x_j) \tag{9.7}$$

$$y_i = x_i - \sin x_i \cos x_i, \qquad x_i = \sqrt{\Omega(m_i)^2 - (Rm_i)^2} \tag{9.8}$$

Effective mass of the baryon

In the presence of constant scalar field over the volume of baryon, the variations of the field induces the spin-orbit interaction, that is neglected in uniform matter consideration. Let the strange quark does not interact with the scalar field.

$$m_{ud} \to m_{ud} - g^q_\sigma\sigma, m_s \to m_s \tag{9.9}$$

where σ represents the scalar field and g^q_σ shown the coupling constant of σ to Up (u) and Down (d) quarks. Then mass of baryon of flavour f as a function of σ depends on R_N^{free}. In a medium

$$M_f \to M_f(m_{u,d} - g^q_\sigma, R_N^{free}). \tag{9.10}$$

Simply a fit of $M_f(\sigma, R_N^{free}) - M_f(0, R_N^{free})$ is made in powers of $m_{u,d} - g^q_\sigma\sigma$, with also coefficients also fitted as polynomials in R_N^{free}.
$\sigma - N$ coupling is defined as

$$g_\sigma = \frac{\partial M_N(\sigma, R_N^{free})}{\partial\sigma}|_{\sigma=0} = -g^q_\sigma \frac{\partial M_N(\sigma, R_N^{free})}{\partial m}|_{m=0}, \tag{9.11}$$

which allows us to eliminate g^q_σ in favour of g_σ. And following expression is formed

$$M_f(\sigma, R_N^{free}) - M_f(0, R_N^{free}) = P_f^{(1)}(R_N^{free})g_\sigma\sigma + P_f^{(2)}(R_N^{free})(g_\sigma\sigma)^2 + ... \tag{9.12}$$

where by construction

$$P_N^{(1)}(R_N^{free}) = -1, \tag{9.13}$$

if the mass is approximately

$$M_f = \frac{N_u\Omega(m_{ud}) + N_s\Omega(m_s)}{R_N^{free}}, \tag{9.14}$$

$$P^1_{\Lambda\Sigma} = -2/3, \qquad P^1_{\Xi} = -1/3. \tag{9.15}$$

Following Kolomeitsev and Voskresensky 2003, $M_f(\sigma)$ becomes

$$M_f(\sigma) = M_f - \omega^\sigma_f g_\sigma \sigma + (d/2)\tilde{\omega}^\sigma_f (g_\sigma \sigma)^2, \tag{9.16}$$

where d is scalar polarisability, values of ω^σ_f & $\tilde{\omega^\sigma_f}$ are given in Table 9.1 and the selected value of $R_{N(free)}$ is 0.8 fm.

	N	Λ	Σ	Ξ
d(fm)	0.15	0.15	0.15	0.15
ω^σ_f	1	0.703	0.614	0.353
$\tilde{\omega^\sigma_f}$	1	0.68	0.673	0.371

TABLE 9.1: Values of d, ω^σ_f, and $\tilde{\omega^\sigma_f}$ for different baryons.

Appendix B

Structural equations

Christoffel symbols and Ricci scalar

$$
\begin{aligned}
\Gamma^{\lambda}_{t\kappa}\Gamma^{\kappa}_{\lambda t} &= (\Gamma^{t}_{tt})^2 + 2\Gamma^{t}_{ti}\Gamma^{i}_{tt} + \Gamma^{i}_{tj}\Gamma^{j}_{it} = 2(\Phi')^2 e^{2\nu-2\Lambda},\\
\Gamma^{\lambda}_{r\kappa}\Gamma^{\kappa}_{\lambda r} &= (\Gamma^{t}_{rt})^2 + 2\Gamma^{t}_{ri}\Gamma^{i}_{tr} + \Gamma^{i}_{rj}\Gamma^{j}_{ir} = (\Phi')^2 + (\Lambda')^2 + \frac{2}{r^2},\\
\Gamma^{\lambda}_{\theta\kappa}\Gamma^{\kappa}_{\lambda\theta} &= (\Gamma^{t}_{\theta t})^2 + 2\Gamma^{t}_{\theta i}\Gamma^{i}_{t\theta} + \Gamma^{i}_{\theta j}\Gamma^{j}_{i\theta} = -2e^{-2\lambda} + \cot^2\theta,\\
\Gamma^{\lambda}_{\phi\kappa}\Gamma^{\kappa}_{\lambda\phi} &= (\Gamma^{t}_{\phi t})^2 + 2\Gamma^{t}_{\phi i}\Gamma^{i}_{t\phi} + \Gamma^{i}_{\phi j}\Gamma^{j}_{i\phi} = -2(\sin^2\theta e^{-2\Lambda} + \cos^2\theta),
\end{aligned}
\tag{9.17}
$$

$$
\begin{aligned}
R^{t}_{rtr} &= -\Phi'' - (\Phi')^2 + \Phi'\Lambda',\\
R^{t}_{\theta t\theta} &= r\Phi' e^{-2\Lambda},\\
R^{t}_{\phi t\phi} &= r\Phi' \sin^2\theta e^{-2\Lambda},\\
R^{r}_{ttr} &= [-\Phi'' - (\Phi')^2 + \Phi'\Lambda']e^{2\Phi-2\Lambda},\\
R^{r}_{\theta r\theta} &= r\Lambda' e^{-2\Lambda},\\
R^{r}_{\phi r\phi} &= r\Lambda' \sin^2\theta e^{-2\Lambda},\\
R^{\theta}_{tt\theta} &= -\Phi' r e^{2(\Phi-\Lambda)},\\
R^{\theta}_{rr\theta} &= -\frac{\Lambda'}{r},\\
R^{\theta}_{\phi\theta\phi} &= \sin^2\theta(1 - e^{-2\Lambda}),\\
R^{\phi}_{tt\phi} &= -\Phi' r e^{2(\Phi-\Lambda)},\\
R^{\phi}_{rr\phi} &= \frac{\Lambda'}{r},\\
R^{\phi}_{\theta\theta\phi} &= -1 + e^{-2\Lambda},
\end{aligned}
\tag{9.18}
$$

Ricci tensors are given by

$$\begin{aligned} R_{tt} &= [-\Phi'\Lambda' + \Phi'' + (\Phi')^2 + 2\frac{\Phi'}{r}]e^{2(\Phi-\Lambda)}, \\ R_{rr} &= -\Phi'' - \Phi'^2 + \Phi'\Lambda' + \frac{2\Lambda'}{r}, \\ R_{\theta\theta} &= [-r\Phi' + r\Lambda' + e^{2\Lambda} - 1]e^{-2\Lambda}, \\ R_{\phi\phi} &= -\sin^2\theta[r\Phi' - r\Lambda' - e^{2\Lambda} + 1]e^{-2\Lambda}. \end{aligned} \tag{9.19}$$

Individual components of mixed Ricci tensors are calculated by the relation

$$R^{\mu}_{\nu} = g^{\mu\lambda}R_{\lambda\nu}, \tag{9.20}$$

and Ricci scalar is obtained from the relation,

$$R = g^{\mu\nu}R_{\mu\nu}, \tag{9.21}$$

Relation between Φ and P

$$T^{\mu}_{\nu;\mu} = 0 = (\epsilon + P)u_{\sigma;\mu}u^{\mu} + P_{,\sigma} + P_{,\mu}\,u^{\mu}u_{\sigma}, \tag{9.22}$$

where σ is the dummy index. One notices that $P_{,r}$ is non-zero and non-trivial component is

$$(\epsilon + P)u_{r;\mu}u^{\mu} + P_{,r} = 0, \tag{9.23}$$

and

$$u_{r;\mu} = \frac{\partial u_r}{\partial x^{\mu}} - \Gamma^{\lambda}_{r\mu}u_{\lambda} = -\Gamma^{\lambda}_{r\mu}u_{\lambda}, \tag{9.24}$$

which gives the desired relation

$$\frac{dP}{dr} = (\epsilon + P)\Gamma^{\lambda}_{r\mu}u_{\lambda}u^{\mu} = -(\epsilon + P)\frac{d\Phi}{dr}. \tag{9.25}$$

Equations of rotating neutron stars

Mixed tensor R^t_ϕ is calculated ($R^t_\phi = R_{\phi\nu}g^{\nu t}$) as,

$$\begin{aligned}R^t_\phi = (-1/2)[&e^{2\nu(r,\theta)}\frac{\partial^2}{\partial r^2}\omega(r,\theta) + e^{2\lambda(r,\theta)}\frac{\partial^2}{\partial\theta^2}\omega(r,\theta) + (\frac{\partial}{\partial\theta}\lambda(r,\theta)) \times e^{2\lambda(r,\theta)}\frac{\partial}{\partial\theta}\omega(r,\theta)\\
&+ (\frac{\partial}{\partial r}\mu(r,\theta))e^{2\mu(r,\theta)}\frac{\partial}{\partial r}\omega(r,\theta) + 3(\frac{\partial}{\partial\theta}\psi(r,\theta))e^{2\lambda(r,\theta)}\frac{\partial}{\partial\theta}\omega(r,\theta)\\
&- (\frac{\partial}{\partial r}\lambda(r,\theta))e^{2\mu(r,\theta)} \times \frac{\partial}{\partial r}\omega(r,\theta) - (\frac{\partial}{\partial r}\omega(r,\theta))e^{2\mu(r,\theta)}\frac{\partial}{\partial r}\nu(r,\theta)\\
&- (\frac{\partial}{\partial\theta}\omega(r,\theta)) \times e^{2\lambda(r,\theta)}\frac{\partial}{\partial\theta}\nu(r,\theta) + 3(\frac{\partial}{\partial r}\psi(r,\theta))e^{2\mu(r,\theta)}\frac{\partial}{\partial r}\omega(r,\theta)\\
&- (\frac{\partial}{\partial\theta}\mu(r,\theta))e^{2\lambda(r,\theta)}\omega(r,\theta)] \times e^{2\psi(r,\theta)-2\nu(r,\theta)-2\lambda(r,\theta)-2\mu(r,\theta)}\end{aligned} \tag{9.26}$$

$$T^t_\phi = -\frac{e^{2\psi(r,\theta)}[\epsilon+P][\Omega-\omega(r,\theta)]}{-e^{2\nu(r,\theta)}+[\Omega-\omega(r,\theta)]^2e^{2\psi(r,\theta)}}, \tag{9.27}$$

$$e^{2\psi} \to r^2\sin^2\theta, \tag{9.28}$$

$$T^t_\phi = \frac{r^2\sin^2\theta[\epsilon+P]\overline{\omega}e^{-2\nu}}{1-\overline{\omega}^2e^{2\psi-2\nu}}, \tag{9.29}$$

$$T^t_\phi = r^2\sin^2\theta[\epsilon+P]\bar{\omega}e^{-2\nu} + O(\Omega^2), \tag{9.30}$$

we have

$$\frac{\partial\lambda}{\partial\theta} = \frac{\partial\nu}{\partial\theta} = \frac{\partial\mu}{\partial\theta} = 0, \tag{9.31}$$

consequently,

$$\begin{aligned}R^t_\phi = -\frac{1}{2}[&e^{2\mu}\frac{\partial^2\omega}{\partial r^2} + e^{2\lambda}\frac{\partial^2\omega}{\partial\theta^2} + \frac{\partial\mu}{\partial r}e^{2\mu}\frac{\partial\omega}{\partial r} - \frac{\partial\lambda}{\partial r}e^{2\mu}\frac{\partial\omega}{\partial r} - \frac{\partial\nu}{\partial r}e^{2\mu}\frac{\partial\omega}{\partial r}\\
&+3\frac{\partial\psi}{\partial r}e^{2\mu}\frac{\partial\omega}{\partial r}]e^{2\psi-2\nu-2\lambda-2\mu}\end{aligned} \tag{9.32}$$

$$\begin{aligned}R^t_\phi = -\frac{1}{2}[&\frac{\partial^2\omega}{\partial r^2} + e^{2\lambda-2\mu}\frac{\partial^2\omega}{\partial\theta^2} + \frac{\partial\mu}{\partial r}\frac{\partial\omega}{\partial r} - \frac{\partial\lambda}{\partial r}\frac{\partial\omega}{\partial r} - \frac{\partial\nu}{\partial r}\frac{\partial\omega}{\partial r}\\
&+3\frac{\partial\psi}{\partial r}\frac{\partial\omega}{\partial r}]e^{2\psi-2\nu-2\lambda}\end{aligned} \tag{9.33}$$

$$R^t_\phi = 8\pi T^t_\phi, \tag{9.34}$$

$$\begin{aligned}-\frac{1}{2}[&\frac{\partial^2\omega}{\partial r^2} + e^{2\lambda-2\mu}\frac{\partial^2\omega}{\partial\theta^2} + \frac{\partial\mu}{\partial r}\frac{\partial\omega}{\partial r} - \frac{\partial\lambda}{\partial r}\frac{\partial\omega}{\partial r} - \frac{\partial\nu}{\partial r}\frac{\partial\omega}{\partial r} + 3\frac{\partial\psi}{\partial r}\frac{\partial\omega}{\partial r}]e^{2\psi-2\nu-2\lambda}\\
&= 8\pi r^2\sin^2\theta[\epsilon+P]\overline{\omega}e^{-2\nu}\end{aligned} \tag{9.35}$$

Bibliography

Abazajian, Kevork (Mar. 2006). 'Linear cosmological structure limits on warm dark matter'. In: *Phys. Rev. D* 73 (6), p. 063513. DOI: 10.1103/PhysRevD.73.063513. URL: https://link.aps.org/doi/10.1103/PhysRevD.73.063513.

Abazajian, Kevork, George M. Fuller and Wallace H. Tucker (2001). 'Direct Detection of Warm Dark Matter in the X-Ray'. In: *The Astrophysical Journal* 562, pp. 593–604.

Abbott, B. P. et al. (2017a). 'GW170817: Observation of Gravitational Waves from a Binary Neutron Star Inspiral'. In: *Phys. Rev. Lett.* 119.16, p. 161101. DOI: 10.1103/PhysRevLett.119.161101. arXiv: 1710.05832 [gr-qc].

— (2018). 'GW170817: Measurements of neutron star radii and equation of state'. In: *Phys. Rev. Lett.* 121.16, p. 161101. DOI: 10.1103/PhysRevLett.121.161101. arXiv: 1805.11581 [gr-qc].

Abbott, B. P. et al. (Oct. 2017b). 'GW170817: Observation of Gravitational Waves from a Binary Neutron Star Inspiral'. In: *Physical Review Letters* 119.16. ISSN: 1079-7114. DOI: 10.1103/physrevlett.119.161101. URL: http://dx.doi.org/10.1103/PhysRevLett.119.161101.

Abbott, B. P. et al. (Sept. 2019). 'GWTC-1: A Gravitational-Wave Transient Catalog of Compact Binary Mergers Observed by LIGO and Virgo during the First and Second Observing Runs'. In: *Physical Review X* 9.3. ISSN: 2160-3308. DOI: 10.1103/physrevx.9.031040. URL: http://dx.doi.org/10.1103/PhysRevX.9.031040.

Abbott, L.F. and P. Sikivie (1983). 'A cosmological bound on the invisible axion'. In: *Physics Letters B* 120.1, pp. 133–136. ISSN: 0370-2693. DOI: https://doi.org/10.1016/0370-2693(83)90638-X.

Aguilar, M. et al. (Aug. 2016). 'Antiproton Flux, Antiproton-to-Proton Flux Ratio, and Properties of Elementary Particle Fluxes in Primary Cosmic Rays Measured with the

Alpha Magnetic Spectrometer on the International Space Station'. In: *Phys. Rev. Lett.* 117 (9), p. 091103. DOI: 10.1103/PhysRevLett.117.091103. URL: https://link.aps.org/doi/10.1103/PhysRevLett.117.091103.

Ahmad, Q. R. et al. (June 2002). 'Direct Evidence for Neutrino Flavor Transformation from Neutral-Current Interactions in the Sudbury Neutrino Observatory'. In: *Phys. Rev. Lett.* 89 (1), p. 011301. DOI: 10.1103/PhysRevLett.89.011301. URL: https://link.aps.org/doi/10.1103/PhysRevLett.89.011301.

Akmal, A., V. R. Pandharipande and D. G. Ravenhall (Sept. 1998). 'Equation of state of nucleon matter and neutron star structure'. In: *Phys. Rev. C* 58 (3), pp. 1804–1828. DOI: 10.1103/PhysRevC.58.1804. URL: https://link.aps.org/doi/10.1103/PhysRevC.58.1804.

Alcock, Charles, Edward Farhi and Angela Olinto (Nov. 1986). 'Strange Stars'. In: *apj* 310, p. 261. DOI: 10.1086/164679.

An, Haipeng et al. (July 2015). 'Direct detection constraints on dark photon dark matter'. In: *Physics Letters B* 747, pp. 331–338. DOI: 10.1016/j.physletb.2015.06.018. URL: https://doi.org/10.1016%5C%2Fj.physletb.2015.06.018.

Antoniadis, John et al. (Apr. 2013a). 'A Massive Pulsar in a Compact Relativistic Binary'. In: *Science* 340.6131. DOI: 10.1126/science.1233232. URL: https://doi.org/10.1126%2Fscience.1233232.

Antoniadis, John et al. (Apr. 2013b). 'A Massive Pulsar in a Compact Relativistic Binary'. In: *Science* 340.6131, p. 448. DOI: 10.1126/science.1233232. arXiv: 1304.6875 [astro-ph.HE].

Antypas, D. et al. (Mar. 2022). 'New Horizons: Scalar and Vector Ultralight Dark Matter'. In: arXiv: 2203.14915 [hep-ex].

Aprile, E. et al. (Oct. 2017). 'First Dark Matter Search Results from the XENON1T Experiment'. In: *Phys. Rev. Lett.* 119 (18), p. 181301. DOI: 10.1103/PhysRevLett.119.181301. URL: https://link.aps.org/doi/10.1103/PhysRevLett.119.181301.

Aprile, E. et al. (July 2022). 'Emission of single and few electrons in XENON1T and limits on light dark matter'. In: *Phys. Rev. D* 106 (2), p. 022001. DOI: 10.1103/PhysRevD.

106.022001. URL: https://link.aps.org/doi/10.1103/PhysRevD.106.022001.

Arnett, W. David and Richard L. Bowers (Apr. 1977). 'A Microscopic Interpretation of Neutron Star Structure'. In: *apjs* 33, p. 415. DOI: 10.1086/190434.

Arzumanov, S. et al. (2015). 'A measurement of the neutron lifetime using the method of storage of ultracold neutrons and detection of inelastically up-scattered neutrons'. In: *Physics Letters B* 745, pp. 79–89. ISSN: 0370-2693. DOI: https://doi.org/10.1016/j.physletb.2015.04.021.

Asztalos, S. J. et al. (May 2002). 'Experimental Constraints on the Axion Dark Matter Halo Density'. In: *The Astrophysical Journal* 571.1, pp. L27–L30. DOI: 10.1086/341130. URL: https://doi.org/10.1086/341130.

Audren, Benjamin et al. (Dec. 2014). 'Strongest model-independent bound on the lifetime of Dark Matter'. In: *Journal of Cosmology and Astroparticle Physics* 2014.12, pp. 028–028. DOI: 10.1088/1475-7516/2014/12/028. URL: https://doi.org/10.1088/1475-7516/2014/12/028.

Baade, W. and F. Zwicky (July 1934). 'Remarks on Super-Novae and Cosmic Rays'. In: *Phys. Rev.* 46 (1), pp. 76–77. DOI: 10.1103/PhysRev.46.76.2. URL: https://link.aps.org/doi/10.1103/PhysRev.46.76.2.

Bahcall, J. N. (Jan. 1978). 'Masses of neutron stars and black holes in X-ray binaries.' In: *araa* 16, pp. 241–264. DOI: 10.1146/annurev.aa.16.090178.001325.

Bahcall, John N. and Richard A. Wolf (Dec. 1965). 'Neutron Stars. II. Neutrino-Cooling and Observability'. In: *Phys. Rev.* 140 (5B), B1452–B1466. DOI: 10.1103/PhysRev.140.B1452. URL: https://link.aps.org/doi/10.1103/PhysRev.140.B1452.

Baker, C. A. et al. (Sept. 2006). 'Improved Experimental Limit on the Electric Dipole Moment of the Neutron'. In: *Phys. Rev. Lett.* 97 (13), p. 131801. DOI: 10.1103/PhysRevLett.97.131801. URL: https://link.aps.org/doi/10.1103/PhysRevLett.97.131801.

Balberg, Shmuel and Nir Barnea (Jan. 1998). 'S-wave pairing of $\Lambda hyperonsindensematter$'. In: *Phys. Rev. C* 57 (1), pp. 409–416. DOI: 10.1103/PhysRevC.57.409. URL: https://link.aps.org/doi/10.1103/PhysRevC.57.409.

Balberg, Shmuel, Itamar Lichtenstadt and Gregory B. Cook (Apr. 1999). 'Roles of Hyperons in Neutron Stars'. In: *The Astrophysical Journal Supplement Series* 121.2, pp. 515–531. DOI: 10.1086/313196. URL: https://doi.org/10.1086/313196.

Bales, M. J. et al. (June 2016). 'Precision Measurement of the Radiative β Decay of the Free Neutron'. In: *Phys. Rev. Lett.* 116 (24), p. 242501. DOI: 10.1103/PhysRevLett.116.242501. URL: https://link.aps.org/doi/10.1103/PhysRevLett.116.242501.

Baym, G and C Pethick (1975). 'Neutron Stars'. In: *Annual Review of Nuclear Science* 25.1, pp. 27–77. DOI: 10.1146/annurev.ns.25.120175.000331. eprint: https://doi.org/10.1146/annurev.ns.25.120175.000331. URL: https://doi.org/10.1146/annurev.ns.25.120175.000331.

Baym, Gordon, Hans A. Bethe and Christopher J Pethick (1971). 'Neutron star matter'. In: *Nuclear Physics A* 175.2, pp. 225–271. ISSN: 0375-9474. DOI: https://doi.org/10.1016/0375-9474(71)90281-8.

Baym, Gordon et al. (Aug. 2018). 'Testing Dark Decays of Baryons in Neutron Stars'. In: *Phys. Rev. Lett.* 121 (6), p. 061801. DOI: 10.1103/PhysRevLett.121.061801. URL: https://link.aps.org/doi/10.1103/PhysRevLett.121.061801.

Beck, D.H. (2019). 'Neutron decay, dark matter and neutron stars'. In: *EPJ Web Conf.* 219, p. 05006. DOI: 10.1051/epjconf/201921905006. URL: https://doi.org/10.1051/epjconf/201921905006.

Bell, Nicole F., Giorgio Busoni and Sandra Robles (June 2019). 'Capture of leptophilic dark matter in neutron stars'. In: *Journal of Cosmology and Astroparticle Physics* 2019.06, pp. 054–054. DOI: 10.1088/1475-7516/2019/06/054. URL: https://doi.org/10.1088%5C%2F1475-7516%5C%2F2019%5C%2F06%5C%2F054.

Bell, Nicole F. et al. (2020). *Nucleon Structure and Strong Interactions in Dark Matter Capture in Neutron Stars*. arXiv: 2012.08918 [hep-ph].

Bennett, C. L. et al. (Sept. 2003). 'First-Year <i<Wilkinson Microwave Anisotropy Probe</i< (<si<WMAP</i<) Observations: Preliminary Maps and Basic Results'. In: *The Astrophysical Journal Supplement Series* 148.1, pp. 1–27. DOI: 10.1086/377253. URL: https://doi.org/10.1086/377253.

Berezhiani, Zurab et al. (Nov. 2021). 'Neutron-mirror neutron mixing and neutron stars'. In: *The European Physical Journal C* 81.11. ISSN: 1434-6052. DOI: 10.1140/epjc/s10052-021-09806-1. URL: http://dx.doi.org/10.1140/epjc/s10052-021-09806-1.

Berryman, Jeffrey M., Susan Gardner and Mohammadreza Zakeri (Jan. 2022). 'Neutron Stars with Baryon Number Violation, Probing Dark Sectors'. In: arXiv: 2201.02637 [hep-ph].

Bertone, Gianfranco and Malcolm Fairbairn (Feb. 2008). 'Compact stars as dark matter probes'. In: *Phys. Rev. D* 77 (4), p. 043515. DOI: 10.1103/PhysRevD.77.043515. URL: https://link.aps.org/doi/10.1103/PhysRevD.77.043515.

Blaschke, D. et al. (Dec. 2009). 'Sequential deconfinement of quark flavors in neutron stars'. In: *Phys. Rev. C* 80 (6), p. 065807. DOI: 10.1103/PhysRevC.80.065807. URL: https://link.aps.org/doi/10.1103/PhysRevC.80.065807.

Bonn, J et al. (2000). 'Results of the Mainz neutrino mass experiment'. In: *Nuclear Physics B - Proceedings Supplements* 87.1. Proceedings of the Sixth International Workshop on Topics in Astroparticle and Underground Physics, pp. 271–274. ISSN: 0920-5632. DOI: https://doi.org/10.1016/S0920-5632(00)00677-0. URL: https://www.sciencedirect.com/science/article/pii/S0920563200006770.

Bonometto, S.A., F. Gabbiani and A. Masiero (1989). 'A monochromatic axino dominated universe'. In: *Physics Letters B* 222.3, pp. 433–437. ISSN: 0370-2693. DOI: https://doi.org/10.1016/0370-2693(89)90339-0.

Borner, Gerhard and Jeffrey M. Cohen (Nov. 1973). 'Rotating Neutron Star Models and Pulsars'. In: *apj* 185, pp. 959–974. DOI: 10.1086/152470.

Bramante, Joseph, Tim Linden and Yu-Dai Tsai (Mar. 2018). 'Searching for dark matter with neutron star mergers and quiet kilonovae'. In: *Phys. Rev. D* 97 (5), p. 055016. DOI:

10.1103/PhysRevD.97.055016. URL: https://link.aps.org/doi/10.1103/PhysRevD.97.055016.

Bullock, James S. and Michael Boylan-Kolchin (2017). 'Small-Scale Challenges to the Λ CDM Paradigm'. In: *Annual Review of Astronomy and Astrophysics* 55.1, pp. 343–387. DOI: 10.1146/annurev-astro-091916-055313. eprint: https://doi.org/10.1146/annurev-astro-091916-055313. URL: https://doi.org/10.1146/annurev-astro-091916-055313.

— (n.d.). 'Small-Scale Challenges to the ΛCDM Paradigm'. In: ().

Buote, David A. et al. (Sept. 2002). '<i<Chandra</i<Evidence of a Flattened, Triaxial Dark Matter Halo in the Elliptical Galaxy NGC 720'. In: *The Astrophysical Journal* 577.1, pp. 183–196. DOI: 10.1086/342158. URL: https://doi.org/10.1086/342158.

Burkert, A. (July 1995). 'The Structure of Dark Matter Halos in Dwarf Galaxies'. In: *The Astrophysical Journal* 447.1, p. L25. DOI: 10.1086/309560. URL: https://dx.doi.org/10.1086/309560.

Busoni, Giorgio (Dec. 2021). 'Capture of Dark Matter in Neutron Stars'. In: arXiv: 2201.00048 [hep-ph].

— (2022). 'Capture of DM in Compact Stars'. In: *PoS* PANIC2021, p. 046. DOI: 10.22323/1.380.0046.

Byrne, J. et al. (Jan. 1996). 'A revised value for the neutron lifetime measured using a Penning trap'. In: *Europhysics Letters* 33.3, p. 187. DOI: 10.1209/epl/i1996-00319-x. URL: https://dx.doi.org/10.1209/epl/i1996-00319-x.

Cadamuro, Davide and Javier Redondo (2012). 'Cosmological bounds on pseudo Nambu-Goldstone bosons'. In: *JCAP* 02, p. 032. DOI: 10.1088/1475-7516/2012/02/032. arXiv: 1110.2895 [hep-ph].

Canuto, V., B. Datta and J. Lodenquai (Apr. 1975). 'Structure of Neutron Star Cores'. In: *apss* 34.1, pp. 223–229. DOI: 10.1007/BF00646762.

Caputo, Andrea et al. (May 2021). 'Dark photon limits: a cookbook'. In: arXiv: 2105.04565 [hep-ph].

Catena, Riccardo and Piero Ullio (Aug. 2010). 'A novel determination of the local dark matter density'. In: *Journal of Cosmology and Astroparticle Physics* 2010.08, p. 004. DOI: 10.1088/1475-7516/2010/08/004. URL: https://dx.doi.org/10.1088/1475-7516/2010/08/004.

Chabanat, E. et al. (1998). 'A Skyrme parametrization from subnuclear to neutron star densities. 2. Nuclei far from stablities'. In: *Nucl. Phys. A* 635. [Erratum: Nucl.Phys.A 643, 441–441 (1998)], pp. 231–256. DOI: 10.1016/S0375-9474(98)00180-8.

Champion, David J. et al. (June 2008). 'An Eccentric Binary Millisecond Pulsar in the Galactic Plane'. In: *Science* 320.5881, p. 1309. DOI: 10.1126/science.1157580. arXiv: 0805.2396 [astro-ph].

Chodos, A. et al. (Oct. 1974). 'Baryon structure in the bag theory'. In: *Phys. Rev. D* 10 (8), pp. 2599–2604. DOI: 10.1103/PhysRevD.10.2599. URL: https://link.aps.org/doi/10.1103/PhysRevD.10.2599.

Cline, James M. and Jonathan M. Cornell (2018). 'Dark decay of the neutron'. In: *JHEP* 07, p. 081. DOI: 10.1007/JHEP07(2018)081. arXiv: 1803.04961 [hep-ph].

Collins, J. C. and M. J. Perry (May 1975). 'Superdense Matter: Neutrons or Asymptotically Free Quarks?' In: *Phys. Rev. Lett.* 34 (21), pp. 1353–1356. DOI: 10.1103/PhysRevLett.34.1353. URL: https://link.aps.org/doi/10.1103/PhysRevLett.34.1353.

Dalfovo, Franco et al. (1999). 'Theory of Bose-Einstein condensation in trapped gases'. In: *Rev. Mod. Phys.* 71, pp. 463–512. DOI: 10.1103/RevModPhys.71.463. arXiv: cond-mat/9806038.

de Groot, M. (Sept. 1977). 'BOOKS (with comments): "Pulsars", by R. N. Manchester and J. H. Taylor'. In: *Irish Astronomical Journal* 13, p. 142.

DeGrand, T. et al. (Oct. 1975). 'Masses and other parameters of the light hadrons'. In: *Phys. Rev. D* 12 (7), pp. 2060–2076. DOI: 10.1103/PhysRevD.12.2060. URL: https://link.aps.org/doi/10.1103/PhysRevD.12.2060.

Demorest, P. B. et al. (Oct. 2010). 'A two-solar-mass neutron star measured using Shapiro delay'. In: *nat* 467.7319, pp. 1081–1083. DOI: 10.1038/nature09466. arXiv: 1010.5788 [astro-ph.HE].

Dine, Michael and Willy Fischler (1983). 'The not-so-harmless axion'. In: *Physics Letters B* 120.1, pp. 137–141. ISSN: 0370-2693. DOI: https://doi.org/10.1016/0370-2693(83)90639-1.

Dolgov, A. D. et al. (Dec. 2013). 'Constraints on millicharged particles from Planck data'. In: *Phys. Rev. D* 88 (11), p. 117701. DOI: 10.1103/PhysRevD.88.117701. URL: https://link.aps.org/doi/10.1103/PhysRevD.88.117701.

Dremin, Igor M. and Aleksei B. Kaidalov (2006). In: *Physics-Uspekhi* 49.3, p. 263. DOI: 10.1070/pu2006v049n03abeh005873. URL: https://doi.org/10.1070/pu2006v049n03abeh005873.

Duine, R.A. and H.T.C. Stoof (2004). 'Atom–molecule coherence in Bose gases'. In: *Physics Reports* 396.3, pp. 115–195. ISSN: 0370-1573. DOI: https://doi.org/10.1016/j.physrep.2004.03.003.

Einasto, Jaan, Ants Kaasik and Enn Saar (July 1974). 'Dynamic evidence on massive coronas of galaxies'. In: *nat* 250.5464, pp. 309–310. DOI: 10.1038/250309a0.

Einstein, Albert (1936). 'Lens-Like Action of a Star by the Deviation of Light in the Gravitational Field'. In: *Science* 84.2188, pp. 506–507. DOI: 10.1126/science.84.2188.506. eprint: https://www.science.org/doi/pdf/10.1126/science.84.2188.506. URL: https://www.science.org/doi/abs/10.1126/science.84.2188.506.

Eisenstein, Daniel J. et al. (Nov. 2005). 'Detection of the Baryon Acoustic Peak in the Large-Scale Correlation Function of SDSS Luminous Red Galaxies'. In: *The Astrophysical Journal* 633.2, pp. 560–574. DOI: 10.1086/466512. URL: https://doi.org/10.1086/466512.

Ellis, John et al. (June 2018). 'Dark matter effects on neutron star properties'. In: *Physical Review D* 97.12. ISSN: 2470-0029. DOI: 10.1103/physrevd.97.123007. URL: http://dx.doi.org/10.1103/PhysRevD.97.123007.

Faber, M. et al. (Sept. 2009). 'Continuum-state and bound-state β^--decay rates of the neutron'. In: *Phys. Rev. C* 80 (3), p. 035503. DOI: 10.1103/PhysRevC.80.035503. URL: https://link.aps.org/doi/10.1103/PhysRevC.80.035503.

Feng, Jonathan L., Arvind Rajaraman and Fumihiro Takayama (July 2003). 'Superweakly Interacting Massive Particles'. In: *Phys. Rev. Lett.* 91 (1), p. 011302. DOI: 10.1103/PhysRevLett.91.011302. URL: https://link.aps.org/doi/10.1103/PhysRevLett.91.011302.

Flanagan, Éanna É. and Tanja Hinderer (Jan. 2008). 'Constraining neutron-star tidal Love numbers with gravitational-wave detectors'. In: *prd* 77.2, 021502, p. 021502. DOI: 10.1103/PhysRevD.77.021502. arXiv: 0709.1915 [astro-ph].

Fornal, Bartosz and Benjamín Grinstein (2020). 'Neutron's dark secret'. In: *Modern Physics Letters A* 35.31, p. 2030019. DOI: 10.1142/S0217732320300190. eprint: https://doi.org/10.1142/S0217732320300190. URL: https://doi.org/10.1142/S0217732320300190.

Fornal, Bartosz and Benjamın Grinstein (May 2018a). 'Dark Matter Interpretation of the Neutron Decay Anomaly'. In: *Phys. Rev. Lett.* 120 (19), p. 191801. DOI: 10.1103/PhysRevLett.120.191801. URL: https://link.aps.org/doi/10.1103/PhysRevLett.120.191801.

— (May 2018b). 'Dark Matter Interpretation of the Neutron Decay Anomaly'. In: *Phys. Rev. Lett.* 120 (19), p. 191801. DOI: 10.1103/PhysRevLett.120.191801. URL: https://link.aps.org/doi/10.1103/PhysRevLett.120.191801.

Fukuda, Y. et al. (Aug. 1998). 'Evidence for Oscillation of Atmospheric Neutrinos'. In: *Phys. Rev. Lett.* 81 (8), pp. 1562–1567. DOI: 10.1103/PhysRevLett.81.1562. URL: https://link.aps.org/doi/10.1103/PhysRevLett.81.1562.

Glendenning, Norman K. (Aug. 1992). 'First-order phase transitions with more than one conserved charge: Consequences for neutron stars'. In: *Phys. Rev. D* 46 (4), pp. 1274–1287. DOI: 10.1103/PhysRevD.46.1274. URL: https://link.aps.org/doi/10.1103/PhysRevD.46.1274.

Gold, T. (May 1968). 'Rotating Neutron Stars as the Origin of the Pulsating Radio Sources'. In: *nat* 218.5143, pp. 731–732. DOI: 10.1038/218731a0.

Gonzalez, F. M. et al. (2021). 'Improved Neutron Lifetime Measurement with UCNτ'. In: *Phys. Rev. Lett.* 127.16, p. 162501. DOI: 10.1103/PhysRevLett.127.162501. arXiv: 2106.10375 [nucl-ex].

Graham, Peter W. et al. (2015). 'Experimental Searches for the Axion and Axion-Like Particles'. In: *Annual Review of Nuclear and Particle Science* 65.1, pp. 485–514. DOI: 10.1146/annurev-nucl-102014-022120. eprint: https://doi.org/10.1146/annurev-nucl-102014-022120. URL: https://doi.org/10.1146/annurev-nucl-102014-022120.

Graham-Smith, Francis (1977). *Pulsars / F. G. Smith*. English. Cambridge University Press Cambridge ; New York, xii, 239 pages : ISBN: 0521212413.

Grinstein, Benjamın, Chris Kouvaris and Niklas Grønlund Nielsen (2019). 'Neutron Star Stability in Light of the Neutron Decay Anomaly'. In: *Phys. Rev. Lett.* 123.9, p. 091601. DOI: 10.1103/PhysRevLett.123.091601. arXiv: 1811.06546 [hep-ph].

Guichon, P.A.M. (1988a). 'A possible quark mechanism for the saturation of nuclear matter'. In: *Physics Letters B* 200.3, pp. 235–240. ISSN: 0370-2693. DOI: https://doi.org/10.1016/0370-2693(88)90762-9.

Guichon, P.A.M. et al. (June 2006). 'Physical origin of density dependent forces of Skyrme type within the quark meson coupling model'. In: *Nuclear Physics A* 772.1-2, pp. 1–19. DOI: 10.1016/j.nuclphysa.2006.04.002. URL: https://doi.org/10.1016%2Fj.nuclphysa.2006.04.002.

Guichon, Pierre A. M. (1988b). 'A Possible Quark Mechanism for the Saturation of Nuclear Matter'. In: *Phys. Lett. B* 200, pp. 235–240. DOI: 10.1016/0370-2693(88)90762-9.

Guichon, Pierre A. M., Anthony W. Thomas and Kazuo Tsushima (2008). 'Binding of hypernuclei in the latest quark-meson coupling model'. In: *Nucl. Phys. A* 814, pp. 66–73. DOI: 10.1016/j.nuclphysa.2008.10.001. arXiv: 0712.1925 [nucl-th].

Guichon, Pierre A. M. et al. (1996). 'The Role of nucleon structure in finite nuclei'. In: *Nucl. Phys. A* 601, pp. 349–379. DOI: 10.1016/0375-9474(96)00033-4. arXiv: nucl-th/9509034.

Hartle, James B. (Dec. 1967). 'Slowly Rotating Relativistic Stars. I. Equations of Structure'. In: *apj* 150, p. 1005. DOI: 10.1086/149400.

Hartle, James B. and Kip S. Thorne (Sept. 1968). 'Slowly Rotating Relativistic Stars. II. Models for Neutron Stars and Supermassive Stars'. In: *apj* 153, p. 807. DOI: 10.1086/149707.

Harvey, David et al. (2015). 'The non-gravitational interactions of dark matter in colliding galaxy clusters'. In: *Science* 347, pp. 1462–1465. DOI: 10.1126/science.1261381. arXiv: 1503.07675 [astro-ph.CO].

Hessels, Jason W. T. et al. (Mar. 2006). 'A Radio Pulsar Spinning at 716 Hz'. In: *Science* 311.5769, pp. 1901–1904. DOI: 10.1126/science.1123430. arXiv: astro-ph/0601337 [astro-ph].

Hewish, A. et al. (Feb. 1968). 'Observation of a Rapidly Pulsating Radio Source'. In: *nat* 217.5130, pp. 709–713. DOI: 10.1038/217709a0.

Hinderer, Tanja (Apr. 2008). 'Tidal Love Numbers of Neutron Stars'. In: *The Astrophysical Journal* 677.2, pp. 1216–1220. ISSN: 1538-4357. DOI: 10.1086/533487. URL: http://dx.doi.org/10.1086/533487.

Hinderer, Tanja et al. (June 2010). 'Tidal deformability of neutron stars with realistic equations of state and their gravitational wave signatures in binary inspiral'. In: *Physical Review D* 81.12. ISSN: 1550-2368. DOI: 10.1103/physrevd.81.123016. URL: http://dx.doi.org/10.1103/PhysRevD.81.123016.

Husain, Wasif, Theo F. Motta and Anthony W. Thomas (Mar. 2022a). 'Consequences of neutron decay inside neutron stars'. In: arXiv: 2203.02758 [hep-ph].

— (Oct. 2022b). 'Consequences of neutron decay inside neutron stars'. In: *Journal of Cosmology and Astroparticle Physics* 2022.10, p. 028. DOI: 10.1088/1475-7516/2022/10/028. URL: https://doi.org/10.1088%2F1475-7516%2F2022%2F10%2F028.

Husain, Wasif and Anthony W Thomas (Nov. 2022). 'Novel neutron decay mode inside neutron stars'. In: *Journal of Physics G: Nuclear and Particle Physics* 50.1, p. 015202. DOI: 10.1088/1361-6471/aca1d5. URL: https://doi.org/10.1088%2F1361-6471%2Faca1d5.

— (Dec. 2020). 'Significance of lower energy density region of neutron star and universalities among neutron star properties'. In: *Journal of Physics: Conference Series* 1643, p. 012066.

DOI: 10.1088/1742-6596/1643/1/012066. URL: https://doi.org/10.1088/1742-6596/1643/1/012066.

— (2021a). 'Hybrid Stars with Hyperons and Strange Quark Matter'. In: *AIP Conf. Proc.* 2319.1. Ed. by Teck-Yong Tou et al., p. 080001. DOI: 10.1063/5.0036994. arXiv: 2010.06750 [hep-ph].

— (Oct. 2021b). 'Possible nature of dark matter'. In: *Journal of Cosmology and Astroparticle Physics* 2021.10, p. 086. ISSN: 1475-7516. DOI: 10.1088/1475-7516/2021/10/086. URL: http://dx.doi.org/10.1088/1475-7516/2021/10/086.

Iosilevskiy, Igor (2010). 'Non-congruent Phase Transitions in Cosmic Matter and in the Laboratory'. In: DOI: 10.48550/ARXIV.1005.4186. URL: https://arxiv.org/abs/1005.4186.

Ivanenko, D. D. and D. F. Kurdgelaidze (1965). 'Hypothesis concerning quark stars'. In: *Astrophysics* 1, pp. 251–252. DOI: 10.1007/BF01042830.

Ivanov, A. N. et al. (June 2018). 'Neutron Dark Matter Decays'. In: arXiv: 1806.10107 [hep-ph].

Kaaret, P. et al. (Feb. 2007). 'Evidence of 1122 Hz X-Ray Burst Oscillations from the Neutron Star X-Ray Transient XTE J1739-285'. In: *The Astrophysical Journal* 657.2, pp. L97–L100. DOI: 10.1086/513270. URL: https://doi.org/10.1086/513270.

Kahn, F. D. and L. Woltjer (Nov. 1959). 'Intergalactic Matter and the Galaxy.' In: *apj* 130, p. 705. DOI: 10.1086/146762.

Kaplan, D. B. and A. E. Nelson (1988). 'Kaon Condensation in Dense Matter'. In: *Nucl. Phys. A* 479. Ed. by J. Speth, p. 273c. DOI: 10.1016/0375-9474(88)90442-3.

Kolomeitsev, Evgeni E. and Dmitri N. Voskresensky (July 2003). 'Negative kaons in dense baryonic matter'. In: *Physical Review C* 68.1. DOI: 10.1103/physrevc.68.015803. URL: https://doi.org/10.1103%2Fphysrevc.68.015803.

Kouvaris, Chris (May 2012). 'Limits on Self-Interacting Dark Matter from Neutron Stars'. In: *Physical Review Letters* 108.19. ISSN: 1079-7114. DOI: 10.1103/physrevlett.108.191301. URL: http://dx.doi.org/10.1103/PhysRevLett.108.191301.

Kouvaris, Chris (July 2013). 'Composite millicharged dark matter'. In: *Physical Review D* 88.1. DOI: 10.1103/physrevd.88.015001. URL: https://doi.org/10.1103%5C%2Fphysrevd.88.015001.

Kouvaris, Chris and Niklas Grønlund Nielsen (Sept. 2015). 'Asymmetric dark matter stars'. In: *Physical Review D* 92.6. ISSN: 1550-2368. DOI: 10.1103/physrevd.92.063526. URL: http://dx.doi.org/10.1103/PhysRevD.92.063526.

Kouvaris, Chris and Peter Tinyakov (Sept. 2010). 'Can neutron stars constrain dark matter?' In: *Phys. Rev. D* 82 (6), p. 063531. DOI: 10.1103/PhysRevD.82.063531. URL: https://link.aps.org/doi/10.1103/PhysRevD.82.063531.

Kurkela, Aleksi, Paul Romatschke and Aleksi Vuorinen (May 2010). 'Cold quark matter'. In: *Phys. Rev. D* 81 (10), p. 105021. DOI: 10.1103/PhysRevD.81.105021. URL: https://link.aps.org/doi/10.1103/PhysRevD.81.105021.

Lattimer, James M. and Bernard F. Schutz (Aug. 2005a). 'Constraining the Equation of State with Moment of Inertia Measurements'. In: *apj* 629.2, pp. 979–984. DOI: 10.1086/431543. arXiv: astro-ph/0411470 [astro-ph].

— (Aug. 2005b). 'Constraining the Equation of State with Moment of Inertia Measurements'. In: *The Astrophysical Journal* 629.2, pp. 979–984. DOI: 10.1086/431543. URL: https://doi.org/10.1086/431543.

Lattimer, James M. and Andrew W. Steiner (Apr. 2014). 'Neutron Star Masses and Radii from Quiescent Low-mass X-Ray Binaries'. In: *apj* 784.2, 123, p. 123. DOI: 10.1088/0004-637X/784/2/123. arXiv: 1305.3242 [astro-ph.HE].

Lattimer, James M. et al. (May 1991). 'Direct URCA process in neutron stars'. In: *Phys. Rev. Lett.* 66 (21), pp. 2701–2704. DOI: 10.1103/PhysRevLett.66.2701. URL: https://link.aps.org/doi/10.1103/PhysRevLett.66.2701.

Lee, Benjamin W. and Steven Weinberg (July 1977). 'Cosmological Lower Bound on Heavy-Neutrino Masses'. In: *Phys. Rev. Lett.* 39 (4), pp. 165–168. DOI: 10.1103/PhysRevLett.39.165. URL: https://link.aps.org/doi/10.1103/PhysRevLett.39.165.

Li, X.Y, T Harko and K.S Cheng (June 2012a). 'Condensate dark matter stars'. In: *Journal of Cosmology and Astroparticle Physics* 2012.06, pp. 001–001. DOI: 10.1088/1475-

7516/2012/06/001. URL: https://doi.org/10.1088/1475-7516/2012/06/001.

Li, X.Y, F.Y Wang and K.S Cheng (Oct. 2012b). 'Gravitational effects of condensate dark matter on compact stellar objects'. In: *Journal of Cosmology and Astroparticle Physics* 2012.10, pp. 031–031. ISSN: 1475-7516. DOI: 10.1088/1475-7516/2012/10/031. URL: http://dx.doi.org/10.1088/1475-7516/2012/10/031.

Lobashev, V. M. et al. (Aug. 1999). 'Direct search for mass of neutrino and anomaly in the tritium beta-spectrum'. In: *Physics Letters B* 460.1-2, pp. 227–235. DOI: 10.1016/S0370-2693(99)00781-9.

Lyne, A. G. and Francis Graham-Smith (1990). *Pulsar astronomy / A.G. Lyne, F. Graham-Smith*. English. Cambridge University Press Cambridge [England] ; New York, xiv, 274 p. : ISBN: 0521326818.

McDaniel, A., T. Jeltema and S. Profumo (May 2021). 'X-ray shapes of elliptical galaxies and implications for self-interacting dark matter'. In: *Journal of Cosmology and Astroparticle Physics* 2021.05, p. 020. DOI: 10.1088/1475-7516/2021/05/020. URL: https://doi.org/10.1088/1475-7516/2021/05/020.

McDermott, Samuel D., Hai-Bo Yu and Kathryn M. Zurek (Mar. 2011). 'Turning off the lights: How dark is dark matter?' In: *Physical Review D* 83.6. DOI: 10.1103/physrevd.83.063509. URL: https://doi.org/10.1103%2Fphysrevd.83.063509.

McKeen, David et al. (2018). 'Neutron stars exclude light dark baryons'. In: *Phys. Rev. Lett.* 121.6, p. 061802. DOI: 10.1103/PhysRevLett.121.061802. arXiv: 1802.08244 [hep-ph].

Merritt, David et al. (Nov. 2006). 'Empirical Models for Dark Matter Halos. I. Nonparametric Construction of Density Profiles and Comparison with Parametric Models'. In: *The Astronomical Journal* 132.6, p. 2685. DOI: 10.1086/508988. URL: https://dx.doi.org/10.1086/508988.

Migdal, A B (Nov. 1977). 'Vacuum polarization in strong fields and pion condensation'. In: *Soviet Physics Uspekhi* 20.11, pp. 879–898. DOI: 10.1070/pu1977v020n11abeh005471. URL: https://doi.org/10.1070/pu1977v020n11abeh005471.

Miller, M. C. et al. (Dec. 2019). 'PSR J0030+0451 Mass and Radius from NICER Data and Implications for the Properties of Neutron Star Matter'. In: 887.1, L24, p. L24. DOI: 10.3847/2041-8213/ab50c5. arXiv: 1912.05705 [astro-ph.HE].

Miller, M. C. et al. (Sept. 2021). 'The Radius of PSR J07406620 from NICER and XMM-Newton Data'. In: *The Astrophysical Journal Letters* 918.2, p. L28. DOI: 10.3847/2041-8213/ac089b. URL: https://doi.org/10.3847%5C%2F2041-8213%2Fac089b.

Motta, T. F., P. A. M. Guichon and A. W. Thomas (2018a). 'Implications of Neutron Star Properties for the Existence of Light Dark Matter'. In: *J. Phys. G* 45.5, 05LT01. DOI: 10.1088/1361-6471/aab689. arXiv: 1802.08427 [nucl-th].

— (2018b). 'Neutron to Dark Matter Decay in Neutron Stars'. In: *Int. J. Mod. Phys. A* 33.31. Ed. by Harald Fritzsch, p. 1844020. DOI: 10.1142/S0217751X18440207. arXiv: 1806.00903 [nucl-th].

Motta, T. F. et al. (2019). 'Isovector Effects in Neutron Stars, Radii and the GW170817 Constraint'. In: *Astrophys. J.* 878.2, p. 159. DOI: 10.3847/1538-4357/ab218e. arXiv: 1904.03794 [nucl-th].

Mukhopadhyay, Somnath et al. (July 2017). 'Compact bifluid hybrid stars: hadronic matter mixed with self-interacting fermionic asymmetric dark matter'. In: *The European Physical Journal C* 77.7. ISSN: 1434-6052. DOI: 10.1140/epjc/s10052-017-5006-3. URL: http://dx.doi.org/10.1140/epjc/s10052-017-5006-3.

Navarro, Julio F., Carlos S. Frenk and Simon D. M. White (May 1996). 'The Structure of Cold Dark Matter Halos'. In: *apj* 462, p. 563. DOI: 10.1086/177173. arXiv: astro-ph/9508025 [astro-ph].

Navarro, Julio F. et al. (Feb. 2010). 'The diversity and similarity of simulated cold dark matter haloes'. In: *mnras* 402.1, pp. 21–34. DOI: 10.1111/j.1365-2966.2009.15878.x. arXiv: 0810.1522 [astro-ph].

Nelson, Ann, Sanjay Reddy and Dake Zhou (2019). 'Dark halos around neutron stars and gravitational waves'. In: *JCAP* 07, p. 012. DOI: 10.1088/1475-7516/2019/07/012. arXiv: 1803.03266 [hep-ph].

Nesti, Fabrizio and Paolo Salucci (July 2013). 'The Dark Matter halo of the Milky Way, AD 2013'. In: *Journal of Cosmology and Astroparticle Physics* 2013.07, p. 016. DOI: 10.1088/1475-7516/2013/07/016. URL: https://dx.doi.org/10.1088/1475-7516/2013/07/016.

Nico, J. S. et al. (May 2005). 'Measurement of the neutron lifetime by counting trapped protons in a cold neutron beam'. In: *Phys. Rev. C* 71 (5), p. 055502. DOI: 10.1103/PhysRevC.71.055502. URL: https://link.aps.org/doi/10.1103/PhysRevC.71.055502.

Nishizaki, Shigeru, Yasuo Yamamoto and Tatsuyuki Takatsuka (Oct. 2002). 'Hyperon-Mixed Neutron Star Matter and Neutron Stars*)'. In: *Progress of Theoretical Physics* 108.4, pp. 703–718. ISSN: 0033-068X. DOI: 10.1143/PTP.108.703. eprint: https://academic.oup.com/ptp/article-pdf/108/4/703/5414579/108-4-703.pdf. URL: https://doi.org/10.1143/PTP.108.703.

Nobile, Eugenio Del, Marco Nardecchia and Paolo Panci (Apr. 2016). 'Millicharge or decay: a critical take on Minimal Dark Matter'. In: *Journal of Cosmology and Astroparticle Physics* 2016.04, pp. 048–048. DOI: 10.1088/1475-7516/2016/04/048. URL: https://doi.org/10.1088%5C%2F1475-7516%5C%2F2016%5C%2F04%5C%2F048.

Oppenheimer, J. R. and G. M. Volkoff (Feb. 1939). 'On Massive Neutron Cores'. In: *Phys. Rev.* 55 (4), pp. 374–381. DOI: 10.1103/PhysRev.55.374. URL: https://link.aps.org/doi/10.1103/PhysRev.55.374.

Ostriker, J. P., P. J. E. Peebles and A. Yahil (Oct. 1974). 'The Size and Mass of Galaxies, and the Mass of the Universe'. In: *apjl* 193, p. L1. DOI: 10.1086/181617.

Özel, Feryal and Paulo Freire (2016). 'Masses, Radii, and the Equation of State of Neutron Stars'. In: *Ann. Rev. Astron. Astrophys.* 54, pp. 401–440. DOI: 10.1146/annurev-astro-081915-023322. arXiv: 1603.02698 [astro-ph.HE].

Pagels, Heinz and Joel R. Primack (Jan. 1982). 'Supersymmetry, Cosmology, and New Physics at Teraelectronvolt Energies'. In: *Phys. Rev. Lett.* 48 (4), pp. 223–226. DOI: 10.1103/PhysRevLett.48.223. URL: https://link.aps.org/doi/10.1103/PhysRevLett.48.223.

Pandharipande, V R (Jan. 1971). 'HYPERONIC MATTER.' In: *Nucl. Phys. A178: No. 1, 123-44(1971)*. DOI: 10.1016/0375-9474(71)90193-X. URL: https://www.osti.gov/biblio/4679056.

Pattie, R. W. et al. (2018). 'Measurement of the neutron lifetime using a magneto-gravitational trap and in situ detection'. In: *Science* 360.6389, pp. 627–632. DOI: 10.1126/science.aan8895. eprint: https://www.science.org/doi/pdf/10.1126/science.aan8895. URL: https://www.science.org/doi/abs/10.1126/science.aan8895.

Peccei, R. D. and Helen R. Quinn (June 1977). 'CP Conservation in the Presence of Pseudoparticles'. In: *Phys. Rev. Lett.* 38 (25), pp. 1440–1443. DOI: 10.1103/PhysRevLett.38.1440. URL: https://link.aps.org/doi/10.1103/PhysRevLett.38.1440.

Pethick, C. J. and H. Smith (2008). *Bose–Einstein Condensation in Dilute Gases*. 2nd ed. Cambridge University Press. DOI: 10.1017/CBO9780511802850.

Pichlmaier, A. et al. (2010). 'Neutron lifetime measurement with the UCN trap-in-trap MAMBO II'. In: *Physics Letters B* 693.3, pp. 221–226. ISSN: 0370-2693. DOI: https://doi.org/10.1016/j.physletb.2010.08.032.

Preskill, John, Mark B. Wise and Frank Wilczek (1983). 'Cosmology of the invisible axion'. In: *Physics Letters B* 120.1, pp. 127–132. ISSN: 0370-2693. DOI: https://doi.org/10.1016/0370-2693(83)90637-8.

Press, W. H. and D. N. Spergel (Sept. 1985). 'Capture by the sun of a galactic population of weakly interacting, massive particles'. In: *apj* 296, pp. 679–684. DOI: 10.1086/163485.

Raffelt, Georg G. (Dec. 1990). 'Astrophysical methods to constrain axions and other novel particle phenomena'. In: *physrep* 198.1-2, pp. 1–113. DOI: 10.1016/0370-1573(90)90054-6.

Rajendran, Surjeet and Harikrishnan Ramani (Feb. 2021). 'Composite solution to the neutron lifetime anomaly'. In: *Physical Review D* 103.3. ISSN: 2470-0029. DOI: 10.1103/physrevd.103.035014. URL: http://dx.doi.org/10.1103/PhysRevD.103.035014.

Ramos, Angels, Jurgen Schaffner-Bielich and Jochen Wambach (2000). 'Kaon Condensation in Neutron Stars'. In: DOI: 10.48550/ARXIV.NUCL-TH/0011003. URL: https://arxiv.org/abs/nucl-th/0011003.

Randall, Scott W. et al. (June 2008). 'Constraints on the Self-Interaction Cross Section of Dark Matter from Numerical Simulations of the Merging Galaxy Cluster 1E 0657-56'. In: *apj* 679.2, pp. 1173–1180. DOI: 10.1086/587859. arXiv: 0704.0261 [astro-ph].

Ransom, Scott M. et al. (Feb. 2005). 'Twenty-One Millisecond Pulsars in Terzan 5 Using the Green Bank Telescope'. In: *Science* 307.5711, pp. 892–896. DOI: 10.1126/science.1108632. arXiv: astro-ph/0501230 [astro-ph].

Regge, Tullio and John A. Wheeler (1957). 'Stability of a Schwarzschild singularity'. In: *Phys. Rev.* 108, pp. 1063–1069. DOI: 10.1103/PhysRev.108.1063.

Rikovska Stone, J. et al. (2007a). 'Cold uniform matter and neutron stars in the quark–meson-coupling model'. In: *Nuclear Physics A* 792.3, pp. 341–369. ISSN: 0375-9474. DOI: https://doi.org/10.1016/j.nuclphysa.2007.05.011.

— (2007b). 'Cold uniform matter and neutron stars in the quark–meson-coupling model'. In: *Nuclear Physics A* 792.3, pp. 341–369. ISSN: 0375-9474. DOI: https://doi.org/10.1016/j.nuclphysa.2007.05.011.

Riley, T. E. et al. (Dec. 2019). 'A iNICER/i View of PSR J00300451: Millisecond Pulsar Parameter Estimation'. In: *The Astrophysical Journal* 887.1, p. L21. DOI: 10.3847/2041-8213/ab481c. URL: https://doi.org/10.3847%2F2041-8213%2Fab481c.

Riley, Thomas E. et al. (Sept. 2021). 'A NICER View of the Massive Pulsar PSR J07406620 Informed by Radio Timing and XMM-Newton Spectroscopy'. In: *The Astrophysical Journal Letters* 918.2, p. L27. DOI: 10.3847/2041-8213/ac0a81. URL: https://doi.org/10.3847%2F2041-8213%2Fac0a81.

Roberts, M. S. and A. H. Rots (Aug. 1973). 'Comparison of Rotation Curves of Different Galaxy Types'. In: *aap* 26, pp. 483–485.

Rubin, V. C., Jr. Ford W. K. and N. Thonnard (Nov. 1978). 'Extended rotation curves of high-luminosity spiral galaxies. IV. Systematic dynamical properties, Sa -> Sc.' In: *apjl* 225, pp. L107–L111. DOI: 10.1086/182804.

Ruderman, M. (Jan. 1972). 'Pulsars: Structure and Dynamics'. In: *araa* 10, p. 427. DOI: 10.1146/annurev.aa.10.090172.002235.

Sawyer, R. F. (Aug. 1972). 'Condensed π^- Phase in Neutron-Star Matter'. In: *Phys. Rev. Lett.* 29 (6), pp. 382–385. DOI: 10.1103/PhysRevLett.29.382. URL: https://link.aps.org/doi/10.1103/PhysRevLett.29.382.

Scalapino, D. J. (Aug. 1972). 'π^- Condensate in Dense Nuclear Matter'. In: *Phys. Rev. Lett.* 29 (6), pp. 386–388. DOI: 10.1103/PhysRevLett.29.386. URL: https://link.aps.org/doi/10.1103/PhysRevLett.29.386.

Serebrov, A. et al. (2005). 'Measurement of the neutron lifetime using a gravitational trap and a low-temperature Fomblin coating'. In: *Physics Letters B* 605.1, pp. 72–78. ISSN: 0370-2693. DOI: https://doi.org/10.1016/j.physletb.2004.11.013.

Serebrov, A. P. et al. (2008). 'Experimental search for neutron: Mirror neutron oscillations using storage of ultracold neutrons'. In: *Phys. Lett. B* 663, pp. 181–185. DOI: 10.1016/j.physletb.2008.04.014. arXiv: 0706.3600 [nucl-ex].

Serebrov, A. P. et al. (May 2018a). 'Neutron lifetime measurements with a large gravitational trap for ultracold neutrons'. In: *Phys. Rev. C* 97 (5), p. 055503. DOI: 10.1103/PhysRevC.97.055503. URL: https://link.aps.org/doi/10.1103/PhysRevC.97.055503.

Serebrov, A. P. et al. (Feb. 2018b). 'Neutron lifetime, dark matter and search for sterile neutrino'. In: arXiv: 1802.06277 [nucl-ex].

Serot, Brian D. and John Dirk Walecka (1986). 'The Relativistic Nuclear Many Body Problem'. In: *Adv. Nucl. Phys.* 16, pp. 1–327.

Shapiro, Stuart L. and Saul A. Teukolsky (1983). *Black holes, white dwarfs, and neutron stars : the physics of compact objects*.

Sikivie, P. (Apr. 1982). 'Axions, Domain Walls, and the Early Universe'. In: *Phys. Rev. Lett.* 48 (17), pp. 1156–1159. DOI: 10.1103/PhysRevLett.48.1156. URL: https://link.aps.org/doi/10.1103/PhysRevLett.48.1156.

— (Oct. 1983). 'Experimental Tests of the "Invisible" Axion'. In: *Phys. Rev. Lett.* 51 (16), pp. 1415–1417. DOI: 10.1103/PhysRevLett.51.1415. URL: https://link.aps.org/doi/10.1103/PhysRevLett.51.1415.

Sivertsson, S et al. (Apr. 2018). 'The localdark matter density from SDSS-SEGUE G-dwarfs'. In: *Monthly Notices of the Royal Astronomical Society* 478.2, pp. 1677–1693. ISSN: 0035-8711. DOI: 10.1093/mnras/sty977. eprint: https://academic.oup.com/mnras/article-pdf/478/2/1677/25059992/sty977.pdf. URL: https://doi.org/10.1093/mnras/sty977.

Spergel, D. N. et al. (Sept. 2003). 'First-Year <i<Wilkinson Microwave Anisotropy Probe</i< (<i<WMAP</i<) Observations: Determination of Cosmological Parameters'. In: *The Astrophysical Journal Supplement Series* 148.1, pp. 175–194. DOI: 10.1086/377226. URL: https://doi.org/10.1086/377226.

Spergel, David N. and Paul J. Steinhardt (2000). 'Observational evidence for selfinteracting cold dark matter'. In: *Phys. Rev. Lett.* 84, pp. 3760–3763. DOI: 10.1103/PhysRevLett.84.3760. arXiv: astro-ph/9909386.

Steigman, Gary and Michael S. Turner (1985). 'Cosmological Constraints on the Properties of Weakly Interacting Massive Particles'. In: *Nucl. Phys. B* 253, pp. 375–386. DOI: 10.1016/0550-3213(85)90537-1.

Steiner, Andrew W., James M. Lattimer and Edward F. Brown (Mar. 2013). 'The Neutron Star Mass-Radius Relation and the Equation of State of Dense Matter'. In: *apjl* 765.1, L5, p. L5. DOI: 10.1088/2041-8205/765/1/L5. arXiv: 1205.6871 [nucl-th].

Steyerl, A. et al. (June 2012). 'Quasielastic scattering in the interaction of ultracold neutrons with a liquid wall and application in a reanalysis of the Mambo I neutron-lifetime experiment'. In: *Phys. Rev. C* 85 (6), p. 065503. DOI: 10.1103/PhysRevC.85.065503. URL: https://link.aps.org/doi/10.1103/PhysRevC.85.065503.

Strumia, Alessandro (Dec. 2021). 'Dark Matter interpretation of the neutron decay anomaly'. In: arXiv: 2112.09111 [hep-ph].

— (Feb. 2022). 'Dark Matter interpretation of the neutron decay anomaly'. In: *Journal of High Energy Physics* 2022.2. DOI: 10.1007/jhep02(2022)067. URL: https://doi.org/10.1007%5C%2Fjhep02%5C%282022%5C%29067.

Takatsuka, T. and R. Tamagaki (1999). 'Superfluidity of Lambda-hyperons admixed in neutron star cores'. In: *Prog. Theor. Phys.* 102, pp. 1043–1048. DOI: 10.1143/PTP.102.1043.

Takatsuka, Tatsuyuki et al. (2006). 'Occurrence of hyperon superfluidity in neutron star cores'. In: *Prog. Theor. Phys.* 115, pp. 355–379. DOI: 10.1143/PTP.115.355. arXiv: nucl-th/0601043.

Tamagaki, Ryozo (Mar. 1993). 'Overview'. In: *Progress of Theoretical Physics Supplement* 112, pp. 1–25. ISSN: 0375-9687. DOI: 10.1143/PTPS.112.1. eprint: https://academic.oup.com/ptps/article-pdf/doi/10.1143/PTPS.112.1/38836198/112-1.pdf. URL: https://doi.org/10.1143/PTPS.112.1.

Tang, Z. et al. (2018a). 'Search for the Neutron Decay n$\rightarrow$ X+γ where X is a dark matter particle'. In: *Phys. Rev. Lett.* 121.2, p. 022505. DOI: 10.1103/PhysRevLett.121.022505. arXiv: 1802.01595 [nucl-ex].

Tang, Z. et al. (July 2018b). 'Search for the Neutron Decay n $\rightarrow$ χ+γ , Where χ is a Dark Matter Particle'. In: *Physical Review Letters* 121.2. ISSN: 1079-7114. DOI: 10.1103/physrevlett.121.022505. URL: http://dx.doi.org/10.1103/PhysRevLett.121.022505.

Tegmark, Max et al. (May 2004). 'Cosmological parameters from SDSS and WMAP'. In: *Phys. Rev. D* 69 (10), p. 103501. DOI: 10.1103/PhysRevD.69.103501. URL: https://link.aps.org/doi/10.1103/PhysRevD.69.103501.

Thomas, A. W. (1984). 'Chiral Symmetry and the BAG Model: A New Starting Point for Nuclear Physics'. In: *Advances in Nuclear Physics: Volume 13*. Ed. by J. W. Negele and Erich Vogt. Boston, MA: Springer US, pp. 1–137. ISBN: 978-1-4613-9892-9. DOI: 10.1007/978-1-4613-9892-9_1. URL: https://doi.org/10.1007/978-1-4613-9892-9_1.

Tolman, Richard C. (1934). 'Effect of Inhomogeneity on Cosmological Models'. In: *Proceedings of the National Academy of Sciences* 20.3, pp. 169–176. ISSN: 0027-8424. DOI: 10.1073/pnas.20.3.169. eprint: https://www.pnas.org/content/20/3/169.full.pdf. URL: https://www.pnas.org/content/20/3/169.

Trimble, V. and M. Rees (Jan. 1970). 'The Expansion Energy of the Crab Nebula'. In: *aplett* 5, p. 93.

Tulin, Sean and Hai-Bo Yu (2018a). 'Dark matter self-interactions and small scale structure'. In: *Physics Reports* 730. Dark matter self-interactions and small scale structure, pp. 1–57.

ISSN: 0370-1573. DOI: https://doi.org/10.1016/j.physrep.2017.11.004.

— (Feb. 2018b). 'Dark matter self-interactions and small scale structure'. In: *Physics Reports* 730, pp. 1–57. DOI: 10.1016/j.physrep.2017.11.004. URL: https://doi.org/10.1016%5C%2Fj.physrep.2017.11.004.

Turner, Michael S. (1990). 'Windows on the Axion'. In: *Phys. Rept.* 197, pp. 67–97. DOI: 10.1016/0370-1573(90)90172-X.

Urbanec, M., J. C. Miller and Z. Stuchlık (Aug. 2013). 'Quadrupole moments of rotating neutron stars and strange stars'. In: *mnras* 433.3, pp. 1903–1909. DOI: 10.1093/mnras/stt858. arXiv: 1301.5925 [astro-ph.SR].

Verbiest, J. P. W. et al. (May 2008). 'Precision Timing of PSR J0437-4715: An Accurate Pulsar Distance, a High Pulsar Mass, and a Limit on the Variation of Newton's Gravitational Constant'. In: *apj* 679.1, pp. 675–680. DOI: 10.1086/529576. arXiv: 0801.2589 [astro-ph].

Weinberg, Steven (Jan. 1978). 'A New Light Boson?' In: *Phys. Rev. Lett.* 40 (4), pp. 223–226. DOI: 10.1103/PhysRevLett.40.223. URL: https://link.aps.org/doi/10.1103/PhysRevLett.40.223.

Wilczek, F. (Jan. 1978). 'Problem of Strong P and T Invariance in the Presence of Instantons'. In: *Phys. Rev. Lett.* 40 (5), pp. 279–282. DOI: 10.1103/PhysRevLett.40.279. URL: https://link.aps.org/doi/10.1103/PhysRevLett.40.279.

Wiringa, R. B. (Jan. 1993). 'From deuterons to neutron stars: variations in nuclear many-body theory'. In: *Rev. Mod. Phys.* 65 (1), pp. 231–242. DOI: 10.1103/RevModPhys.65.231. URL: https://link.aps.org/doi/10.1103/RevModPhys.65.231.

Yue, A. T. et al. (Nov. 2013). 'Improved Determination of the Neutron Lifetime'. In: *Phys. Rev. Lett.* 111 (22), p. 222501. DOI: 10.1103/PhysRevLett.111.222501. URL: https://link.aps.org/doi/10.1103/PhysRevLett.111.222501.

Zavala, Jesús and Carlos S. Frenk (2019). 'Dark Matter Haloes and Subhaloes'. In: *Galaxies* 7.4. ISSN: 2075-4434. DOI: 10.3390/galaxies7040081. URL: https://www.mdpi.com/2075-4434/7/4/81.

Zwicky, F. (Oct. 1937). ‘On the Masses of Nebulae and of Clusters of Nebulae’. In: *apj* 86, p. 217. DOI: 10.1086/143864.